Role of the spleen in *Plasmodium vivax*: a reticulocyte-prone non-lethal malaria

Mireia Ferrer Almirall

Role of the spleen in *Plasmodium vivax*: a reticulocyte-prone non-lethal malaria

Memòria presentada per Mireia Ferrer Almirall per aspirar al títol de Doctora per la Universitat de Barcelona

Director de tesi: Prof. Hernando A. del Portillo Obando

Línia de Recerca: Salut Internacional

Programa de Doctorat en Medicina

Facultat de Medicina

Centre de Recerca en Salut Internacional de Barcelona (CRESIB)

Hospital Clínic/IDIBAPS-Universitat de Barcelona

El Prof. Hernando A. del Portillo, investigador ICREA del Centre de Recerca en Salut Internacional de Barcelona (CRESIB), certifica que la tesi titulada "**Role of the spleen in *Plasmodium vivax*: a reticulocyte-prone non-lethal malaria**" presentada per la Mireia Ferrer Almirall ha estat realitzada sota la seva direcció, i compleix tots els requisits que dicta la normativa vigent per a la presentació de tesis doctorals com a compendi d'articles a la Facultat de Medicina de la Universitat de Barcelona. Així mateix, certifica la seva contribució equitativa, científica i experimental, en els treballs presentats en coautoria.

Prof. Hernando A. del Portillo

Barcelona, novembre del 2011

A la meva família.

« C'est comme si la réalité était continuellement derrière les rideaux qu'on arrache... Il y en a encore une autre... toujours une autre. Mais j'ai l'impression ou l'illusion que je fais des progrès tous les jours. C'est cela qui me fait agir, comme si on devait bel et bien arriver à comprendre le noyau de la vie. »

[A. Giacometti]

ARTICLES QUE CONSTITUEIXEN LA TESI DOCTORAL

1) **Intravital microscopy of the spleen in a rodent malaria model: quantitative analysis of parasite mobility and blood flow**

Mireia Ferrer*, Lorena Martin-Jaular*, Maria Calvo, Hernando A. Del Portillo.

Journal of Visualized Experiments (acceptat a publicació: Oct 2011)

Factor d'impacte / Quartil: veure nota de l'editora#

2) **Strain-specific spleen remodelling in *Plasmodium yoelii* infections in Balb/c mice facilitates adherence and spleen macrophage-clearance escape**

Lorena Martin-Jaular*, Mireia Ferrer*, Maria Calvo, Anna Rosanas-Urgell, Susana Kalko, Stefanie Graewe, Guadalupe Soria, Núria Cortadellas, Jaume Ordi, Anna Planas, James Burns, Volker Heussler, Hernando A. del Portillo.

Cellular Microbiology, 2011 Jan;13(1):109-22

Factor d'Impacte / Quartil: 5.625 / 1 (Infectious Diseases)

3) **Adhesion of *Plasmodium vivax* infected reticulocytes to the human spleen**

Mireia Ferrer, Stefanie Lopes, Juliana Leite, Bruna Carvalho, Wanessa Neiras, Paulo Nogueira, Fabio T. M. Costa, Marcus V. G. Lacerda, and Hernando A. del Portillo.

Treball no publicat

4) **Spleen plasmablastic proliferation in untreated *Plasmodium vivax* infection**

Marcus Lacerda, André M. Siqueira, Belisa Magalhães, Gisely Melo, Paola Castillo, Mireia Ferrer, Lorena Martin-Jaular, Carmen Fernandez-Becerra, Jaume Ordi, Antonio Martinez, Hernando A. del Portillo.

Sotmès a **Blood** (Oct 2011)

---

* Coautoria.

#The Journal of Visualized Experiments is a peer-reviewed, PubMed-indexed journal. It does not currently have an impact factor, but is actively being tracked by Thompson Reuters and expects to be assigned one within the 2011 (Thompson Reuters tracks a journal for about 12 months prior to assigning an IF and they began tracking JoVE in 2010). The average JoVE article currently gets abut 2,000 views a month with a total of about 10,000 views per year.

Table of content

List of abbreviations

17X: *P. yoelii* 17X reticulocyte-prone non lethal strain

17XL: *P. Yoelii* 17XL normocyte-prone lethal strain

CM: cerebral malaria

CT: computed tomography

DC : dendritic cells

ECM: experimental cerebral malaria

FITC: fluorescein isothiocyanate

GFP: green fluorescence protein

hpi / dpi: hour post-infection / day post-infection

IVM: intravital microscopy

µm (or um) / mm: micrometer / millimeter

min / sec: minute / second

MZ: marginal zone

MZM: marginal zone macrophage

MMM : marginal metalophilic macrophages

MRI: magnetic resonance imaging

P.: *Plasmodium*

pRBC: parasitized red blood cell

RBC: red blood cell

WHO: World Health Organization

1 General introduction

Infectious diseases are a major concern for human welfare. Their causative agents (viruses, protozoa, bacteria or fungi) have complex life cycles, often involving more than one host, where they occasionate a broad range of affections and disease severity. Vector-borne parasitic diseases, including malaria, trypanosomiasis, Chagas disease, leishmaniasis, filariasis, and schistosomiasis, affect humans mainly in the tropics and subtropics, where environmental, socioeconomic and biological factors contribute to their transmission and settlement. Key questions arise when trying to understand how parasites resist in their hosts and populations. How do parasites interact with their hosts? How they monitor/adapt/evade host responses to survive? How they influence vector behavior and fitness? Integrated research tools are needed to understand the mechanisms underlying disease, from molecular to evolutionary level, that lead to the development of effective intervention strategies (Matthews, 2011).

1.1 *Malaria disease: an overview*

Malaria is an ancient disease that has accompanied human evolution for over 50.000 years (Garnham, 1966). The infectious organism was first identified in 1880 by Dr. Laveran inside the red blood cells of soldiers suffering from malaria. It is caused by a protozoan parasite of the genus *Plasmodium* (*P.*) that is transmitted to humans through the bite of the female mosquito *Anopheles*. In humans, the parasite develops silently in the liver before reaching the blood stage, where cyclic invasion, damage and rupture of red blood cells bear mild to severe clinical complications, including death. Symptomatology consists of flu-like fever, chills, headache, muscle ache, anemia and vomits, often recurring in cycles after subsiding. Four species of *Plasmodium* account for the disease (*P. falciparum, P. vivax, P. malariae* and *P. ovale*), with a fifth species, *P. knowlesi*, being recently described from zoonotic phenomenon (Singh *et al.*, 2004). In addition, several species of *Plasmodium* exist that can infect birds, reptiles, monkeys, chimpanzees and rodents (Garnham, 1967; Escalante and Ayala, 1994; Cox, 2010). *P. falciparum* and *P. vivax* are responsible for the majority of morbidity and mortality associated with malaria, being *P. falciparum* the most life-threatening.

To date, several strategies for disease control have been directed to the interruption of vector transmission and development of antimalaric drugs and vaccines to eliminate parasite infection. Of note, while the major bulk of research has been conducted in *P. falciparum* species, little is known on the other species accounting for large morbidity in several countries, namely *P. vivax*. The technological advances enabling the sequencing of the *P. vivax* genome (Carlton *et al.*, 2008) and a recent call for global malaria eradication together have placed new emphasis on the potential and importance of addressing *P. vivax* as a major public health problem (Mueller *et al.*, 2009; Alonso *et al.*, 2011).

1.2 *Focus on* Plasmodium vivax *malaria*

P. vivax is the most widespread malaria and responsible each year for 100-300 million clinical cases (figure 1, (Mendis *et al.*, 2001; Guerra *et al.*, 2010)). Despite being long considered a benign disease, it shatters human welfare of all ages by producing chronic and reemergent infections that contribute to a major arrest on the socioeconomic development in endemic areas. Moreover, severe clinical cases are increasingly being reported, including respiratory distress, spleen rupture, coma and death. Outside sub-Saharan Africa, *P. vivax* is mostly sympatric with *P. falciparum* and mixed infections are common (Mendis *et al.*, 2001; Price *et al.*, 2007; Guerra *et al.*, 2010). As present tools against *P. falciparum* will not suffice to control *P. vivax*, there is an urgent need for understanding the unique biology, epidemiology and pathology of this neglected parasite (Mueller *et al.*, 2009).

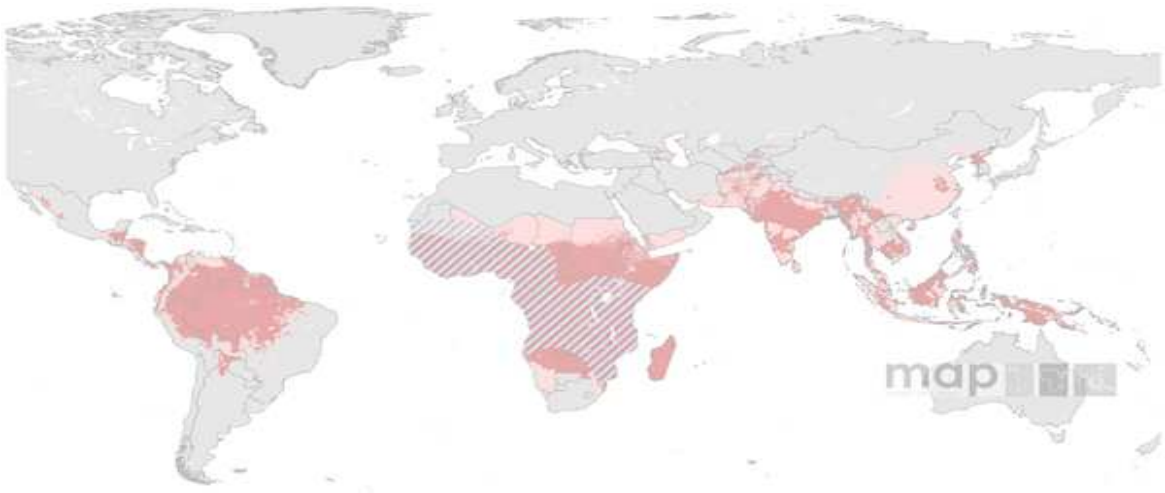

Figure 1- *Plasmodium vivax* malaria transmission in 2009. Risk areas are defined as stable (red), unstable (pink) or no transmission (gray). Areas modulated by Duffy negativity trait are hatched (source: (Guerra *et al.*, 2010)).

1.2.1 Life cycle and pathogenesis

P. vivax biology and life cycle (figure 2) differ from that of *P. falciparum* in different aspects. The most obvious features are: (i) the formation of dormant stages in the liver, called hypnozoites, that can reactivate weeks-months later and cause clinical relapses (Krotoski, 1985). This allows the parasite to be kept in reservoirs in the liver, which, in temperate zones where the presence of mosquitos is seasonal, ensures transmission and propagation of the species. In addition, (ii) round gametocytes appear in the circulation before the onset of clinical symptoms (Boyd and Kitchen, 1937), favoring its transmission before drug treatment; and (iii) mosquito vectors from areas where *P. vivax* is more prevalent are outdoor biting and antropophilic, thus making control measures based on impregnated bed nets of limited value (Mueller *et al.*, 2009). (iv) *P. vivax* invades preferentially, if not exclusively, reticulocytes (Kitchen, 1938). Of note, invasion requires binding of the Duffy binding protein to the Duffy antigen expressed by the host cell (Miller *et al.*, 1976; Batchelor *et al.*, 2011), explaining its absence from West Africa, where Duffy-negative individuals predominate (figure 1). Yet, cases of *P. vivax* infection in Duffy-negative individuals have been recently reported (Ryan *et al.*, 2006; Cavasini *et al.*, 2007). (v) The surface membrane of infected reticulocytes suffers invaginations, called caveola vesicles (Aikawa, 1988), which function remains unknown. Differently, *P. falciparum* induces protuberances in the erythrocyte membrane, called knobs, that contain parasite-encoded proteins involved in pathogenesis (Kilejian, 1979).

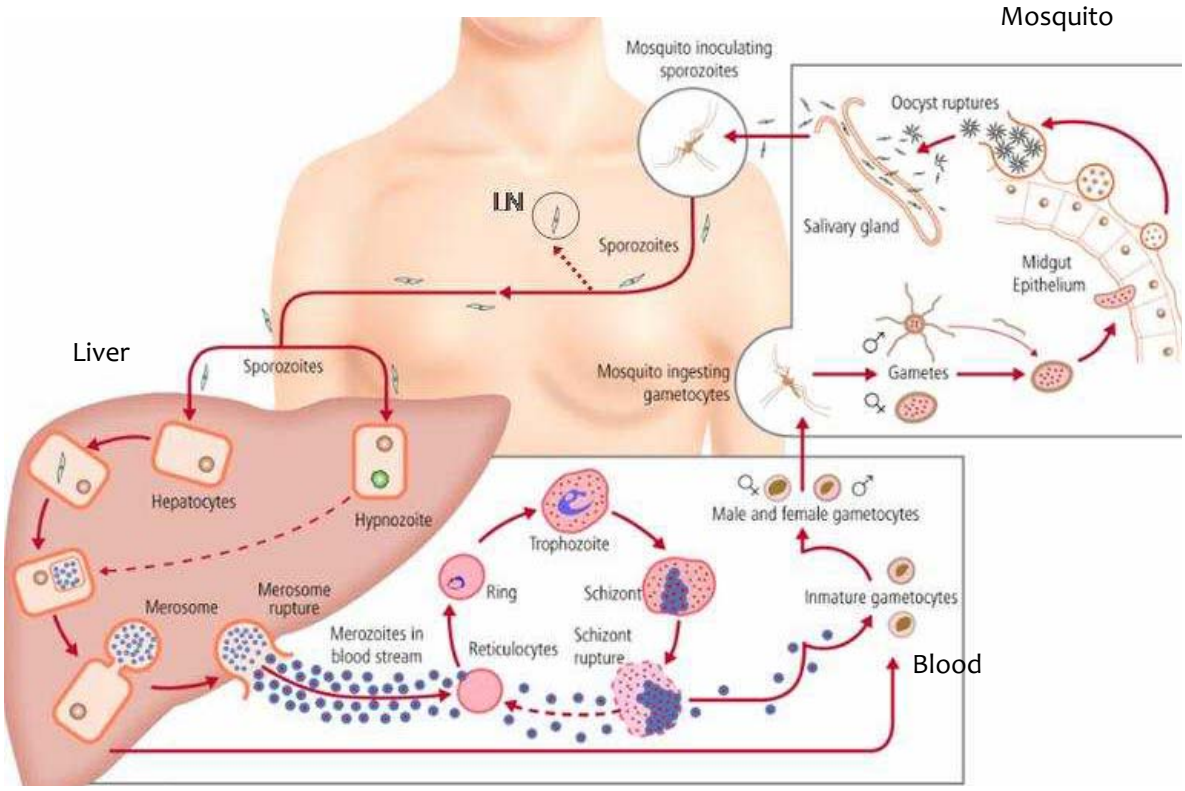

Figure 2- ***Plasmodium vivax*** **life cycle.** Upon mosquito bite, tens of sporozoites are inoculated to the skin, where a large proportion remain in the dermis and can be destroyed by local macrophages, while some enter the lymphatics and the blood circulation to finally reach the lymph nodes (LN) and the liver (Amino *et al.*, 2006). The circulating sporozoites that reach the liver sinusoids migrate through the parenchyma to settle in a final hepatocyte. Invasion of the hepatocyte occurs through the formation of a parasitophorous vacuole that supports parasite growth and development into thousands of infective merozoites. Some forms, termed hypnozoites, can remain dormant in the liver for weeks-months and eventually cause relapses of the infection (Krotoski, 1985). Merozoites are then released to the circulatory system through budding and disruption of host-cell derived vesicles called merosomes that protect them from macrophage uptake (Frevert *et al.*, 2005; Sturm *et al.*, 2006). The erythrocytic cycle of infection lasts 48 hours and is initiated by merozoite invasion of red blood cells. Within red blood cells, parasites remodel the host cell membrane and undergo a trophic period in which they feed from the host cytoplasm and proteinic hemoglobine transforming it to the so-called malaria pigment or hemozoin within the parasite food vacuole. Resulting trophozoites multiply into schizonts that finally rupture and liberate merozoites to reinvade new reticulocytes and perpetuate the asexual cycle. As an alternative to the erythrocytic schizogony, the parasite can differentiate to gametocytes that upon uptake by a feeding mosquito will fuse and complete the life cycle. (source: (Mueller *et al.*, 2009)).

1.2.1.1 Variant genes and the spleen

Pathology in malaria is associated with the capacity of infected red blood cells (pRBCs) to escape immune responses and establish chronic infections. The spleen is the main organ involved in the development of the immune response and in elimination of pRBCs (Bowdler, 2002; Engwerda *et al.*, 2005; Buffet *et al.*, 2009). In the case of *P. falciparum*, parasite-induced modifications of the host cell membrane via export of variant proteins encoded in subtelomeric multigene variant families of the parasite genome (like *var, rif* and *stevor*) (Baruch *et al.*, 1995; Smith *et al.*, 1995; Su *et al.*, 1995; Gardner *et al.*, 2002) unleash a set of phenomena related to pathogenesis: (i) antigenic variation, that refers to the expression of antigenically diverse proteins at the surface of pRBCs to avoid antibody recognition (Brown and Brown, 1965); (ii) rosette formation, through aggregation of pRBCs to uninfected erythrocytes, that contributes to microvascular obstruction of blood flow (David *et al.*, 1988); and (iii) cytoadherence of pRBCs to host cells, by which sequestration of mature stage pRBCs in the deep capillaries of internal organs avoids passage through the spleen, where these cells would be targeted for destruction (Bignami and Bastianelli, 1889; Miller *et al.*, 1994).

Unlike *P. falciparum*, it has been long accepted that no sequestration occurs in *P. vivax* malaria due to the presence of all circulating stages in peripheral blood and absence of knob formation, thus having an obligate passage through the spleen. Questions thus arise as to how this reticulocyte-prone parasite avoids spleen clearance and establishes chronic infections. Studies from *P. vivax* patients have reported antigenic variation and the capacity of mature stage RBCs to form rosettes (Udagama *et al.*, 1987; Udomsanpetch *et al.*, 1995). Moreover, a subtelomeric multigene variant superfamily termed *vir* has been identified in *P. vivax* (del Portillo *et al.*, 2001), that shares homology with members of multigene families from other *Plasmodium* species, like the *rif/stevor* in *P. falciparum* (Fernandez-Becerra *et al.*, 2009). Notably, with the availability of the complete genome sequence of the Salvador I strain of *P. vivax* (Carlton *et al.*, 2008), additional subtelomeric gene families have been recently identified. It is therefore tempting to speculate that subtelomeric variant proteins of *P. vivax,* like those of *P. falciparum*, are associated with pathology. In fact, because of their immunogenic and immunovariant properties, together with diverse subcellular

localization in pRBCs (Fernandez-Becerra *et al.*, 2005), it has been hypothetized that VIR proteins might play a role in immune evasion other than antigenic variation, i.e. in mediating adhesion to the spleen to facilitate the establishment of chronic infections (del Portillo *et al.*, 2004). Of importance, recent studies have reported adhesion of *P. vivax*-pRBCs in lungs and placenta *in vitro* (Carvalho *et al.*, 2010), challenging this current view on the lack of sequestration in *P. vivax*. Thus, there is a renewed interest to move forward on the knowledge of this neglected parasite and reevaluate obsolete paradigms.

1.3 *In this thesis*

Knowledge of the role of the spleen in *P. vivax* malaria has been hindered by the lack of a continuous *in vitro* culture of the parasite and by the ethical and technical constraints of studying this organ in humans. To overcome these limitations, research in the pathogenesis of malaria has been majorly enabled by the use of animal models of malaria that mimick different aspects of disease and the implementation of imaging technologies and other biotechnologic tools that allow for the study of static and dynamic events in physiologic conditions. Advances in the understanding of human pathology will ultimately rely on extrapolation and adaptation of tools that allow for a more translational research in the biomedical field.

Section 2 consists of a revision of the structure and function of the spleen and of its role in malaria infection from what is known from human patients and rodent models.

Section 3 provides a revision of imaging tools and main findings important for dilucidating mechanisms of infection and pathology in rodent malaria and human patients.

Results are presented as three articles and a report. In **articles 1** and **2**, we have used the rodent malaria model of Balb/c mice infected with the reticulocyte-prone non-lethal *P. yoelii* 17X strain, resembling *P. vivax*, and the normocyte-prone lethal *P. yoelii* 17XL strain, resembling *P. falciparum*. To investigate the dynamic characteristics of parasite-spleen interactions, we implemented intravital microscopy of the spleen and developed a methodology for quantification of pRBC mobility and blood flow (**Article 1**). We further studied the structure and function of the spleen in infection, where application of different technologies sinergized to build a model of infection where *P.yoelii* 17X-pRBCs induces remodelling of the spleen through the formation of barrier cells to which pRBCs adhere to escape from macrophage clearance and likely establish chronic infections (**Article 2**).

With the aim to extrapolate the observations performed in the rodent malaria model to human vivax malaria, we implemented magnetic resonance imaging of the mouse spleen to assess differences in remodeling *in vivo* (**Article 2**). As well, we addressed *in vitro* the adhesion properties of *P. vivax*-infected reticulocytes from human patients to

cryosections of human spleens and explored the role of VIR proteins in such an adhesion (**Report 3**). Finally, the misfortune of a *P. vivax* patient undergoing splenectomy due to traumatic spleen rupture provided a unique sample to assess the immunopathology and detect the presence of *P. vivax*-pRBCs in this organ (**Article 4**).

Our data suggest that in reticulocyte-prone non-lethal malaria, passage through the spleen is different from what is known in other *Plasmodium* species and open new avenues for functional/structural studies of this lymphoid organ in malaria.

2 The spleen in malaria: a double-edged sword

Splenomegaly, *albeit* variably, is a hallmark of malaria disease and spleen rupture is mostly associated with malaria infections. A central role for the spleen in clearing particles from the blood was first acknowledged by Ponfick in 1885 (cited in (Lewis, 1983)), though it was not until 1952 that concerns about the increased susceptiblity of splenectomized patients to infections raised the first investigations on the immunological aspects of this organ (King and Shumacker, 1952). Indeed, the spleen carries tripartite actions to fight malaria including removal of parasitized erythrocytes, generation of immune responses and supply of new red blood cells (reviewed in (Engwerda *et al.*, 2005)). However, parasite and host interplay seems to be historically coevolved to a state of "morbid peace", which highlights the need for further research on the mechanisms employed by each counterpart to fully understand the role of the spleen in pathology and chronic infections in malaria.

2.1 *The spleen: normal structure and function*

The spleen consists of a three-dimensionally compartmentalized parenchyma enclosed within a dense capsule of connective tissue (Bowdler, 2002). Trabeculae stemming from the capsule support larger vasculature that branches like a tree into smaller arterial vessels. The origin of the spleen diverges from other lymphoid organs. During embriogenesis, a multilobular mass derives from mesenchymal tissue forming a sponge-like reticular cell meshwork that is progressively vascularized and colonized by hematopoietic and lymphoid cells (Chadburn, 2000; Mebius and Kraal, 2005). Three main compartments arise within a complex structure that account for its unique function: (i) the white pulp, a lymphoid area composed of T and B cell zones where immune responses develop (ii) the marginal zone, with specialized macrophages lining between red and white pulp compartments and (iii) the red pulp, where blood is filtered through an entramated reticuloendothelial system (figure 3).

2.1.1 Splenic compartments

White pulp

The organization of the lymphoid compartment of the spleen, similar to the lymph nodes, is maintained through specific interactions with the stroma and chemokine levels, whose expression is dependent on lymphotoxin β receptor (LT-βR) or tumor necrosis factor receptor 1 (TNFR1) engagement (Ngo *et al.*, 1999). Two lymphocyte populations seggregate into differentiate zones forming sheaths around branching arterial vessels. The inner zone, T cell zone or periarteriolar lymphoid sheath (PALS) (figure 3C), is where T cells reside and can interact with interdigitating dendritic cells and passing B cells to develop adaptive immune responses. It is surrounded by the B cell zone (figure 3B), organized in follicles that undergo antigen-specific B cell clonal expansion and immunoglobulin isotype switching upon activation by follicular dendritic cells and helping T (Th) cells (Engwerda *et al.*, 2005). With respect to other lymphoid organs, the spleen is highly irrigated and has only efferent lymphatic vessels for lymphocyte egress.

Marginal zone

The marginal zone (MZ) forms a rim around the white pulp and supports transit of cells from the blood to this region. It consists of a marginal sinus lined by reticular cells and banded by specific subsets of macrophages (the marginal metallophilic macrophages (MMM), situated at the white pulp border, and the marginal zone macrophages (MZM), adjacent to the red pulp) that play important functions in the uptake of particulate matter and bacteria from the blood (Dijkstra *et al.*, 1985). Other cells localize in between, such as B cells involved in T cell-independent responses and a variety of trafficking populations including DC and T cells (Engwerda *et al.*, 2005; Mebius and Kraal, 2005) (figure 3D).

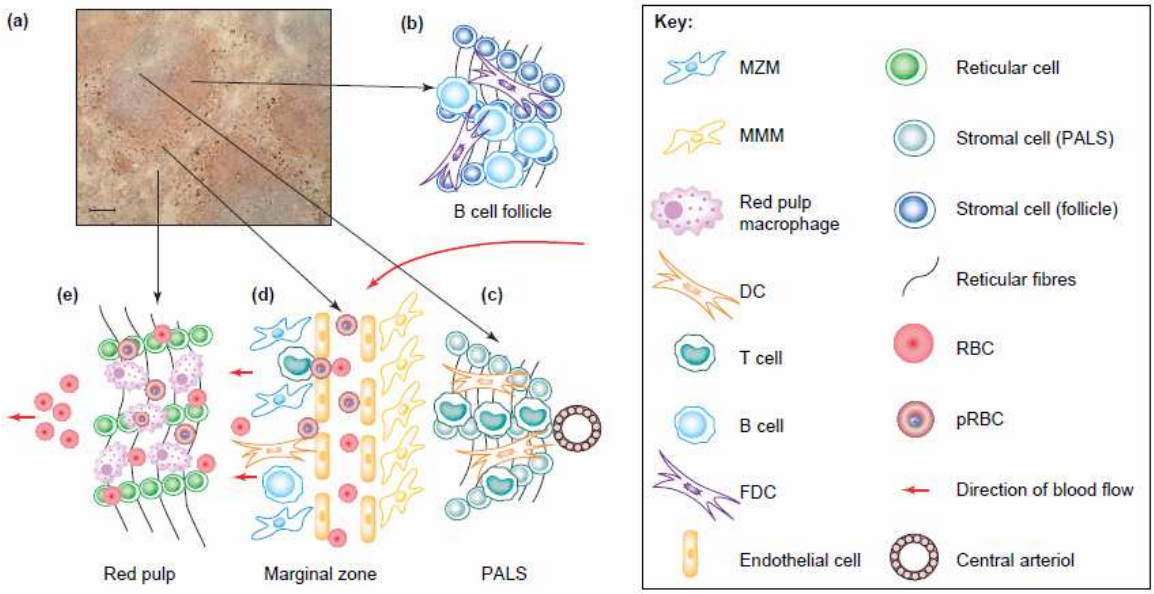

Figure 3- Splenic compartments and cellular composition. A: Histological section of a rodent spleen. **B:** B cell follicle. **C:** PALS. **D:** Marginal zone. **E:** Red pulp. (source: (Engwerda *et al.*, 2005))

Recirculating lymphocytes enter the spleen within this region and are directed to the white pulp via fibroblast channels without crossing an endothelium (Steiniger *et al.*, 2001; Bajenoff *et al.*, 2008). Moreover, similar to lymph nodes, rapid transport of small molecules through the lymphoid compartments has been reported to occur via a tubular network, termed conduit system (Gretz *et al.*, 2000; Nolte *et al.*, 2003). This way, small blood-borne molecules, such as cytokines, chemokines and antigens, can directly reach the splenic white pulp compartment (Nolte *et al.*, 2003; Lokmic *et al.*, 2008). As discrepancy in localization of different molecules with similar weights was

observed, 3D configuration or electrostatic charges of molecules were suggested to be determinant for transport within the conduits. These tubular structures consist of collagen fibers ensheathed with reticular fibroblasts expressing ER-TR7 antigen, that can produce and bind signal factors and chemokines important for the organization of the lymphoid compartment, such as CXCL13 or CCL21, responsible for B or T-cell migration respectively (Nolte *et al.*, 2003).

Red pulp

The red pulp conforms 70-80% of the volume of the spleen (van Krieken *et al.*, 1985). It consists of sinuses and cords that display unique architectural and microcirculatory features related to its function. The splenic cords, or cords of Billroth, are open spaces, devoid of endothelial lining, populated by highly active macrophages along with reticular fibers and reticular cells (Chadburn, 2000). Blood particles and cells, including erythrocytes, hematopoietic cells, granulocytes, circulating monocytes and activated lymphocytes, extravasate from arterioles within these spaces, thus facilitating immune surveillance of blood-borne material (Saito *et al.*, 1988) (figure 3E and figure 4).

Normal red blood cells are rapidly collected from the cords by passing through the interendothelial slits of venous sinuses, whereas abnormal and old erythrocytes exhibiting low deformability are trapped within these spaces for phagocytosis (Mebius and Kraal, 2005). In addition to erythrophagocytosis, which is an important function of the spleen for iron recycling, squeezing of erythrocytes through the slits can leave behind rigid intracytoplasmatic particulate matter, including oxidized hemozoin (Heinz bodies), nuclear remnants (Howell Jolly bodies) and malarial parasites, preserving erythrocyte viability, a process named "pitting" (Schnitzer *et*

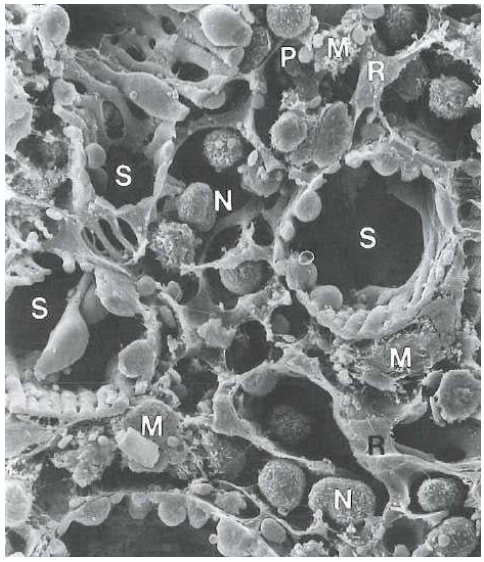

Figure 4- Scanning electron micrograph of the red pulp of the human spleen. The open spaces of the splenic cords are conformed by an entramated meshwork of reticular cells (R) containing macrophages (M), leukocytes (N), blood platelets and erythrocytes (E). Erythrocytes are collected in venous sinuses (S) by squeezing through the interendothelial slits (source: (Bowdler, 2002)).

al., 1972; Chadburn, 2000). Furthermore, contractility of the stress fibers that sheath the venous sinuses permits modulation of the slits to help in the retention of erythrocytes as a reservoir for anemia conditions (Mebius and Kraal, 2005).

Therefore, the red pulp offers a microenvironment adapted to accomplish diverse functions such as blood filtration, removal of aging erythrocytes, iron recycling, pitting and development of innate and adaptive immune effector mechanisms, like antibody secretion by plasma cells. In some cases, the spleen undertakes hematopoietic and cellular reservoir functions (Chadburn, 2000). Indeed, the physicochemical and electrocharge/adhesive nature of the reticular meshwork allows for entrapment of reticulocytes in the red pulp, where they can undergo final maturation (Moghimi, 1995). Moreover, Swirski and collaborators elegantly showed the presence of clusters of monocytes stored in the cords of subcapsular red pulp for rapid deployment upon inflammatory stimuli (Swirski *et al.*, 2009).

Box 1: Differences between mouse and human spleen

Three main differences exist between mouse and human spleen regarding the marginal zone, vascular layout and hematopoietic function. On one hand, the marginal zone in human spleen lacks of a marginal sinus and is divided into an inner and outer compartment by specialized fibroblasts. It is surrounded by an additional perifollicular zone, where some blood vessels terminate in capillaries sheathed by macrophages and blood-filled spaces without endothelial lining can be found (Steiniger *et al.*, 2001; Mebius and Kraal, 2005). On the other, the human and rat spleens are sinusoidal whereas the mouse spleen is non-sinusoidal. The first consists of a honeycombed reticular meshwork of venous sinuses, in which endothelial cells align longitudinally in a barrel-like shape (Mebius and Kraal, 2005) sustained by a fenestrated basement membrane and adventitial reticular cells. This forces blood to squeeze through the interendothelial slits before entering the lumen of venous sinuses. Differently, in non-sinusoidal spleens, blood flows through open-ended pulp venules provided of flat endothelium, a conventional basement membrane and adventitial reticular cells, thus offering little impedance to entrance of red blood cells. Finally, while the rodent spleen is a major site for extramedullary erythropoiesis, this function is lost in normal adult human spleens, being restricted to some pathologic conditions, including malaria (Bowdler, 2002).

2.1.2 Microcirculation and clearing function

Blood flow in the spleen is complex and heterogeneous, with distinguished circulations that arm the filtering capacity and immune clearance functions of the organ. Blood enters the spleen through the splenic artery, at the hilus. It then divides into trabecular

arteries that become central arterioles, surrounded by lymphoid tissue, and branch into smaller arterioles that terminate in the marginal sinus, marginal zone or the red pulp. Early investigations using microcorrosion casts methods and electron microscopy of spleen sections identified two types of circulation, open and closed (Schmidt *et al.*, 1993). Ninety percent of the total splenic blood flow enters the marginal zone and travels through the adjacent venous sinuses, bypassing the reticular meshwork of the red pulp in a fast pathway, called closed circulation. In humans, part of the blood enters the perifollicular zone. The other 10% percolates through the marginal zone or directly enters the red pulp meshwork, filling the cordal open-system, and will follow a slow circulation through collection by venous sinuses. Blood collected in sinuses merges in the trabeculae veins and is drained through the efferent splenic vein at the hilus (Bowdler, 2002; Cesta, 2006). The spleen flow closely affects clearing functions. The open circulation provides two checkpoints at the red pulp and marginal zone where macrophages and other immune cells can survey red blood cells and blood-borne particles (figure 3D). Hence, mechanisms exist to regulate mass and velocity of cell passage through these compartments. First, innervation of the splenic capsule and trabeculae makes it responsive to sympathetic stimuli to regulate entry and storage of red blood cells. Second, the myoelastic tissue of efferent splenic veins confers elasticity to change its diameter and modulate efflux. Last, blood flow through the filtration beds of the red pulp in human spleens is controlled by modulating the size of interendothelial slits in venous sinuses, through contractility of fibers. In addition, the presence of contractile fibroblasts cells located in filtration beds has been described to grant normal basal filtration in human and murine spleens (Weiss, 1991; Moghimi, 1995).

2.2 *The spleen in malaria*

> *"So powerful is the splenic response, so nicely does it interweave host and parasite, that one is moved to speculate that the very structure of the spleen, as that of hemoglobins, may have been evolutionarily driven by malaria."* (Weiss, 1990)

During the erythrocytic stage of malaria infection, the spleen is the main immune responsive organ and undertakes important functions to fight the pathogen, including elimination of pRBCs, development of innate and adaptive immune responses and production of new red blood cells to compensate for anemia (Bowdler, 2002; Engwerda *et al.*, 2005; Mebius and Kraal, 2005; Buffet *et al.*, 2009). But parasite counteracts by modulating immunity and disorganizing the splenic architecture, which difficults host victory and eventually provokes imbalanced immune responses that may cause severe disease. Thus, concern raises about the two sides of the spleen: protective or pathologic?

2.2.1 Insights from splenectomy

The spleen plays an important role both in parasite destruction and in modulating expression of parasite antigens on the surface of the infected RBC. Avoidance of passage through the spleen has been postulated to be the driving force for parasite sequestration and antigenic variation in *P. falciparum* (Barnwell *et al.*, 1983; David *et al.*, 1983). On the one hand, splenectomized patients in natural infections with *P. falciparum* contained circulating forms of all stages, thus suggesting impaired sequestration of mature stage pRBCs (Demar *et al.*, 2004). On the other, removal of this organ in *P. knowlesi* infected monkeys caused a notable decrease in expression of variant genes, which was restored upon reinfection of monkeys with an intact spleen (Barnwell *et al.*, 1983; David *et al.*, 1983). Thus, the spleen plays a major role in modulating the expression of variant proteins in malaria parasites.

The relevance of the spleen for control of malaria infection comes from direct evaluation of splenectomized human patients and rodent models. Several cases of *P. falciparum*-infected patients suffering splenectomy under different immunological conditions have been reported (reviewed in (Buffet *et al.*, 2011)). In immune individuals, the absence of a spleen also aggravated the course of the disease and antibody-mediated clearance of pRBCs was overtaken by other organs though with less

efficicency. The spleen was also found to play a role in chronifying infection, since removal of the spleen in a chronic carrier led to a significant increase in peripheral parasite loads and acute attack (Bachmann *et al.*, 2009). As well, clearance of pRBCs in drug-treated patients was retarded upon splenectomy. Thus, while the spleen may not be essential for parasite clearance in partially immune, splenectomized patients, it exerts a major protective role in non-immune patients, via innate response of macrophages or mechanical retention, since splenectomy of both *P. falciparum* or *P. vivax* non-immune patients (Looareesuwan *et al.*, 1993; Chotivanich *et al.*, 2000) aggravated severity and death of malaria. As well, higher numbers of parasitemia and of circulating mature forms were found. Similar observations have been performed in *P. chabaudi-* or *P. yoelii*-infected mice (Sayles *et al.*, 1991; Yap and Stevenson, 1994), with prolonged waves of parasitemias and impaired parasite clearance (box 2 and table 1).

Of interest, *P. yoelii* 17X infection in mice from distinct backgrounds responded differently to splenectomy: DBA/2 mice were not adversely affected by removal of the spleen, while C57BL/6 or Balb/c mice failed to resolve infection. The lower parasitemia levels in splenectomized mice were attributed to the lack of spleen-derived reticulocytes for parasitation (Sayles *et al.*, 1991). Thereafter, host genotype may influence splenic response to infection, in which alternative mechanisms, such as pRBC phagocytosis in the liver and/or bone marrow hematopoiesis, may supply its function.

The acute course of rodent models of non-lethal malaria follows two phases, one characterized by rising parasitemia and minimal immunity, named "precrisis", and another of immune-mediated falling parasitemia, termed "crisis". Splenectomy of *P. chabaudi adami*-mouse and *P. berghei*-rat infected models during crisis abrogated immunity and increased parasitemia (Quinn and Wyler, 1980; Yadava *et al.*, 1996), highlighting the role of the spleen in parasite killing during this period. Moreover, Weiss and collaborators found that splenectomy aggravated 17X non-lethal and ameliorated 17XL lethal malaria (Weiss, 1991).

Box 2: Rodent malaria models

Experimental models have been developed to tackle different aspects of malaria disease and immunity. Four major rodent *Plasmodium* species, naturally infecting African Thicket Rats (*P. berghei, P. yoelii, P. chabaudi* and *P.vinckei*), have been adapted to infect laboratory rats and mouse strains of distinct genetic backgrounds, whereby infection courses with variable virulence depending on the *Plasmodium*-mouse strain combination (Landau and Boulard, 1978; Sanni *et al.*, 2002) (table 2). Lethality normally reflects discontrolled immune responses, hyperparasitemia and anemia lead to multiorgan failure. *P. berghei* ANKA infection in mice causes cerebral malaria (ECM) complications with neurologic symptoms similar to humans. Non-lethal infection is characterized by an initial acute phase of increasing parasitemia followed by parasite clearance, which in some cases can recrudesce in a second wave of low grade parasitemia (2waves). These models are used to investigate the immune mechanisms involved in controlling infection and disease severity. The course of *P. yoelii* 17X strain causes a self-resolving reticulocyte-prone infection and induces structural and functional changes of the spleen that might help to gain insight into the immunopathogenesis of *P. vivax* malaria.

Implementation of reverse genetic tools to some *Plasmodium* species has provided insights into the mechanisms involved in invasion, parasite growth, antigenic variation and virulence at mosquito and mammal stages. To date, several knockout and transgenic parasites expressing reporter molecules have been constructed to facilitate research (Janse *et al.*, 2011). Although no single model reflects exactly infections in humans, they may help to dissect the complex mechanisms governing pathogenic and immune states and provides a "modifiable system" to address opportune questions. When taken together, they may ultimately unveil information on the mechanisms involved in human malaria.

Plasmodium	Mouse strain	Outcome	Tropism	Immune response	Application to study	References
P.vinckei vinckei	Balb/c	L	N		Chemotherapy, immunity	Perlmann *et al.*, 1995
P.vinckei petteri	Balb/c	NL	N			Caillard *et al.*, 1995
P.chabaudi chabaudi AS	C57BL/6	NL, 2waves	N	IL-12 inflammatory, B cells short lived	Immunopathogenesis	Achtman *et al.*, 2003, Yap *et al.*, 1994,
	A/J	L	N	Th2 early		Stevenson *et al.*, 1995
P.chabaudi chabaudi AS vir	C57BL/6	L/NL	N		Sequestration Antigenic variation	Krucken *et al.*, 2005
P.chabaudi adami	Balb/c	NL, 2waves	N	Th1/Th2 switch Ab-independent	Immunopathogenesis	Yadava *et al.*, 1996, Alves *et al.*, 1996, Helmby *et al.*, 2000
P.yoelii 17XL	Balb/c	L	N>R		Immunopathogenesis ECM Vaccine development	Weiss *et al.*, 1989
	C57BL/6	L	N>R	TGF-B at 24hpi		De Souza *et al.*, 1997
P.yoelii YM	C57BL/6	L	N>R			
P.yoelii 17X	Balb/c	NL	R	Th1/Th2 switch	Spleen response (barrier cells, hematopoiesis) Immunopathogenesis	Weiss *et al.*, 1986
	C57BL/6	NL	R	CD8-Tcell, TGF-B at 10dpi		Omer *et al.*, 2003, Asami *et al.*, 1992
P.berghei ANKA	C57BL/6	L	N/R	CD4/CD8 T cell	ECM Sequestration	Asami *et al.*, 1992, Franke-Fayard *et al.*, 2005
P.berghei ANKA	Wistar rat	NL	N/R		Immunopathogenesis	Wyler *et al.*, 1981

Table 1- Rodent models of malaria with lethal (L) or non-lethal (NL) outcome, normocyte-prone (N) or reticulocyte-prone (R) infection. Ab: antibody. Dpi: day post-infection. ECM: experimental cerebral malaria. (Adapted from (Sanni *et al.*, 2002; Lamb *et al.*, 2006))

Whether protective immunity to *Plasmodium* parasites can be generated in the spleen was proved through adoptive transfer of splenocytes from *P. chabaudi*-infected mice to susceptible splenectomized mice, after which they gained resistance to infection (Winkel and Good, 1991; Yap and Stevenson, 1994). Of note, protection was abrogated by B-cell, but not T-cell, depletion of splenocytes prior to transfer (Yap and Stevenson, 1994). Another study using immune mice to *P. vinckei vinckei* lethal infection showed reversal of immunity by splenectomy, as well as by *in vivo* depletion of CD4 T cells in immune mice, though it remained unaffected in the absence of B cells. Further, adoptive transfer of splenic CD4 T cells from immune to naive mice didn't confered immunity, thus suggesting an interdependent role between CD4 T cells and the malarial spleen in generating protective immune responses (Kumar *et al.*, 1989). Strikingly, priming of CD4 and CD8 T cells in the spleen upon *P. berghei* infection was found to contribute to development of experimental cerebral malaria (ECM), which was reversed by splenectomy or depletion of T cells (Hermsen *et al.*, 1998). The appearance of severe complications in human infections has also been related to the presence of a spleen (Baird, 2007). Hence, the spleen is a double-edged sword with several factors influencing the outcome of the disease. Unveiling the changes and immune effector mechanisms in the spleen during malaria infection is of importance for new interventions.

2.2.2 Immune defense

Macrophages at the first line

Macrophages have a central role in the uptake of circulating pRBCs. During the acute stage of infection, the cellularity and phagocytic activity of the spleen are increased. Enhanced phagocytic activity of the reticuloendothelial system, including macrophages, endothelial and reticular cells, is observed in pathological conditions (Moghimi, 1995). Red pulp macrophages are highly active cells that can mediate opsonic or non-opsonic phagocytosis. *In vitro* phagocytic assays with *P. falciparum* showed opsonization of *P. falciparum*-pRBCs by antibodies that led to macrophage clearance via TNF-α production and release of nitric oxid (Li and Li, 1987), whereas CD36-mediated non-opsonic clearance occurred through unspecific activation by T cells and without increase of the TNF-α proinflammatory cytokine (McGilvray *et al.*,

2000). Opsonic clearance of pRBCs was corroborated in the murine model of *P. chabaudi*-infected mice through binding of strain-specific acute phase-derived sera (Mota *et al.*, 1998).

Host response to *P. yoelii* 17X infection was characterized by a dramatic accumulation of monocytes and macrophages in the blood, liver and spleen, with enhanced endocytic and secretory capabilities (Lee *et al.*, 1986). Moreover, high numbers of inflammatory monocytes, identified as $CD11b^{high}Ly6C^{high}$ cells, appeared in the spleens of *P. chabaudi* infected mice as part of a second wave of mechanisms controlling postpeak parasitemia (Achtman *et al.*, 2003; Sponaas *et al.*, 2009). Protective effect of these monocytes in malaria infection was thought to be achieved through *in vivo* phagocytosis of pRBCs and release of reactive oxygen intermediates, as well as initiation of adaptive responses.

Adaptive responses

Both T and B cell responses were found to play a role in protection to human and rodent malaria. Investigation of the mechanisms involved in resistance to rodent malaria infection highlighted the importance of an early inflammatory response, mediated by interferon γ (IFN-γ), that self limited upon peak parasitemia through tumor growth factor β (TGF-β) production and switched to a Th2 response. The interleukin 12 (IL-12) was purposed as an early host factor bridging innate and adaptive immunity (Stevenson *et al.*, 1995). The encounter of parasite antigen by dendritic cells (DC) in red pulp stimulates their maturation and migration to T cell areas where they activate antigen-specific T cells (Engwerda *et al.*, 2005). Importantly, pRBCs and parasite-derived soluble factors were found to modulate DC function in *P. falciparum* (Urban *et al.*, 1999) and *P. yoelii* (Orengo *et al.*, 2008) infections, respectively.

During Th2 response, primed B cells position in the red pulp to deliver antibodies into the circulation (Engwerda *et al.*, 2005). Antibody-dependent immunity in *P. falciparum* malaria has proved to be short-lived, revealing deficient induction of memory B cells. Histological analysis of the spleens from patients dying of malaria showed architectural disorganization of the white pulp and loss of maginal zone B cells (Urban *et al.*, 2005). Deficient B-cell responses were similarly accompanied by disorganized germinal centers in a *P. berghei* susceptible model (Carvalho *et al.*, 2007). In contrast, *P. chabaudi*

resistant mice were able to develop a protective B cell response through extrafollicular growth of plasma cells and formation of germinal centers, in spite of temporary loss of white pulp integrity (Achtman *et al.*, 2003).

Thus, balanced and opportune development of cellular and humoral immune responses in the course of infection might dictate the outcome of the disease. In fact, comparative analysis of the expression pattern in 17X and 17XL infected spleens identified distinct cellular processes related to metabolic perturbations, erythropoiesis, B-cell immune responses and other innate and cellular immune responses (Schaecher *et al.*, 2005). However, controversy exists on the significance of this antibody-dependent clearance function in protective immunity, and rather point to circulatory and structural changes of the spleen as the main effector mechanism mediating transition to an immune state (Wyler *et al.*, 1981; Grun *et al.*, 1985).

2.2.3 Remodeling of the malarial spleen

To control infection, the splenic structures rapidly enlarge and reorganize increasing its filtering capacity and pRBC removal. The spleen-parasite interplay has evolved different physical and biological mechanisms that orchestrate compartmentalized immune responses and control hyperactivation of immune cells important for parasite/host survival (Serghides *et al.*, 2003; Wong and Rodriguez, 2008). Distribution of *P. chabaudi* pRBCs in the spleens of infected Balb/c mice differed from that of bacteria, implicating a role for red pulp or marginal zone macrophages in each infection, respectively (Yadava *et al.*, 1996). Though pRBCs seemed to avoid a fully functional marginal zone and be directed to filtration beds of the red pulp, a study using a more virulent strain of *P. chabaudi* in C57BL/6 mice revealed loss of MZ macrophages concomitant with impaired pRBC trapping by the red pulp (Krucken *et al.*, 2005). During precrisis, changes in the MZ occurred that led to closure of the circulation throughout infection. Proinflammatory TNF-α signalling was involved in loss of MZM and MMM. Interestingly, mice deficient in LT-βR or TNFR, in which loss of MZM was prevented, exhibited incomplete closure with enhanced survival of mice (Krucken *et al.*, 2005). Similarly, avirulent infections caused by *P. yoelii* 17X and *P. chabaudi adami* parasites in Balb/c mice showed only transient splenic closure during the late precrisis phase (Weiss *et al.*, 1986; Alves *et al.*, 1996). Thus, the magnitude and

dynamics of spleen closing during the course of infection might influence the outcome of the disease.

Barrier cells

Weiss et al suggested that the actions of the spleen aggravate the lethal malaria and ameliorate the non-lethal (Weiss, 1991). Extensive ultrastructural microscopic studies revealed differences of the rodent malarial spleen between *P. yoelii* 17X or 17XL infection. Though the stromal and erythropoietic splenic responses were similar between non-lethal and lethal models, erythroid stores were not effectively protected in the last, leading to fierce parasitization and phagocytic uptake of pRBCs that ended up with host death (Weiss, 1989). By contrast, the formation of a competent blood-spleen barrier in the non-lethal malaria models, *P. yoelii* 17X and *P. chabaudi*, caused limited acces of blood into the filtration beds, thus preventing discontrolled parasitization of reticulocytes and macrophage activation (Weiss, 1989; Alves *et al.*, 1996). This way, the spleen provides a safe microenvironment for erythropoiesis, lympho-plasmacytopoiesis and monocyte to macrophage differentiation (Weiss *et al.*, 1986) (figure 5).

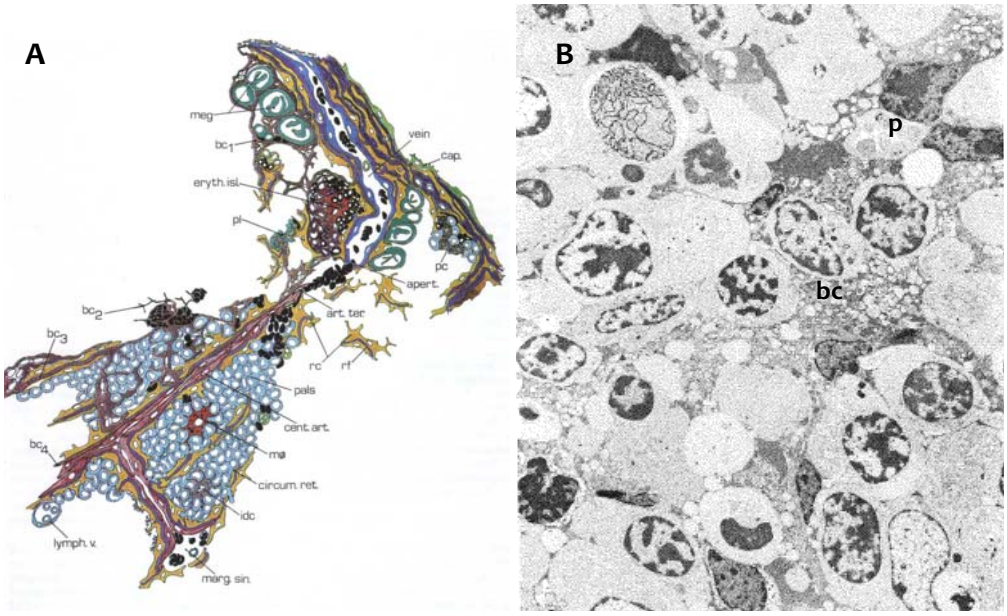

Figure 5- Spleen blood barrier in murine non-lethal malaria. A: Schematic representation of the murine spleen blood barrier formation upon malaria infection. (Weiss, 1990) **B:** Electron micrograph of the red pulp in day 7 of non-lethal *P. yoelii* malaria, showing a syncitial meshwork formed by activated reticular cells (bc), a pRBC (p) and free cells including macrophages, plasma cells and erythroblasts. (Weiss *et al.*, 1986)

The blood spleen barrier was defined by Weiss and collaborators as a complex system of branched syncytial sheets formed by highly active fibroblastic stromal cells termed "barrier cells" (Weiss *et al.*, 1986). They might derive from activation of reticular cells in the filtration beds or in the capsule-trabeculae, or from circulating progenitors that enter the splenic pulp. Indeed, mesenchymal stem cells follow a specific differentiation pathway, likely that of vascular smooth muscle cells, to constitute the supportive environment in hematopoietic tissues (Charbord, 2003). Normally present in the bone marrow (mouse and human) and spleen (mouse) in limited numbers, barrier cells are quickly mobilized in response to hematopoietic or immunologic stress (Weiss, 1991). The interleukin 1 (IL-1) is a potent inducer of cytokines related to mesenchymal stromal cells, like platelet-derived growth factor (PDGF) and TGF-β (Charbord, 2003). Interestingly, administration of IL-1 induced barrier cell formation and protected from lethality and ECM outcome in *P. yoelii* 17XL and *P. berghei* infections, respectively (Weiss, 1990; Alves *et al.*, 1996).

Closing of the splenic circulation in non-lethal murine malaria occurred before the peak parasitemia and was restored during crisis. Dismantling of barrier cells during crisis facilitated (i) release of reticulocytes produced in the sealed-off locules of filtration beds, thus relieving anemia, and (ii) trapping of circulating pRBCs, being damaged by spleen produced factors to become crisis forms (Weiss *et al.*, 1986). Thus, interposition of barrier cells within filtration beds in response to malarial infection and other stress conditions is envisaged to modulate splenic clearance capacities, ranging from hyper to asplenic functions (Weiss, 1990).

2.2.4 Mechanical trapping

Deformability of erythrocytes was found to be critical for their removal in sinusoidal spleens, i.e. human and rat spleens. Early studies by Wyler and Quinn in *P. berghei* infected rats showed impaired splenic trapping of infected and heat-induced abnormal erythrocytes during precrisis (Quinn and Wyler, 1980; Wyler *et al.*, 1981), a period characterized by splenomegaly, decreased cordal blood flow and extramedullary erythropoiesis, which was restored before the onset of crisis, a period of massive destruction of pRBCs. The authors hypothesized that two defense mechanisms might act in concert during precrisis: (i) obstruction of the cords by erythroid precursors

might cause closing of the circulation and (ii) secretion of soluble factors by cordal macrophages might retard intracellular development of the parasite (Wyler *et al.*, 1981). In the crisis period that follows, the altered rheologic properties of erythrocytes are a major determinant of their trapping and removal by the spleen (Wyler *et al.*, 1981). In *P. falciparum*, removal of crisis forms or drug treated pRBCs is achieved without a significant reduction of RBCs. This process, known as "pitting" (Schnitzer *et al.*, 1972), refers to a unique function of the spleen, in which mechanical trapping of circulating pRBCs facilitates parasite engulfment by macrophages or neutrophils leaving the host cell intact, except for parasite proteins that remain on the erythrocyte membrane, like the ring surface antigen RESA (Chotivanich *et al.*, 2000).

2.2.5 Summary, remarks and gaps

Studies in rodent models have revealed key cellular and immune events that take place early in infection that might confer resistance to malaria (summarized in figure 6).

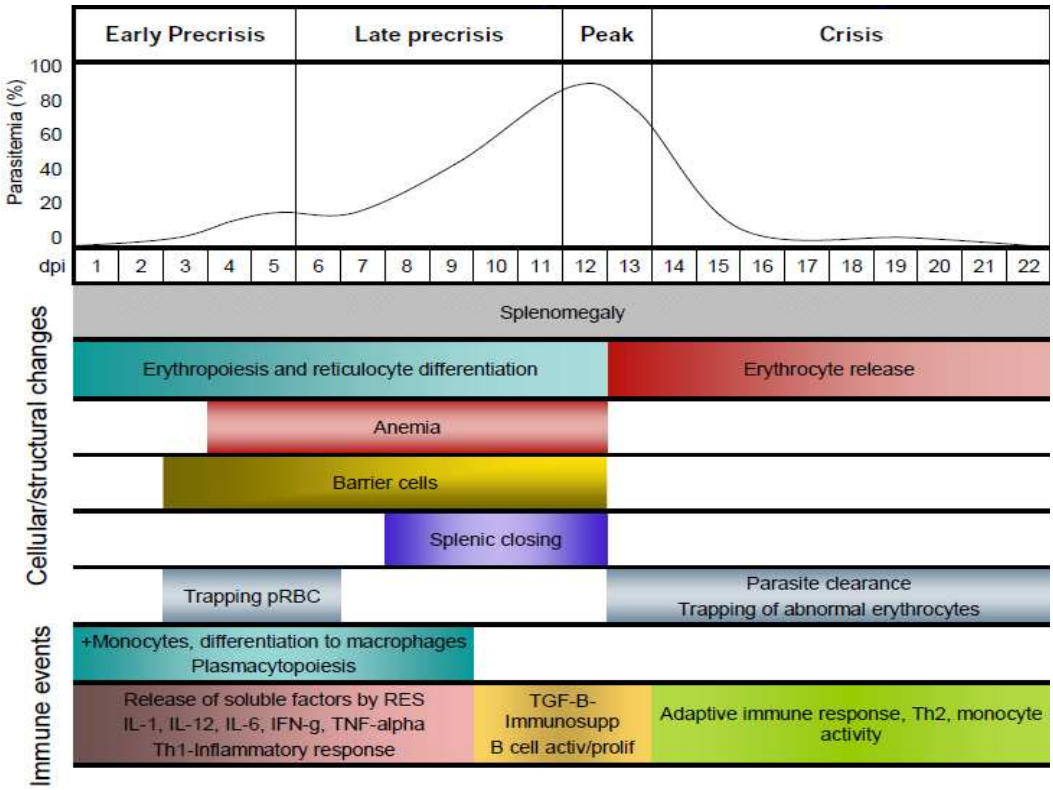

Figure 6- Spleen events in mice resistant to infection. Structural remodeling, differences in hematopoiesis (Asami *et al.*, 1992) and immune responses (Schaecher *et al.*, 2005) may influence the outcome of the disease. Induction of an inflammatory response (mediated by IL-12, IFN-γ and TNF-α) seems to be necessary to control parasitemia at first stage, whereas subsequent development of immunosuppressive responses that mediate Th2 switching may be beneficial to prevent severe host tissue damage. RES: reticulodendothelial system.

Investigation of the mechanisms underlying spleen infections in humans is mostly restricted to clinical observations, exploration of feasible biopsies and post-mortem analysis of fixed tissue sections. Outstandingly, Buffet and collaborators developed a system for ex vivo perfusion of intact human spleens that preserved parenchymal structure, vascular flow and metabolic activity for up to 6 hours (Buffet *et al.*, 2006). These studies showed for the first time the "ex vivo" physiology of this blood filtratory organ and added important insights into the mechanisms of pRBC clearance in an intact spleen, independent from parasite-priming and serum factors. Continuous usage of this model for *P. falciparum*, as well as for *P. vivax* (once a continuous *in vitro* culture system for blood stages have been developed), further guarants a deeper insight into spleen physiology in malaria infections.

Understanding the spatiotemporal events that occur during human and experimental infections and the parasite-spleen interactions *in vivo* remains challenging. A major breakthrough in the biology of malaria parasites was enabling intravital imaging approaches to study *in vivo* the dynamics of parasite infection in the rodent host. With the advent of non-invasive imaging technologies in the biomedical field, exploration of organs in the living host is now feasible and offers great potential for translational research from rodent models to human disease.

3 Imaging tools to investigate parasite-host interactions: from mouse models to human disease

Investigation of the mechanisms underlying infection in humans is mostly restricted to clinical observations, exploration of feasible biopsies and postmortem analysis of fixed tissue sections. These studies, though being highly valuable, represent unlinked pieces that need to be puzzled out. With the advent of new technologies in the biomedical field, the understanding of the spatio-temporal events that parasites undergo in their hosts is beginning to be challenged. Thus, implementation of imaging techniques to rodent models of infection, together with important biotechnological advances in genetic engineering of microorganisms/cells and the development of reporter molecules, has shed light to the dynamic patterns of pathogen transmission, cell invasion, dissemination and immunity from the molecular to the whole body level.

3.1 *From big to small: an overview of imaging tools*

Diverse imaging modes have been engineered based on energy-matter interactions. Their suitability to image live small animal models depends on their specific features and the spatiotemporal resolution achieved (reviewed in (Weissleder, 2002; Kherlopian *et al.*, 2008)). On one hand, non-invasive imaging techniques, such as magnetic resonance imaging (MRI), radiotracer modalities (scintigraphy, positron emission tomography (PET) and single-photon emission computed tomography (SPECT)), X-ray computed tomography (CT), ultrasound and bioluminiscence systems, permit whole body imaging with repeated observations of the same subject over longitudinal studies. Though they can penetrate deep into the tissues, low spatiotemporal resolution is reached (50µm-mm, min-sec). Some applications of these techniques include biodistribution analyses, metabolite tracking, cell migration and imaging of tissue architecture and vascularity (table 2A). On the other hand, intravital microscopy techniques (IVM) have been extensively used to image dynamic molecular and cellular events within tissues, achieving high spatiotemporal resolution (µm/sec). As it is based on light interactions, it usually requires surgical exposure of the organ of study and imaging is restricted to short depths beyond the exposed surface (table 2B). Probes have been developed to enhance all *in vivo* imaging techniques. MRI and CT rely on endogenous tissue contrast to generate the signal while the others require the administration of contrast agents or reporter probes. In IVM, fluorescence signal is obtained from endogenous tissue structures or from reporter fluorescent probes (summarized in table 2). Moreover, transgenic animal models that express fluorescent proteins in specific cell subsets facilitate study of pathogen-host interactions.

A	Bioluminiscence	Nuclear imaging Scintigraphy, SPECT, PET	Ultrasound imaging	Magnetic Resonance Imaging	X-ray computed tomography imaging
Principle	Luminiscence emerges from luciferase-catalyzed conversion of a substrate administered to the body, luciferin, to oxyluciferin, thus reporting its location.	Radiolabelled compounds uptaken by the body emit γ-radiation that is captured on external detectors to form an image. Different modalities provide 2D (scintigraphy) or 3D images (SPECT). PET uses coincidence detection to image functional processes.	Ultrasound waves are used to generate images based on acoustic echoes.	Unpaired nuclear spins (H+ in water and organic compounds) align when placed into a magnetic field (1,5-3Tesla). A temporary radiofrequency pulse is given to change the alignment of the spins, emitting a detectable radiofreq signal when they return to relaxed state.	CT uses X-rays to obtain 3D images by rotating an X-ray source around the subject and measuring the intensity of transmitted X-rays from different angles.
Sample	Live samples. Whole-body or ex vivo imaging.	Whole body	Whole body	Whole body	Whole body
Contrast agent/probes	Luciferins	Isotopes, radionuclides	Microbubbles	Gadolinium, iron oxide particles	Iodine
Space **Time** **Depth**	Several mm Min Cm	1-2mm Min No limit	50um Min mm	10-100um Min-hours No limit	50um Min No limit
Advantages	Non-invasive. High sensitivity. Simple use.	High sensitivity, direct measure of biochemistry and functional activity, molecular detail	Non-invasive. Fast acquisition. Blood flow monitoring.	High soft tissue contrast, high spatial resolution. No biological risks. Preselectable contrast.	Faster and higher spatial resolution than MRI
Limitations	Requires substrate oxidization for luminiscence.	Spatial resolution, PET radioisotopes have short half lives, only one tracer/exp, Radioactivity, High cost cyclotrons	Air and bone artifacts. Low penetrability.	Sensitivity, acquisition speed.	Negative side effects of X-rays limit repeated imaging. Low contrast between soft tissues.
Application	Gene expression, cell tracking. Time-course follow up and distribution of molecules.	Tumor imaging, therapeutic effects, metabolic activity, receptor interaction, concentration and distribution of molecules.	Vascular and interventional imaging.	Anatomical imaging, functional information can be obtained using different modalities.	Tumor imaging, bone, anatomical details

B	Fluorescence microscopy			
	Spinning-disk confocal	Multiphoton	Laser scanning confocal	Epifluorescence widefield
Principle	A specimen is irradiate with a desired and specific band of wavelengths, which is absorbed by the fluorophores, causing them to emit light of longer wavelengths. The much weaker emitted fluorescence is separated from the excitation light through the use of a spectral emission filter.			
	Mercury lamp or wave-specific lasers, light passes through multihole before and after specimen illumination.	Pulsed long-wave laser. Two or more photons simultaneously absorbed by a fluorophore and produce excitation on the focal plane.	Wave-specific laser, pinhole before detector removes out-of-focus light.	Fluorescent illumination uses Mercury or Xenon lamp or LEDs, excitation/emission filters.
Sample	Fixed or live samples. Intravital microscopy of tissues or ex vivo imaging.			
Contrast agent/probes	Photoproteins, fluorochromes, quantum dots and other dyes. Endogenous contrast (autofluorescence).			
Space **Time** **Depth**	15nm-1um Sec-hours <400-800um			
Advantages	Serial acquisition of optical slices taken at increasing depths allow 3D reconstruction. Fast acquisition. Reduced photobleaching.	Greater imaging depth and minimal photobleaching and toxicity. Provides 3D optical sectioning through exc/em only on the focal plane. Generation of second harmonic signal.	Serial acquisition of optical slices taken at increasing depths allow 3D reconstruction. Fast acquisition and high resolution images.	Easy to manipulate. Acquisition of subjects changing from focal plane. Used for thin specimens
Limitations	Lower spatial resolution than confocal microscopy. Needs sensitive cameras.	Slow switching between wavelengths for two color acquisition. Limited choice of fluorophores.	Limited to short depths. Slight phototoxicity and photobleaching	Phototozicity and photobleaching. Light coming from out-of-focus can give noisy images. Sequential acquisition in two colors. Lower depths.
Application	Anatomical, physiological, molecular. Visualization of cell structures. Imaging intracellular proteins and colocalization analysis in confocal microscopy. Dynamic imaging, cell tracking. Signal specificity obtained from fluorochromes.			

Table 2- Features of imaging techniques and their applications. A: Non-invasive imaging. **B:** Intravital microscopy modalities.

3.2 *Intravital microscopy: imaging cell dynamics*

Intravital microscopy has served to capture pathogens and immune cells "in action". Early in the 19th century, bright field microscopy was used in inflammation studies to image leukocytes in the vasculature of translucent organs by Cohnheim (1889) and Wagner (1839). A century later, fluorescence-based techniques permitted visualization of specific individual cells and rapidly progressed to provide a wide spectrum of tools for the examination of living material with high spatiotemporal resolution (McGavern and Dustin, 2009). Several organs have been successfully imaged using widefield or confocal systems and multiphoton microscopy approaches, with the last offering the advantage of increased tissue penetration with reduced photodamage (reviewed in (Halin *et al.*, 2005) and summarized in table 2B).

Endogenous contrast such as autofluorescence and second harmonic signals can be used by some techniques to illuminate cells and characteristic tissue structures (Frevert *et al.*, 2005; Peters *et al.*, 2008). Interestingly, there exist several fluorescent probes that can be incorporated to facilitate identification of structures and cells in situ (reviewed in (Coombes and Robey, 2010)). Among them, (i) fluorescent labelled dextrans or plasma proteins of different sizes, quantum dots and small dyes with different affinities may be injected intravenously during the experiment to define the blood vasculature and permeability (Molitoris and Sandoval, 2005); (ii) fluorescent antibodies have been used *in vivo* to identify specific cells (Sipkins *et al.*, 2005); and (iii) adoptive transfer of ex vivo labelled cell populations (i.e. labelling of leukocytes and erythrocytes with fluorescein isothiocyanate (FITC), pkH26 or Carboxyfluorescein succinimidyl ester (CFSE)) is commonly used for cell trafficking investigations (Miller *et al.*, 2003). Moreover, transgenic cells and animals can be engineered to express fluorescent proteins under specific promoters. Since the application of green fluorescent protein (GFP)-transgenic organisms in *in vivo* imaging in 1994, other fluorescent reporters such as red fluorescent protein (RFP) and its derivatives have been developed to provide enhanced and stable fluorescences (Graewe *et al.*, 2009). For example, *Plasmodium* transgenic lines for GFP or RFP derivatives, like tdTomato and mCherry, have been created to unveil dynamics of parasite behavior and to image

parasite-host cell interactions in GFP-expressing cell subsets of transgenic mouse strains (Frevert *et al.*, 2005).

With the implementation of intravital microscopy to experimental models of malaria, the journey of malaria parasites to the blood is revealed much more complex than originally thought (Amino *et al.*, 2005; Heussler and Doerig, 2006). Moreover, *in vivo* imaging of parasite-host interactions in the context of immunity and disease paves the way for the understending of malaria pathogenesis (figure 7).

3.2.1 Insights into the *Plasmodium* life cycle

Preerythrocytic stages

Until the advent of intravital imaging, sporozoites were thought to directly travel to the hepatocyte where all protective cellular immune responses against irradiated sporozoites and circumsporozoite (CSP) protein were thought to be elicited. A key stop on the parasite's journey in the rodent host has been discovered using *in vivo* imaging (Amino *et al.*, 2006). Their study showed various fates for the sporozoites inoculated to the skin of mice: (i) a large proportion remained at the inoculation site for up to six hours, (ii) some parasites entered the peripheral circulation towards the liver and (iii) about 20% were drained to regional lymph nodes. The dynamics of sporozoite mobility in the skin was elegantly assessed using epifluorescence and spinning disk confocal microscopy on the ear of mice infected with GFP-transgenic *P. berghei* sporozoites. The active mobility of sporozoites within the mosquito and upon deposition into the skin (Frischknecht *et al.*, 2004; Vanderberg and Frevert, 2004) was predicted to be a selective advantage for transmission. Indeed, sporozoites were imaged gliding in the dermis and interacting with blood vessel walls or drifting along lymphatics vessels, identified by intradermal injection of fluorescent dextran. Once in the lymph nodes, ex vivo imaging of dissected organs over time showed internalization of most of the sporozoites by DC, suggesting a role for these cells in priming T lymphocytes with parasite antigens (Amino *et al.*, 2006; Chakravarty *et al.*, 2007) (figure 7A). Of note, some sporozoites partially matured into exoerythrocytic forms inside the lymph nodes (Amino *et al.*, 2006) and the skin (Gueirard *et al.*, 2010), similarly to what has been described in the liver (Sturm *et al.*, 2006).

Sporozoites that enter blood vessels rapidly reach the liver and infect hepatocytes. Using TIE2-GFP and lys-EGFP-ki mice that express GFP in endothelial and phagocytic cells, respectively, sporozoites were observed to initially arrest in the sinusoids by proteoglycan interactions with stellate cells and then migrate through the sinusoidal cell layer composed of fenestrated endothelium and Kupffer cells (Frevert *et al.*, 2005). Once in the liver parenchyma, they transmigrated through several hepatocytes before settling down in a final cell and eventually differentiating into exoerythrocytic forms (EEF), as had been demonstrated *in vitro* (Mota *et al.*, 2001). In their study, Frevert and collaborators observed diverse mobility patterns and velocities employed by the parasites to cross different host tissue barriers and cells: sporozoites are transported in the sinusoidal bloodstream at 11,2 µm/sec, slow down by gliding along sinusoidal cells (1,4 µm/sec), traverse Kupffer cells (0,3 µm/sec) and transmigrate through hepatocytes (1,6 µm/sec), likely guided by the three-dimensional structural components of the tissue (Frevert *et al.*, 2005) (figure 7B).

While transmigrating through the liver parenchyma, sporozoites leave behind a trail of dead hepatocytes until they finally infect an hepatocyte by formation of a parasitophorous vacuole where they mature into EEFs (Mota *et al.*, 2001). At 40 to 56 hours post-infection (hpi), budding of EEF-infected hepatocyte membrane liberates vesicles filled of merozoites into the sinusoid lumen, without exhibiting host cell damage (van de Sand *et al.*, 2005; Sturm *et al.*, 2006) (figure 7B, inset). Therefore, release of the so-called "extrusomes" (Tarun *et al.*, 2006) or "merosomes" (Sturm *et al.*, 2006), depending on EEF maturity, is a mechanism exploited by the parasite to silently reach the blood circulation. Of importance, *in vivo* observation of these events accounts for prolonged exposure of sample to laser light, which makes the high-speed spinning disk confocal microscope best suited to diminish photobleaching and cell damage while providing rapid image acquisition (Thiberge *et al.*, 2007).

Interlude

How newly developed merozoites are liberated into the circulation and initiate RBC invasion has been recently unveiled by Baer and collaborators and involves passage through the lung capillaries. Merosomes released from the liver into the bloodstream contain thousands of infective merozoites surrounded by host cell membrane that

camuflage them from immune surveillance. On their way, blood shear forces favour resizing and fragmentation of merosomes, thus facilitating passage through the vasculature without disruption. Their study suggested that merosomes travel through the right ventricle of the heart and arrest in the lungs but do not disseminate further as they were absent from other organs such as the spleen, kidney or brain. Ex vivo confocal microscopy of lungs of mice infected with *P. yoelii* 17X strain expressing GFP showed in real time merosome accumulation in the sinusoids followed by desintegration and release of free merozoites into the lung microvasculature where they readily encountered erythrocytes to parasitize (Baer *et al.*, 2007) (figure 7C).

Erythrocytic stages

The development of individual *P. falciparum* parasites in erythrocytes has been recently documented using four-dimensional imaging, challenging our current view on protein export in malaria (Gruring *et al.*, 2011).

3.2.2 Insights into tissue pathogenesis

The distribution and sequestration patterns of infected red blood cells in rodent host tissues have been assessed by whole-body bioluminiscence imaging (Franke-Fayard *et al.*, 2005) (figure 7D); however, few studies have explored *in vivo* the mechanisms and dynamics of parasite sequestration. Implementation of IVM to image the brain microvasculature in rodent models of ECM has provided insights into the role of several host receptors and parasite ligands *in vivo*. For example, the intercellular adhesion molecule 1 (ICAM-1) has been implicated in cytoadherence of pRBCs to the vascular endothelium (Kaul *et al.*, 1998), but neither ICAM-1 nor P-selectin were found to mediate leukocyte recruitment during ECM in *P. berghei*-infected mice despite exhibiting many hallmarks of inflammatory responses (Piccio *et al.*, 2002; Chang *et al.*, 2003), eventually leading to vascular collapse (Cabrales and Carvalho, 2010) (figure 7E).

In the field of immunology, adoptive transfer of fluorescently-labelled T cells has been used to image leukocyte recruitment and migration within lymphoid organs (Grayson *et al.*, 2001; Cahalan *et al.*, 2002) and inflamed tissues (Khandoga *et al.*, 2009). Implementation of IVM to the spleen was first accomplished by Grayson *et al.* to assess T cell recruitment in the white pulp (Grayson *et al.*, 2001), which migration was later

suggested to be directed by fibroblast channels originating in the MZ (Grayson *et al.*, 2003; Bajenoff *et al.*, 2008). Other studies using two-photon microscopy have reported T-DC synapses in the MZ (Morelli *et al.*, 2003) and red pulp of the spleen (Mittelbrunn *et al.*, 2009). As well, clustering of T cells in the white pulp was visualized ex vivo in *Listeria* experimental infections (Aoshi *et al.*, 2008) and another study reported clusters of monocytes in the cords of subcapsular red pulp that functioned as storage for their rapid deployment to regulate inflammation (Swirski *et al.*, 2009) (figure 7F).

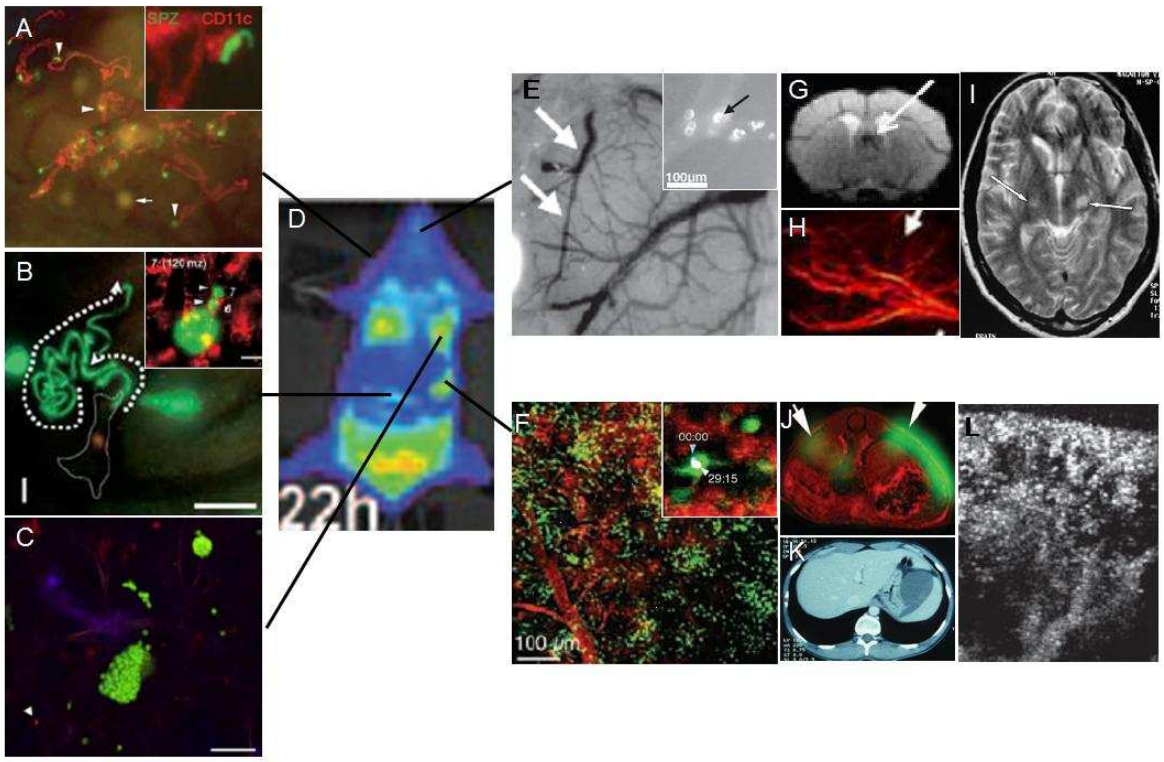

Figure 7- Summary of findings from *in vivo* imaging. **A-C**: Intravital microscopy of pre-erythrocytic stages in different organs. **A:** Mobility of *P. berghei* (*Pb*)-sporozoites in the skin and interaction with DC in the lymph nodes (inset) (Amino *et al.*, 2006). **B:** Traversal of liver parenchima by *Pb*-sporozoites (Frevert *et al.*, 2005) and merosome budding in a blood vessel (inset, (Sturm *et al.*, 2006)). **C:** Lung merosomes in *Pb* (Baer *et al.*, 2007). **D:** Whole-body bioluminiscence of *Pb*-infected mouse showing accumulation of luminiscent schizonts at 22 hours post-infection in the spleen, lungs and adipose tissue (Franke-Fayard *et al.*, 2005). **E:** IVM of brain microcirculation showing points of blood flow obstruction by adhesion of *Pb*-pRBC and leukocytes to capillaries (inset) (Cabrales and Carvalho, 2010). **F:** IVM of GFP-monocytes in the subcapsular splenic red pulp with microcirculation stained in red (Swirski *et al.*, 2009). **G-L:** Non-invasive imaging. **G:** T2-weighted MRI of mouse brain in cerebral malaria (CM) showing edema (Penet *et al.*, 2005). **H:** MRI-angiography of brain in CM showing blood flow obstruction (Togbe *et al.*, 2008). **I:** T2-w MRI of human brain in *P. falciparum*-CM (Vyas *et al.*, 2010). **J:** Abdominal MRI-SPECT of a mouse injected with labeled macrophages showing accumulation in the spleen (Gorantla *et al.*, 2006). **K:** Abdominal CT scan of a *P. vivax* patient suffering splenic rupture (Imbert *et al.*, 2009). **L:** Ultrasonography of the human spleen microcirculation injected with Gd-DTPA contrast agent (Buffet *et al.*, 2006).

3.3 *Non-invasive Imaging: towards biomedical imaging*

With the advent of non-invasive imaging techniques in the medical field, a consistent bridge is being built that helps to extrapolate research from animal models to human disease.

3.3.1 Magnetic Resonance Imaging

Magnetic resonance imaging offers a variety of tools to obtain functional, anatomical and molecular information with high contrast in soft tissues (reviewed in (Weissleder, 2002), table 2A), like the brain. This technique relies on the magnetic moments of atoms with unpaired nuclear spins, such as hydrogen contained in water and organic compounds. Under a strong magnetic field, typically 1,5-3 Tesla for human scanners, nuclei spins align parallel to the field and measures can be obtained from the time required to realign after applying disturbing radiofrequency pulses. Thus, relaxation times (T1 and T2) and proton density-weighted images provide variable image contrast that relates to specific tissue characteristics.

Efforts are being made to enhance MRI contrast and sensitivity, such as development of imaging sequences that accentuate the paramagnetic properties of the blood, i.e. susceptibility-weighted imaging (Tong *et al.*, 2008), and the introduction of contrast agents based on chelates of gadolinium (Gd-DTPA) and a variety of ferromagnetic nanoparticles (MPIOs) that amplify MR signal and can be targeted to specific tissues/cells for further drug delivery (McAteer *et al.*, 2008; von Zur Muhlen *et al.*, 2008).

Insights into human cerebral malaria

Clinical performance of MRI has helped in the diagnosis of cerebral malaria in patients with neurological manifestations, excluding other neuropathies that course similarly and enabling opportune and rapid treatment. MRI findings in three out of twelve patients who had suffered from CM the past days or weeks presented anomalies attributable to two types of lesions (Cordoliani *et al.*, 1998). First, the MR pattern in T1 and T2-weighted images showed hyperintense nodules corresponding to cortical hemorrhagic infarcts, which could reflect pRBC blockage of capillaries. Second, using

T2 and fluid attenuated inversion-recovery (FLAIR) sequences, hyperintensity in white matter was observed, with diffuse areas characteristic of edema and bilateral foci indicating gliosis, likely due to ischemic toxicity (Cordoliani *et al.*, 1998). Of note, in a patient with similar MRI findings, clinical care and treatment with antimalarials reversed almost completely CM brain lesions (Vyas *et al.*, 2010).

3.3.2 Computed Tomography: findings in human malarial spleen

Several organs become enlarged during infection, being splenomegaly a hallmark of malaria disease. During malaria infection, changes in splenic architecture and cellularity result in tissue enlargement, infarction and/or ultimately rupture. Extensive studies have documented altered imaging features associated to splenic abnormalities in humans (De Schepper *et al.*, 2005; Elsayes *et al.*, 2005; Karakas *et al.*, 2005). For instance, arterial phase CT scans revealed an abnormal enhancement of malarial splenic parenchyma that progressively regressed to a normal pattern -where differences in blood flow between red and white pulp become apparent (Karakas *et al.*, 2005)- after antimalarial treatment. The lack of heterogeneity observed reflected histopathological findings of capillary necrosis, sinus thrombosis and splenic congestion (Bae and Jeon, 2006). Both *P. falciparum* and *P. vivax* malaria cases have been reported to induce splenic infarction based on CT images showing hypodense heterogeneous multifocal areas (Bonnard *et al.*, 2005; Kim *et al.*, 2007). This pathology seems to be increasing among non-immune travelers despite antimalarial prophylaxis and may eventually trigger splenic rupture, which is a life-threatening complication in malaria disease (Bonnard *et al.*, 2005; Choudhury *et al.*, 2008). Analysis of 55 cases of malarial splenic rupture revealed several features associated to this lesion, namely splenic enlargement and capsule distension, regardless of the causative *Plasmodium* species. Of note, splenomegaly and risk of splenic rupture were still exacerbated in *P. vivax* malaria and non-immune patients (Imbert *et al.*, 2009) (figure 7L).

The role of the spleen in malaria pathogenesis is controversial since on one hand, it may be of importance in the development of immune responses and protection to severe disease upon reexposure, but, on the other, discontrolled inflammatory responses and reticuloendothelial hyperplasia may cause vascular dysfunction and severe organ failure (Choudhury *et al.*, 2008; Imbert *et al.*, 2009). Though splenectomy

has long been the treatment of choice for this pathology, new interventions are committed to conservative management that takes advantage of CT, ultrasonography and/or MR scans for diagnosis and daily monitoring of tissue recovery (Choudhury *et al.*, 2008).

4 Relevance and hypothesis

Malaria is a global health problem and the recurrent infections and emergence of virulent strains resistant to antimalarics highlight the need to find strategies not only for control but eradication of malaria. *P. vivax* has unique biological characteristics that distinguish it from *P. falciparum*. Progress in understanding the biology of *P. vivax* and its interaction with the host will help define new avenues for contributing to the control, elimination and eradication of malaria.

Based on work of Weiss and collaborators, whose electron microscopy studies of the malarial spleen showed the formation of a blood spleen barrier (Weiss *et al.*, 1986), together with the identification of the *vir* multigene superfamily (del Portillo *et al.*, 2001), it was hypothetized by our group that *P. vivax* infection induces remodeling of the spleen through the formation of barrier cells to which pRBCs cytoadhere through variant proteins or unidentified ligands. In doing so, they may be physically protected to escape macrophage clearance. Moreover, the spleen undertakes erythropoietic/hematopoietic functions during infection, whereby merozoites released from pRBCs will encounter newly formed reticulocytes to parasitize, eventually establishing chronic infections (del Portillo *et al.*, 2004).

Working hypothesis on the mechanism of spleen-clearance evasion in reticulocyte-prone non-lethal malaria.

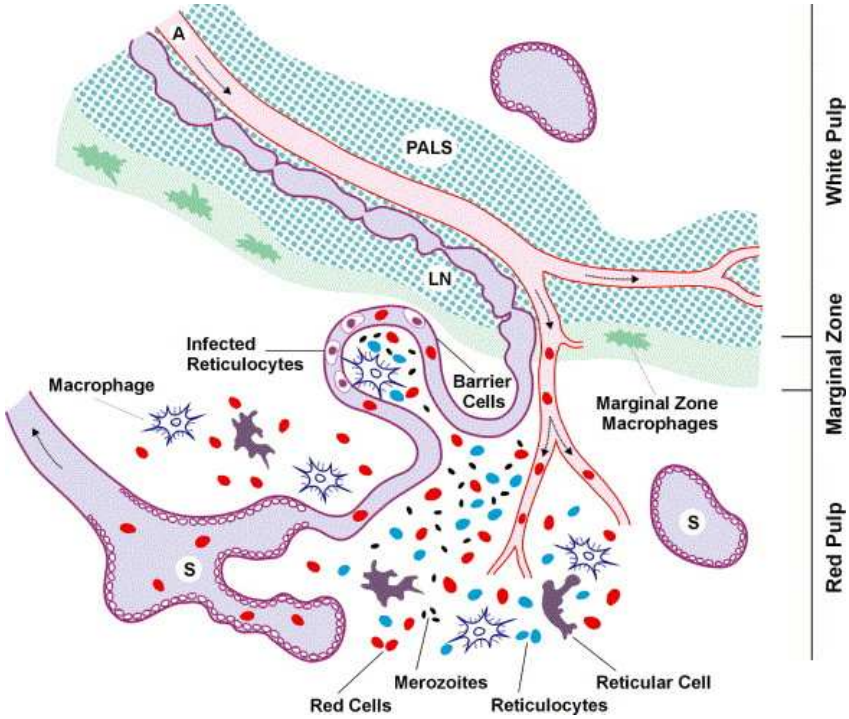

RBCs enter the open spaces of the red pulp and are collected by venous sinuses (S). Macrophages eliminate infected reticulocytes. The induction of barrier cells to which infected reticulocytes cytoadhere facilitates macrophage-clearance escape and establishment of chronic infections.

5 Objectives

The main objective of this thesis is to investigate the role of the spleen in reticulocyte-prone non-lethal malaria in order to gain insight into the mechanisms used by the parasite to escape spleen clearance and establish chronic infections.

Specific objectives

1) To establish and characterize the rodent malaria model of *Balb/c* mice infected with GFP transgenic *P. yoelii* 17X parasites, lethal and non-lethal strains.

2) To perform time-course differential analysis of the structural and functional changes of the spleen in lethal and non-lethal infections through global expression microarray analysis and immunohistological assays, with special attention to the role of barrier cells.

3) To implement IVM approaches to the rodent malarial spleen during blood-stage infection in order to image parasite-spleen interactions in real-time, *in vivo*, and perform quantitative measures of mobility parameters and blood flow.

4) To implement magnetic resonance imaging to the spleen in the rodent malaria model to assess differences in the spleen between lethal and non-lethal strains, with the final aim to implement a protocol for non-invasive imaging of the spleen in human malaria patients.

5) To study the adhesion of pRBCs to rodent and human spleens *in vitro* to gain insight into the role of VIR proteins in such adhesion.

6) To investigate parasite-spleen interactions in human vivax malaria.

6 Results

Results are presented as a compendium of articles and a report:

1) **Intravital microscopy of the spleen in a rodent malaria model: quantitative analysis of parasite mobility and blood flow**

Mireia Ferrer*, Lorena Martin-Jaular*, Maria Calvo, Hernando A. Del Portillo.

Journal of Visualized Experiments (accepted Oct 2011)

2) **Strain-specific spleen remodelling in *Plasmodium yoelii* infections in Balb/c mice facilitates adherence and spleen macrophage-clearance escape**

Lorena Martin-Jaular*, Mireia Ferrer*, Maria Calvo, Anna Rosanas-Urgell, Susana Kalko, Stefanie Graewe, Guadalupe Soria, Núria Cortadellas, Jaume Ordi, Anna Planas, James Burns, Volker Heussler, Hernando A. del Portillo.

Cellular Microbiology, 2011 Jan;13(1):109-22

3) **Adhesion of *Plasmodium vivax* infected reticulocytes to the human spleen**

Mireia Ferrer, Stefanie Lopes, Juliana Leite, Bruna Carvalho, Wanessa Neiras, Paulo Nogueira, Fabio T. M. Costa, Marcus V. G. Lacerda, and Hernando A. del Portillo.

Unpublished work

4) **Spleen plasmablastic proliferation in untreated *Plasmodium vivax* infection**

Marcus Lacerda, André M. Siqueira, Belisa Magalhães, Gisely Melo, Paola Castillo, Mireia Ferrer#, Lorena Martin-Jaular, Carmen Fernandez-Becerra, Jaume Ordi, Antonio Martinez, Hernando del Portillo.

Submitted to *Blood* (Oct 2011).

---

* Equally contributed.

Contribution: Performed nested PCR and IHF analyses.

6.1 *Intravital microscopy of the spleen in a rodent malaria model: quantitative analysis of parasite mobility and blood flow*

6.1.1 Summary

Objectives

To implement intravital microscopy of the spleen in a rodent malaria model and develop methodologies for quantitative imaging of GFP-expressing malaria parasites on its passage through the spleen, blood flow and visualization of microcirculatory structures.

Results

1. Intravital microscopy of the spleen of *P. yoelii-Balb/c* rodent malaria model allowed visualization in real-time of the passage of parasites through the spleen.
2. By using FITC-labelled RBCs injected intravenously to control mice, normal behavior of red blood cells in the spleen was assessed. Injection of vascular dyes allowed identification of the microcirculatory structure of the spleen, with slow/open and fast/closed compartments.
3. Blood flow was calculated using RBC reflection contrast and vascular dyes in splenic vessels of different diameters. Velocity of RBC and pRBC was measured using fluorescence microscopy.
4. Quantitative analysis of parasite mobility in the slow compartment was achieved with the help of Z-coded coloured images to define different mobility parameters that describe adhesion *in vivo*. Manual procedures using ImageJ free software were implemented to follow the fast moving particles in blood flow.
5. Reduced velocity, lack of directionality and increased residence times of pRBCs in the spleen are used to report adhesion *in vivo*. Thus we provide a new tool to conduct *in vivo* studies of adherence in malaria blood stages.

6.1.2 Article 1

Video Article

Intravital Microscopy of the Spleen in a Rodent Malaria Model: Quantitative Analysis of Parasite Mobility and Blood Flow

Mireia Ferrer[1,*], Lorena Martin-Jaular[1,*], Maria Calvo[2], Hernando A. del Portillo[1,3]

[1]Department of poverty related diseases, Barcelona Centre for International Health Research
[2]Confocal Microscopy Unit, University of Barcelona- Scientific and Technological Centers
[3]Institució Catalana de Recerca i Estudis Avançats (ICREA)

[*]These authors contributed equally

URL: http://www.jove.com/details.php?id=3609
DOI: 10.3791/3609

Keywords: intravital microscopy, gfp, malaria, spleen, mobility, adhesion, Plasmodium yoelii, Balb/c mice,

Date Published: //

Citation: Ferrer, M., Martin-Jaular, L., Calvo, M., del Portillo, H.A. Intravital Microscopy of the Spleen in a Rodent Malaria Model: Quantitative Analysis of Parasite Mobility and Blood Flow. J. Vis. Exp. (), e3609, DOI : 10.3791/3609 ().

Abstract

The advent of intravital microscopy in experimental rodent malaria models has allowed major advances to the knowledge of parasite-host interactions [1,2]. Thus, in vivo imaging of malaria parasites during pre-erythrocytic stages have revealed the active entrance of parasites into skin lymph nodes [3], the complete development of the parasite in the skin [4], and the formation of a hepatocyte-derived merosome to assure migration and release of merozoites into the blood stream [5]. Moreover, the development of individual parasites in erythrocytes has been recently documented using 4D imaging and challenged our current view on protein export in malaria [6]. Thus, intravital imaging has radically changed our view on key events in *Plasmodium* development. Unfortunately, studies of the dynamic passage of malaria parasites through the spleen, a major lymphoid organ exquisitely adapted to clear infected red blood cells are lacking due to technical constraints.

Using the murine model of malaria *Plasmodium yoelii* in Balb/c mice, we have implemented intravital imaging of the spleen and reported a differential remodeling of it and adherence of parasitized red blood cells (pRBCs) to barrier cells of fibroblastic origin in the red pulp during infection with the non-lethal parasite line *P.yoelii* 17X as opposed to infections with the *P.yoelii* 17XL lethal parasite line [7]. To reach these conclusions, a specific methodology using ImageJ free software was developed to enable characterization of the fast three-dimensional movement of single-pRBCs. Results obtained with this protocol allow determining velocity, directionality and residence time of parasites in the spleen, all parameters addressing adherence in vivo. In addition, we report the methodology for blood flow quantification using intravital microscopy and the use of different colouring agents to gain insight into the complex microcirculatory structure of the spleen.

Ethics statement

All the animal studies were performed at the animal facilities of University of Barcelona in accordance with guidelines and protocols approved by the Ethics Committee for Animal Experimentation of the University of Barcelona CEEA-UB (Protocol No DMAH: 5429). Female Balb/c mice of 6-8 weeks of age were obtained from Charles River Laboratories.

Video Link

The video component of this article can be found at http://www.jove.com/details.php?id=3609

Protocol

This method was used in the research reported in [7].

1. Animal infection with green fluorescent protein (GFP) transgenic parasites

1. *P. yoelii*–GFP transgenic lines of 17XL and 17X were generated using the same vectors, targeting strategy and protocols described elsewhere for *P. berghei*[8]. They express the mutant 3 variant of GFP [9] under the ubiquitous promoter of *P. berghei* elongation factor 1 (*Pbeef1a*), which directs constitutive expression of GFP to parasite cytosol during the entire intra-erythrocytic developmental cycle.
2. Inject animals intraperitoneally with parasitized red blood cells (pRBCs) of *P. yoelii*-GFP transgenic lines 17XL and 17X obtained from the tail blood of donor mice at 5-10% parasitemia and diluted in PBS. Use a dose of $5x10^5$ pRBCs/mouse to reach a peripheral parasitemia of 1% at day 3 post-infection (p.i.).
3. At day 3 p.i., check that parasitemia of mice infected with both parasite lines is the same by doing a blood smear with a drop of tail blood followed by Giemsa staining and observation under a light microscope with a 100x oil objective. Parasitemia is estimated by calculating the percentage of pRBCs over total RBCs in three optical fields of approximately 300 RBCs.
4. Control animals injected with FITC-labeled RBCs can be used to characterize the movement of these cells in normal spleens.

2. Labeling of red blood cells with FITC and injection to control animals

1. Collect 1 ml of total blood through cardiac puncture of a Balb/c mouse in 200 µl of PBS containing ethylene diamine tetraacetic acid (EDTA) (100 g/L, pH 7.4) and wash the RBC pellet in PBS/EDTA (0.1 g/L, pH 7.4) through centrifugation at 300 xg for 5 minutes (min) at room temperature (RT).
2. Resuspend 200 µl of the RBC pellet in 300 µl of PBS/EDTA (0.1 g/L, pH 8) containing FITC (10 g/L) and incubate for 2 hours at room temperature in the dark with gentle agitation. After that time, the supernatant is removed and the cells washed five times (300 xg, 5 min, RT) in PBS/EDTA (0.1 g/L, pH 7.4).
3. For in vivo experiments, dilute 10 µl of the FITC-labeled RBC pellet in 200 µl of PBS and inject intravenously to a Balb/c mouse in order to reach 1% FITC-RBCs in circulation.

3. Surgical procedures

1. Prepare injectable anesthetic composed of 100 mg/kg of Ketamine and 5 mg/kg of Midazolam per dose according to the weight of the animal. Inject the mouse intraperitoneally with one dose of anesthetic. Readminister half of the dose every 30 min to maintain the mouse full-time anesthetized.
2. Keep the mouse warm and verify that the mouse is completely anesthetized (usually after 5-20 min) by pinching the foot pad before proceeding.
3. In order to facilitate intravenous administration of substances during the course of the experiment, cannulate the tail vein of the mouse using a 27G cannula. Check that the needle is well positioned inside the vein by injecting 20-50 µl of saline buffer and seal it with tape. If it obstructs, repeat the cannulation upstream of the vein. Be careful to not introduce air bubbles.
4. Expose the inferior part of the spleen through a small incision in the skin and musculature at the left dorsal side of the animal. Place the spleen where less breath movement is observed and apply PBS on the surface exposed to keep it clean of the mouse hair and hydrated.
5. Seal a cover-slip of 60x24mm with cyanoacrylate adhesive (Super Glue-3 Loctite) to the skin surrounding the spleen to allow visualization.

4. Imaging of living parasites in the spleen

1. Intravital microscopy experiments were carried out in a Leica TCS-SP5 confocal microscope (Leica Microsystems, Heidelberg, Germany) equipped with an incubation system with temperature control, an APO 63x glycerol immersion objective lens (NA 1.3), resonant scanner at 8000 lines/s and an Argon (488 nm) and HeNe (594 nm, 633 nm) lasers. Additional lasers, such as blue diode (405 nm) and diode-pump-solid state (561 nm), may be required for excitation of probes listed in Table 1.
2. Place the animal on the stage of the microscope with the cover-slipped spleen facing down to the objective. A general view of the microcirculatory structure of the spleen can be optionally visualized using a 20x objective. RBC reflection contrast will be helpful to select different regions of interest to image at higher magnification afterwards.
3. Focus the selected regions of interest with 63x glycerol immersion objective lens using tissue autofluorescence. GFP parasites are observed passing through different areas of the spleen.
4. Fluorescence is recorded on two different channels (excitation/emission wavelength 488/505-580 nm for FITC/GFP and 488/570-630 nm for tissue autofluorescence) with the pinhole set to 3.0 Airy units. RBC reflection (488/480-495 nm), together with fluorescent dyes to label the blood vasculature (see Table 1), are used to obtain additional information on the zone being imaged and in the blood flow experiments described below.
5. Capture images through five Z-stacks covering a depth of 8 µm because of the three-dimensionality of the organ, at a speed of 8 kHz to generate videos of 1.5 min.
6. Record videos of different zones of the spleen for quantitative analysis.

5. Intravital microscopy of the microvasculature of the spleen and image acquisition for blood flow measurement

1. Vital fluorescent probes dissolved in isotonic saline can be injected to the tail vein during the experiment to image the vasculature and gain insight into the structure of the spleen. A list of probes and their application is presented in Table 1 [10].
2. To label the vascular system with fluorescent dextran, prepare 1 mg of 70 kDa dextran labeled with Texas Red in 100 µl of saline buffer.
3. Use the cannulated tail vein to inject the fluorescent dextran to the animal being imaged.
4. Set the vessels horizontally, in the direction of laser scanning, by optical field rotation (not affecting speed). Use xy and xt line scanning modes in the central lumen of the vessel. Use bidirectional scanning with a line average of 32 at a speed of 8 kHz to obtain an image of 512x512 pixels.
5. Acquire images of vessels on three different channels (excitation/emission wavelength 488/505-580 nm, 594/605-660 nm, 488/480-495 nm for FITC/GFP, dextran– Texas Red and erythrocyte reflection, respectively).
6. Take images of vessels with different diameters and over different phases of the cardiac cycle to compensate for fluctuations. In these images, the streaks resulting from moving cells will be used to quantify blood flow [11].

6. Image processing and quantitative analysis of parasite mobility using ImageJ software

1. Create a real-time video from the image sequence generated using ImageJ software (version 1.39o, Wayne Rasband, NIH, www.macbiophotonics.ca).
2. Open the ".lif" file in ImageJ keeping "xyzct" sequence and separated channels.
3. Register some useful information from the metadata file: dblvoxelX-voxel-width, dblvoxelY-voxel-height, dblvoxelZ-voxel-depth and frame interval between consecutive Z-frames and between stacks. This information will be used for calibration.
4. Substract autofluorescence (channel 2) to the GFP-parasite images (channel 1). Filter the images with Gaussian Blur=1. Please recall that using gaussian blur filter in images needs to be declared for publications. Save file "animal1_m1_substract.seq".
5. A Z-coded color video is created as supportive material for quantitative analysis of parasite mobility, as it will facilitate single-particle identification in fast moving particles and Z-movement characterization.
6. Convert the stack to Image 5D, with third dimension being the Z and fourth dimension being the time. Give a different color to each Z and overlay.
7. Project all the Z using maximum intensity over all the time frames to create a Z-coded color video. Save as "animal1_m1_Z_color.avi".

8. Classify and label all the particles that appear in the first 10 time frames of the video according to the number of frames of residence (from 1 to 10). In each video, 20 particles will be tracked following the proportions obtained. In total, 120 parasites will be quantified from 3 animals, using six videos/animal representing different zones of the spleen.
9. Report the frames of residence on each Z and over the entire movie for all the particles to be quantified.
10. Perform 4D (x,y,z,t) manual tracking of particles using the MTrackJ plugin (written by E. Meijering). Open the file "animal1_m1_substract.seq" as Image 5D and set image properties using the information registered before from pixel width, height, depth (in µm) and stack interval (in sec). Configure the track settings as follows: "move to next time" and "apply local cursor-bright centroid/25x25pixel". Configure displaying: "show origin", "show image", "show active track", "show only tracks present in current channels", "show only track point at current time".
11. Add a track for each particle. Consider movement in Z-axis only if displacement is higher than 6 µm (average diameter for a pRBC). Follow the particle over a maximum of 100 frames.
12. Save the x, y, z and t coordinates measured from the track as "animal1_m1_p1".xls.
13. Measures for displacement ($D=SQRT((x_{final}-x_{inital})^2+(y_{final}-y_{inital})^2+(z_{final}-z_{inital})^2$); path length ($P=\Sigma_{n=0\rightarrow final}\ SQRT((x_{n+1}-x_n)^2+(y_{n+1}-y_n)^2+(z_{n+1}-z_n)^2$) with n indicating each position tracked; mean velocity and residence time can be calculated using the values from x,y,z,t coordinates tracked calibrated according to the data registered. Directionality of the particles is defined as the quotient of displacement vs. path length, with values of close to 1 indicating directed movement and values of close to 0 indicating restrained movement [12]. A template for calculations is facilitated enclosed.

7. Calculation of volumetric blood flow

1. Volumetric blood flow is estimated as $Q=V*\pi*D_v^2/4$, with V, erythrocyte velocity over the cross section and D_v, lumen vessel diameter [11].
2. To calculate *V*, measure the angles (θ) of five particle streaks showing bright reflection (RBC) and four particle streaks showing green fluorescence (pRBC-GFP) in each xt image using ImageJ software. Measure lumen vessel diameter on the xy image.
3. The velocity is then expressed as $V=1/\tan(\theta)*D_e/D_v$ to normalize for erythrocyte (D_e=6 µm) and lumen vessel diameters.
4. Quantify a minimum of three vessels with different diameters and five xt images for each vessel.

8. Statistical analysis

1. For statistical analysis, plot directionality, mean velocity and residence time as density distributions and use the equality-of-medians test in STATA (IC10) to assess differences between the two parasite lines.

9. Representative Results

Intravital imaging of GFP parasites in the spleen revealed differences in mobility between the two strains of parasites. Quantitative analysis of mobility parameters of single parasites indicated reduced velocity, lack of directionality and augmented residence time of parasites of mice infected with 17X strain. Moreover, volumetric blood flow in vessels was not altered between strains [7]. The technical procedure is presented in Figure 1A. Figure 1B shows a general view of a normal spleen of a mouse injected with FITC-labeled RBCs, with a zoom in into the red pulp and another to a vessel (Figure 1B, zoom in 1 and 2, respectively). Vasculature was evidenced by injecting 70 kDa Dextran-Texas Red together with erythrocyte reflection contrast. Other fluorescent dyes summarized in Table 1 can be used to gain information on the organ being imaged, such as Hoechst (Figure 1C, 1D).

Real-time imaging of parasites of the 17XL and 17X strain is presented in Movies 1 and 2, with some 17X-pRBC (Movie 2) showing a rolling-circle behavior. Quantitative analysis of mobility parameters was achieved through tracking of individual parasites with the help of Z-coded color images. Figure 2A shows a Z-projection of a Z-coded color stack, where the encircled particle appears moving in different planes. Figure 2B and 2C represent the tracks for different parasites in 17X and 17XL infection, respectively. Results from directionality and residence time of all the particles quantified are presented as a density distribution map of parasite population in Figure 2D and 2E, respectively. To monitor blood flow in the spleen using intravital microscopy, the streaks obtained in xt images of the central lumen of vessels resulting from the erythrocyte movement were measured to calculate velocity [11]. The images show a xy scan of a vessel (Figure 2F) with the corresponding xt line scan (Figure 2G).

Fluorescent Probe	Localization	1 photon Excitation (nm)	2 photon Excitation (nm)	Detected emission (nm)	Quantity/ mouse weight
Hoechst 33342	Membrane-permeant DNA-binding probe. It labels nuclei of all cells (live and dead) after Intravenous injection.	405	800	410-480	12.5 g/Kg
Propidium iodide	Membrane-impermeant DNA-binding probe. It labels nuclei of cells with compromised membrane (apoptotic and necrotic cells).	561	800	570-650	250 mg/Kg
70,000 mol wt Dextran-Fluorescent (FITC, Texas Red)	Fluid-phase marker that enhances contrast of plasma.	FITC 488 Texas Red 594	800	500-540 600-650	50 mg/Kg
Sodium Fluorescein	Bulk fluid-phase albumin marker that enhances contrast of plasma.	488	800	500-540	2 mmol/Kg
Evans Blue	Bulk fluid-phase albumin marker that enhances contrast of plasma.	633	nd	645-700	20 mg/Kg
Rhodamine R6	Vital probe that accumulates in active mitochondria. It labels endothelia and circulating white cells after intravenous injection.	561	800	570-650	25 mg/Kg
Fluospheres- 1micron diameter	Beads that are uptaken by cells with phagocytic activity.	488	800	500-540	nd
Alexa488-labeled fibrin IIβ chain-specific antibody	Probe that labels fibrin IIβ chain	488	800	500-540	0.3 mg/Kg

Table 1. Fluorescent probes for intravital microscopy. Vital fluorescent dyes with different localizations that may be used to label the spleen in vivo. Excitation/emission (Exc/em) ranges to be used with one-photon (or two-photon microscopy) are provided. The dose indicated is dissolved in 0.1-0.2 ml of saline buffer and injected to the tail vein of the mouse. [nd: not determined in this study.

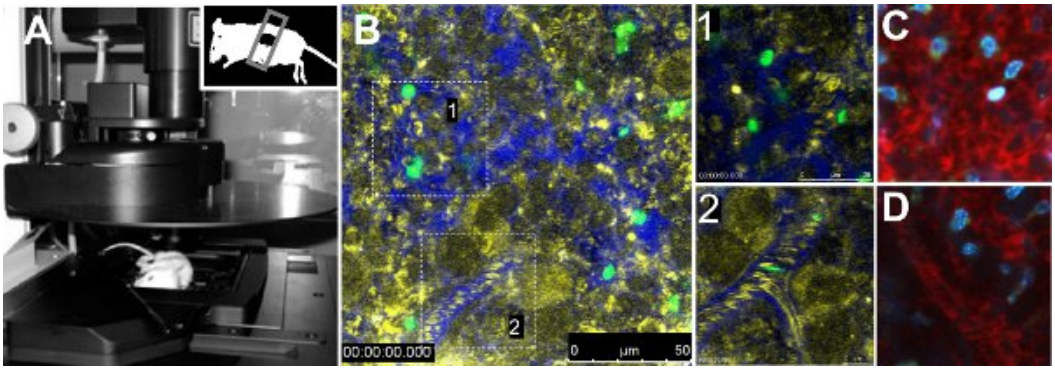

Figure 1. Intravital microscopy of the spleen. A. Leica TCS-SP5 confocal microscope with one mouse placed on the stage of the microscope. The mouse has the inferior part of the spleen exposed and sealed with a cover-slip. **B.** Image of a representative area of the spleen of a non-infected animal injected with FITC-labeled RBCs and 70 kDa Dextran- Texas Red to visualize the vasculature. Reflection (yellow), Dextran (blue) and FITC-RBCs (green) are shown. Blow-ups in white boxes represent open-circulation (1) and close-circulation (2) areas. Open-circulation **(C)** and close-circulation**(D)** stained with 70 kDa dextran (red) and Hoechst 33342 (blue).

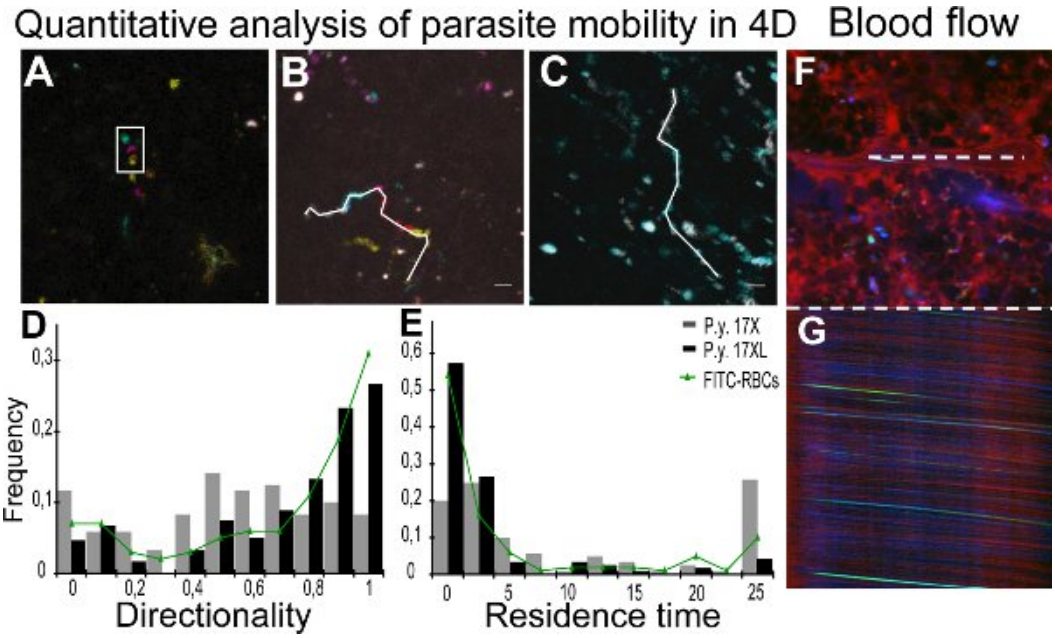

Figure 2. Quantification of parasite mobility and blood flow. **A-C**. Quantitative analysis of particle movement in the four dimensions (4D) is facilitated by using color-coded image processing. **A.** Tracking was performed with the depth information from Z-coded color images, represented using maximum intensity projection of five different depths. White rectangle represents the same particle at different Z in one time point. Different positions are due to time lapses between the acquisition of different Z images. Depth code: yellow (0 µm), orange (2 µm), pink (4 µm), blue (6 µm), green (8 µm). **B, C.** Time projections of particle movement with each time interval coloured as: gray (0-2.4 sec), cyan (2.4-4.8 sec), magenta (4.8-7.0 sec), red (7.0-9.4 sec) and yellow (9.4-11.8 sec). White line represents 4D manual tracking of particles of 17X (11.8 s) **(B)** and 17XL (4.8 sec) **(C)** GFP parasites using MTrackJ. **D,E.** Distribution of the density of GFP particles by values of directionality **(D)** and residence time **(E)**. Data correspond to 120 particles of each line of parasites and 100 FITC-labeled RBCs from three independent experiments analysed with the equality-of-medians test. The 17X/17XL/FITC-RBCs medians are 0.53/0.75/0.85 **(D)** and 4.61/0.67/0.9 sec **(E).** Differences between the two lines in **(D)** and **(E)** are statistically significant ($P < 0.001$). Differences between FITC-labeled RBCs and 17XL parasites are not statistically significant ($P > 0.05$). **F,G.** Spleen blood flow measurements. Representation of xy image **(F)** and xt image **(G)** from a line-scan of the central lumen of the same vessel (white line). Spleen vessel showing plasma with 70 kDa dextran (red), pRBC (green) and erythrocyte reflection (blue).

Movies 1 and 2. Time-lapse intravital microscopy images of the murine spleen infected with 17XL **(1)** or 17X **(2)** GFP-transgenic parasites at 10% parasitemia (Z-maximum projection). Parasite and tissue autofluorescence are shown in green and red respectively. Scale bars represent 10 µm and the time interval is in sec.
Click here to watch Movie 1.
Click here to watch Movie 2.

Discussion

The implementation of intravital microscopy of the spleen in this rodent malaria model opened the possibility of investigating the dynamic passage of parasites through this organ which until now has been considered a "black-box" due to technical considerations. In here, a major effort was put to adapt a quantitative method that allows comparative analysis of different parasite lines at the single and population levels. In contrast to other tissues and cells that had been imaged before in malaria [3,5], imaging the passage of pRBCs through the spleen needs to take into consideration the three-dimensionality and compartmentalization of the organ, the presence of different circulations with fast and slow flux [13], as well as the rapid erythrocyte velocities. With this aim, a specific methodology using online available ImageJ software was developed to enable single parasite

tracking, mobility analysis and comparison between lines at the population level. However, the application of automatic software that solves identification and tracking of single parasites in this context is still needed. Of note, the parameters used to describe parasite mobility have been previously described in other studies to report lymphocyte recruitment and adhesion in vivo [12,14,15]. Thus, this methodology and parameters should be considered a new tool to the in vivo studies of adherence in malaria. In the future, we will use this technology to gain insight into the immunobiology and parasite-spleen cell interactions by imaging infection in transgenic mice expressing fluorescent reporter genes in different cells. Moreover, the generation of transgenic parasites expressing fluorescent markers other than GFP may be used in combination to image dual infections in this model.

In vivo imaging is a powerful tool to study the dynamic interplay of parasites within their hosts. However, there exist several factors affecting cell mobility that must be taken into consideration. Changes in the tissue architecture in response to infection with different *Plasmodium* strains can modify cell passage and interaction with the tissue [7,16] and the rheological properties of red blood cells, as well as changes in the hematocrit or other hematologic parameters, can affect blood flow and hence the interaction of cells with the tissue. For this reason, we recommend to analyze vessel blood flow with the procedure provided. To avoid any confounding effects, we imaged the spleen of infected mice at a time point when hematocrit, reticulocytemia and parasite tropism is comparable in both infections [7].

The resolution of this technique allows for the observation of single fluorescent cells passing through the spleen at earlier time points (<1% parasitemia). However, quantitative analysis of the dynamic behavior of parasites was performed at 1% parasitemia, when sufficient numbers of pRBCs were observed passing through the spleen at time lapses that allow tracking of single cell movement. In movies 1 and 2, which correspond to animals at 10% parasitemia, we showed the general pattern of parasite passage through the spleen in each infection; however, quantitative analysis of moving cells was performed in movies from animals at 1% parasitemia, where single cells are easily followed. Due to the rapid three-dimensional movement of infected red blood cells, we couldn't differentiate between developmental stages of the parasite, as different fluorescence intensities could be attributed to different depths or penetrability of the laser.

With this procedure, fluorescent cells can be visualized in the subcapsular zone of the spleen, composed mainly of red pulp [17]. By using plasma dyes, we could discern between the fast/closed and slow/open circulations of the red pulp. Other studies have reported imaging of fluorescent T-cells in the white pulp using confocal [18] or two-photon microscopy [19], with the last offering greater tissue penetration. In those, off-line analysis and ex vivo characterization of the zone being imaged is an important factor to accurately interpret the data. Thus, efforts to enlighten the microcirculatory structure of the spleen, as well as the development of probes that label specific cells and structures, are of importance to facilitate the study of parasite-host interactions.

Disclosures

No conflicts of interest declared.

Acknowledgements

We are particularly grateful to S. Graewe and V. Heussler for the initial training and continuous input in intravital microscopy of malaria parasites, to J. Burns for donating GFP transgenic parasites, to A. Bosch (Confocal Unit, CCiT-UB, IDIBAPS) for assistance in image analysis and quantification and to P. Astola for technical assistance. We thank R. Tous and I. Caralt for video production. MF is a recipient of a graduate fellowship from the Generality of Catalonia. HAP is an ICREA research professor. Work in the laboratory of HAP is funded by the European Community's Seventh Framework Programme (FP7/2007-2013) under grant agreement N° 242095, by the Private Foundation CELLEX (Catalonia, Spain), and by the Spanish Ministry of Science and Innovation (SAF2009-07760).

References

1. Amino, R., Menard, R., Frischknecht, F. In vivo imaging of malaria parasites--recent advances and future directions. *Curr Opin Microbiol* 2005, **8:** 407-414.
2. Heussler, V. & Doerig, C. In vivo imaging enters parasitology. *Trends Parasitol* 2006, **22:** 192-195.
3. Amino, R., Thiberge, S., Blazquez, S., Baldacci, P., Renaud, O., Shorte, S. *et al*. Imaging malaria sporozoites in the dermis of the mammalian host. *Nat Protoc* 2007, **2:** 1705-1712.
4. Gueirard, P., Tavares, J., Thiberge, S., Bernex, F., Ishino, T., Milon G. *et al*. Development of the malaria parasite in the skin of the mammalian host. *Proc Natl Acad Sci U S A* 2010, **107:** 18640-18645.
5. Sturm, A., Amino, R., van de Sand, C., Regen, T., Retzlaff, S., Rennenberg, A. *et al*. Manipulation of host hepatocytes by the malaria parasite for delivery into liver sinusoids. *Science* 2006, **313:** 1287-1290.
6. Gruring, C., Heiber, A., Kruse, F., Ungefehr, J., Gilberger, T.W. & Spielmann, T. Development and host cell modifications of Plasmodium falciparum blood stages in four dimensions. *Nat Commun* 2011, **2:** 165.
7. Martin-Jaular, L., Ferrer, M., Calvo, M., Rosanas-Urgell, A., Kalko, S., Graewe, S. *et al*. Strain-specific spleen remodelling in Plasmodium yoelii infections in Balb/c mice facilitates adherence and spleen macrophage-clearance escape. *Cell Microbiol* 2011, **13:** 109-122.
8. Franke-Fayard, B., Trueman, H., Ramesar, J., Mendoza, J., van der Keur. M., van der Linden, R. *et al*. A Plasmodium berghei reference line that constitutively expresses GFP at a high level throughout the complete life cycle. *Mol Biochem Parasitol* 2004, **137:** 23-33.
9. Cormack, B.P., Valdivia, R.H. & Falkow, S. FACS-optimized mutants of the green fluorescent protein (GFP). *Gene* 1996, **173:** 33-38.
10. Dunn, K.W., Sandoval, R.M., Kelly, K.J., Dagher, P.C., Tanner, G.A., Atkinson, S.J. *et al*. Functional studies of the kidney of living animals using multicolor two-photon microscopy. *Am J Physiol Cell Physiol* 2002, **283:** C905-C916.
11. Zhong, Z., Petrig, B.L., Qi, X., Burns, S.A. In vivo measurement of erythrocyte velocity and retinal blood flow using adaptive optics scanning laser ophthalmoscopy. *Opt Express* 2008, **16:** 12746-12756.
12. Miller, M.J., Wei, S.H., Parker, I. & Cahalan, M.D. Two-photon imaging of lymphocyte motility and antigen response in intact lymph node. *Science* 2002, **296:** 1869-1873.
13. Bowdler, A.J. The complete spleen. 2002. Totowa: Humana Press. Ref Type: Edited Book
14. Grayson, M.H., Hotchkiss, R.S., Karl, I.E., Holtzman, M.J. & Chaplin D.D. Intravital microscopy comparing T lymphocyte trafficking to the spleen and the mesenteric lymph node. *Am J Physiol Heart Circ Physiol* 2003, **284:** H2213-H2226.
15. Khandoga, A.G., Khandoga, A., Reichel, C.A., Bihari, P., Rehberg, M. & Krombach, F. In vivo imaging and quantitative analysis of leukocyte directional migration and polarization in inflamed tissue. *PLoS One* 2009, **4:** e4693.

16. Weiss, L., Geduldig, U., & Weidanz, W. Mechanisms of splenic control of murine malaria: reticular cell activation and the development of a blood-spleen barrier. *Am J Anat* 1986, **176:** 251-285.
17. Swirski, F.K., Nahrendorf, M., Etzrodt, M., Wildgruber, M., Cortez-Retamozo, V., Panizzi, P. *et al*. Identification of splenic reservoir monocytes and their deployment to inflammatory sites. *Science* 2009, **325:** 612-616.
18. Grayson, M.H., Chaplin, D.D., Karl, I.E., Hotchkiss, R.S. Confocal fluorescent intravital microscopy of the murine spleen. *J Immunol Methods* 2001, **256:** 55-63.
19. Bajenoff, M., Glaichenhaus, N., Germain, R.N. Fibroblastic reticular cells guide T lymphocyte entry into and migration within the splenic T cell zone. *J Immunol* 2008, **181:** 3947-3954.

6.2 *Strain-specific spleen remodelling in* Plasmodium yoelii *infections in Balb/c mice facilitates adherence and spleen macrophage-clearance escape*

6.2.1 Summary

Objectives

To use the rodent malaria model of Balb/c mice infected with the reticulocyte-prone non-lethal *P. yoelii* 17X strain and the normocyte-prone lethal *P. yoelii* 17XL strain to elucidate the mechanism involved in spleen-clearance escape of the non-lethal strain.

Results

1. Significantly higher numbers of *P. yoelii* 17X as compared to *P. yoelii* 17XL were found in the red pulp of the spleen, which could not be explained by higher macrophage uptake.
2. Real-time *in vivo* imaging of GFP transgenic *P. yoelii* parasites in the spleen of *Balb/c* mice revealed reduced motility, lack of directionality and increased residence time in the non-lethal strain, while spleen closure and spleen blood flow were similar in both infections. These parameters reveal *in vivo* adherence of the *P. yoelii* 17X line to spleen cells.
3. Visualization of *P. yoelii* 17X infected spleens under electron microscopy suggests adhesion of pRBCs to barrier cells. *In vitro* adhesion of pRBCs to spleen-derived fibrocytic cells was also reported.
4. Global expression analyses of spleens from mice experimentally infected with *P. yoelii* has identified putative molecular markers of barrier cells from fibroblast origin. Expression of fibroblast growth factor 8 (FGF8) associates with the formation of a spleen tissue barrier in infections with 17X parasites. Laser confocal microscopy of the spleen of Balb/c mice infected with *P. yoelii* 17X confirms the existence of a tissue barrier as originally proposed by L. Weiss.
5. MRI confirms differential remodelling of the spleen in the 17X strain.

6.2.2 Article 2

VOLUME 13 NUMBER 1 JANUARY 2011 www.cell-micro.com ISSN 1462-5822

cellular microbiology

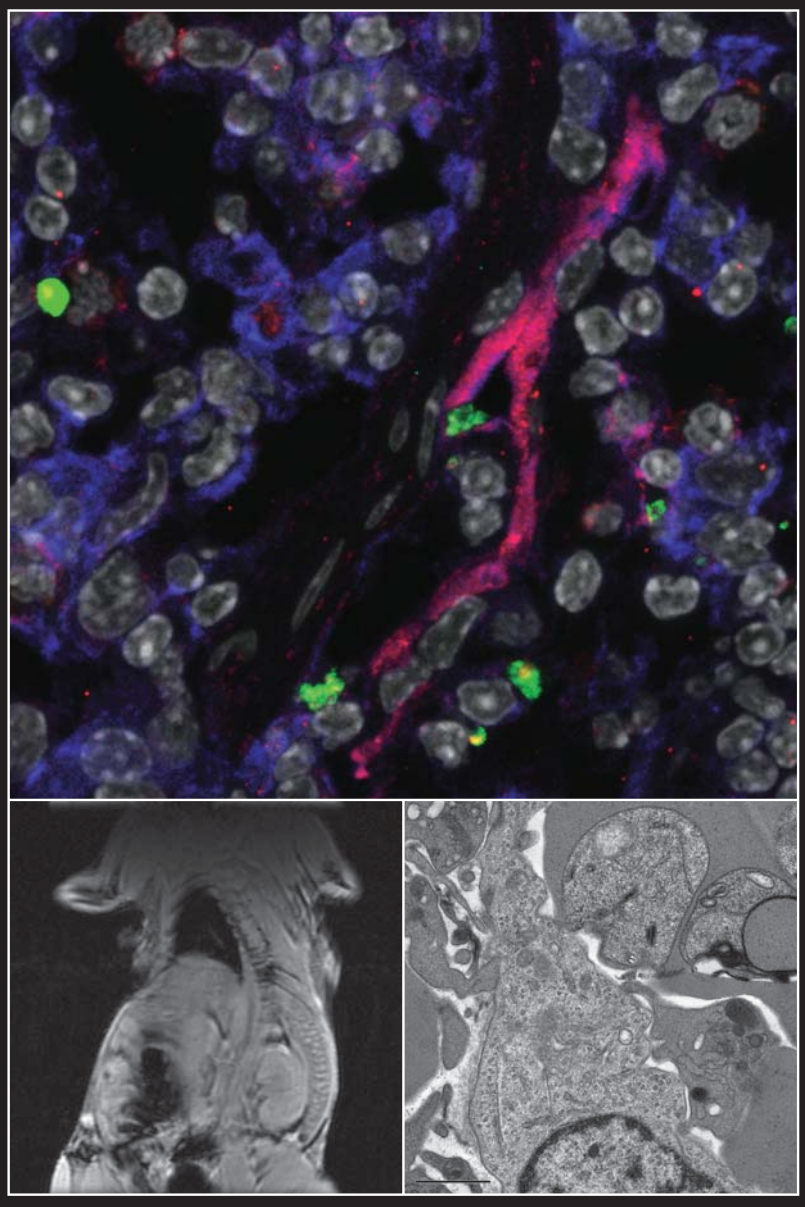

Thematic reviews:
Exosomes

Human papillomavirus infection

Endocytosis and toxicity

WILEY-BLACKWELL 59

Cellular Microbiology (2011) **13**(1), 109–122
doi:10.1111/j.1462-5822.2010.01523.x
First published online 1 October 2010

Strain-specific spleen remodelling in *Plasmodium yoelii* infections in Balb/c mice facilitates adherence and spleen macrophage-clearance escape

Lorena Martin-Jaular,[1†] Mireia Ferrer,[1†] Maria Calvo,[2] Anna Rosanas-Urgell,[1] Susana Kalko,[3] Stefanie Graewe,[4] Guadalupe Soria,[5,6] Núria Cortadellas,[7] Jaume Ordi,[8] Anna Planas,[5,6] James Burns,[9] Volker Heussler[4] and Hernando A. del Portillo[1,10*]

[1]*Barcelona Centre for International Health Research, Barcelona, Spain.*
[2]*Unitat de Microscòpia Confocal, Serveis Cientificotècnics, Facultat de Medicina, Universitat de Barcelona- IDIBAPS, Barcelona, Spain.*
[3]*Bioinformatics Unit, IDIBAPS, Hospital Clinic, Barcelona, Spain.*
[4]*Bernhard Nocht Institute for Tropical Medicine, Department of Molecular Parasitology, Malaria laboratory, Hamburg, Germany.*
[5]*Department of Brain Ischemia and Neurodegeneration, Institut d'Investigacions Biomèdiques de Barcelona (IIBB)-Consejo Superior de Investigaciones Científicas (CSIC), Institut d'Investigacions Biomèdiques August Pi i Sunyer (IDIBAPS), Barcelona, Spain.*
[6]*Unitat de Ressonància Magnètica Experimental, Plataforma d'Imatge, IDIBAPS, Barcelona, Spain.*
[7]*Unitat de Microscòpia Electrònica, Serveis Cientificotècnics, Facultat de Medicina, Universitat de Barcelona- IDIBAPS, Barcelona, Spain.*
[8]*Department of Anatomical Pathology, Hospital Clinic, Barcelona, Spain.*
[9]*Department of Microbiology and Immunology, Drexell University Medical College, Queen Lane, PA, USA.*
[10]*Institució Catalana de Recerca i Estudis Avançats (ICREA), Barcelona, Spain.*

Summary

Knowledge of the dynamic features of the processes driven by malaria parasites in the spleen is lacking. To gain insight into the function and structure of the spleen in malaria, we have implemented intravital microscopy and magnetic resonance imaging of the mouse spleen in experimental infections with non-lethal (17X) and lethal (17XL) *Plasmodium yoelii* strains. Noticeably, there was higher parasite accumulation, reduced motility, loss of directionality, increased residence time and altered magnetic resonance only in the spleens of mice infected with 17X. Moreover, these differences were associated with the formation of a strain-specific induced spleen tissue barrier of fibroblastic origin, with red pulp macrophage-clearance evasion and with adherence of infected red blood cells to this barrier. Our data suggest that in this reticulocyte-prone non-lethal rodent malaria model, passage through the spleen is different from what is known in other *Plasmodium* species and open new avenues for functional/structural studies of this lymphoid organ in malaria.

Introduction

The spleen is a complex organ that is perfectly adapted to selectively filtering and destroying senescent red blood cells (RBCs), infectious microorganisms and *Plasmodium*-infected RBCs (pRBCs) (Bowdler, 2002). Such filtering capacity is related to the complex structure of the spleen as it consists of a trabecular complex structure formed by: (i) the white pulp, lymphoid tissue containing the majority of immune effector cells, (ii) the red pulp, a reticular meshwork where destruction of senescent, aberrant RBCs and pRBCs occurs and (iii) a marginal zone lying between the white pulp and the red pulp, where inert particles, bacteria and viruses are eliminated. In addition, blood enters the spleen through a central artery that branches into capillaries, most of which empty into the filtration beds of the red pulp before reaching the venous system in a so-called open system. The spleen is therefore a complex organ whose 3D structure consists of distinct microanatomical zones exquisitely adapted to performing different functions.

The *Plasmodium yoelii* rodent model has been extensively used to study molecular aspects of virulence in

Received 7 July, 2010; revised 25 August, 2010; accepted 25 August, 2010. *For correspondence. E-mail hernandoa.delportillo@cresib.cat; Tel. +34 690737229; Fax +34 932271850.
†These two authors contributed equally to this work.

malaria mainly because of the existence of strains with different cellular tropisms, growth curves and clinical outcomes, such as the reticulocyte-prone non-lethal *P. yoelii* 17X strain and the normocyte-prone lethal *P. yoelii* 17XL strain (Pattaradilokrat *et al*., 2008). Noticeably, in experimental infections of Balb/c mice with the *P. yoelii* 17X strain, the open circulation of the spleen is temporarily changed to a closed circulation with the formation of syncytial layers of fibroblasts that form physical barriers, termed barrier cells (Weiss *et al*., 1986). Closing of the circulation was demonstrated by the absence of carbon particles in red pulp filtration beds following injection of infected mice during precrisis (a period of increasing parasitaemia). Precrisis was also characterized by intense spleen erythropoiesis and it was thus proposed that barriers cells protect immature RBCs from destruction by parasites before maturation and release into circulation to compensate for the anaemia caused by these experimental infections. In striking contrast, barrier cell-dependent remodelling did not occur in infections with the *P. yoelii* 17XL strain in Balb/c mice (Weiss *et al*., 1986).

Several promising methodologies have been developed enabling intravital and magnetic resonance imaging (MRI) of cells within their *in vivo* tissue environment in malaria (Amino *et al*., 2006; Heussler and Doerig, 2006; Sturm *et al*., 2006; Penet *et al*., 2007). We have implemented these techniques to address the dynamic features of the passage of *P. yoelii* 17X and 17XL strains through the spleen of Balb/c mice and have revisited global transcriptional analysis and histopathology of this organ in these experimental infections. Our data demonstrate that *P. yoelii* 17X induces a spleen blood barrier of fibroblastic origin to which infected reticulocytes adhere facilitating macrophage-clearance escape.

Results

Construction and characterization of P. yoelii *17X and 17XL clonal lines expressing green fluorescent protein (GFP)*

To implement intravital imaging, transgenic lines of the *P. yoelii* 17X and 17XL strains expressing the mutant 3 variant of GFP from *Aequorea victoria* were constructed (JB), using the vector and conditions previously described in *Plasmodium berghei* (Franke-Fayard *et al*., 2004). Analysis of GFP transgenic parasites revealed that GFP expression did not alter growth curves and tropism when compared with the original strains (Fig. S1). Clonal transgenic lines from 17X and 17XL were obtained through standard methodologies and used throughout this study.

Red pulp from spleens of animals infected with 17X contains a significantly higher number of parasites than red pulp from animals infected with 17XL

To investigate early spleen events (3–4 days post infection, p.i.) following the induction but not the complete formation of a spleen blood barrier of fibroblastic origin (Weiss *et al*., 1986), when no confounding effects are observed as a result of the complexity of infection in this model (Table 1), we performed immunohistofluorescence analysis of cryosections of spleens stained with anti-GFP antibody. Noticeably, quantification of GFP parasites in the red pulp of the spleen showed a 3.8-fold increase in 17X parasites compared with 17XL parasites on day 3 p.i. (Fig. 1A–C). Comparable results were obtained in cryosections of spleens stained with Giemsa and visualized under polarized light microscopy, which detects parasites because of the refringent properties of haemozoin (Fig. S2). Similar quantification of 17X and 17XL parasites

Table 1. Balb/c – GFP *P. yoelii* 17X *and* 17XL murine malaria model.

Day p.i.	3				4			
Line	L-GFP	L	NL-GFP	NL	L-GFP	L	NL-GFP	NL
Parasitaemia (%)	1.1 ± 0.3	1.1 ± 0.2	1.1 ± 0.2	1.1 ± 0.2	9.9 ± 1.4	10.3 ± 0.4	9.2 ± 0.6	9.8 ± 0.2
Reticulocytemia (%)	2.7 ± 0.4	2.9 ± 0.7	2.5 ± 0.4	2.8 ± 0.5	2.3 ± 0.3	2.4 ± 0.5	2.9 ± 0.5	2.7 ± 0.3
pRet/pRBCs (%)	60.0 ± 9.1	62.8 ± 4.6	69.2 ± 9.5	72.7 ± 5.8	23.4 ± 5.1	24.7 ± 4.0	32.2 ± 10.0	38.0 ± 14.6
ring/pRBCs (%)	31.4		30.8		39.2		31.8	
troph/pRBCs (%)	64.7		62.7		57.3		63.5	
sch/pRBCs (%)	3.9		6.7		3.4		4.8	
S. w. (g)	0.1 ± 0.0	0.1 ± 0.0	0.1 ± 0.0	0.1 ± 0.0	0.3 ± 0.0	0.3 ± 0.0	0.3 ± 0.0	2.2 ± 0.0
RP/WP	2.3 ± 0.3		2.0 ± 0.2		0.8 ± 0.2		0.8 ± 0.1	

Different parameters were calculated in Balb/c mice infected with wild-type and transgenic parasites on days 3 and 4 p.i. when all experiments were done. Parasitaemias were calculated in groups of 12 animals. Reticulocytemia and percentage of parasitized reticulocytes (pRet) were measured in at least six mice per group. Percentages of asexual forms [rings, trophozoites (troph) and schizonts (sch)] were assessed in four mice per group counting at least 250 pRBCs per animal. Spleen weight (S.w.) and ratio of red pulp to white pulp area (RP/WP) were measured in 3–4 animals per group. The results are expressed as mean ± SEM. Statistical analysis was used to compare differences between the lethal and non-lethal group on those days, with no significant differences found.

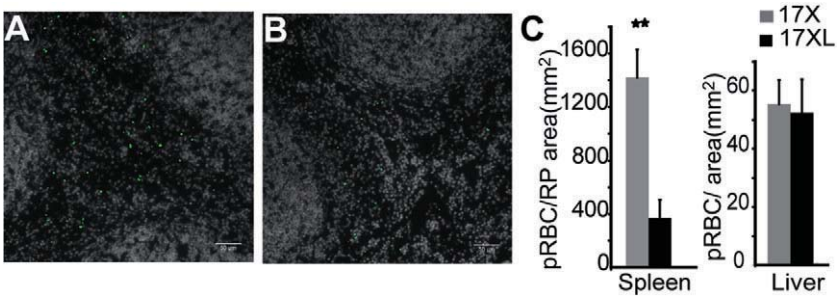

Fig. 1. Increased retention of *P. yoelii* 17X GFP parasites in the red pulp of the spleen.
A, B. Wide-field fluorescence microscopy images of GFP transgenic parasites (green) and nucleic acids (gray) on immunostained cryosections of the spleen of mice infected with 17X (A) or 17XL (B) parasites on day 3 p.i., corresponding to 1% peripheral parasitaemia. pRBCs accumulate in the red pulp, the area with less density of nuclei. Scale bars represent 50 μm.
C. Quantification of parasite retention in the red pulp of the spleen and the liver in selected areas of 0.2 mm^2 and 0.4 mm^2, respectively, expressed as number of particles per area (pRBC mm^{-2}). Values are the mean ± SEM of four mice (analysed with Student's *t*-test). Differences are statistically significant (**$P < 0.01$).

in cryosections of the liver (Fig. 1C) revealed no differences in numbers, indicating that the higher 17X parasite retention was specific to the red pulp of the spleen.

Differences in parasite load in the red pulp of the spleen cannot be explained by macrophage activity

The differences observed in the accumulation of parasites in the red pulp of the spleen during experimental infections with *P. yoelii* 17X and 17XL could be due to differences in parasite engulfment by macrophages or other phagocytic cells. In order to test this hypothesis, Balb/c mice were infected with the *P. yoelii* GFP transgenic lines. Thereafter, splenocytes were stained with F4/80 antibody specific for red pulp macrophages and analysed by flow cytometry (Fig. 2A). The number of macrophages containing parasites was calculated as the percentage of $F4/80^+GFP^+$ cells as a function of $F4/80^+$ cells. As we could not determine numbers of double-positive cells on day 3 p.i. as a result of the scarcity of $F4/80^+GFP^+$ cells, we performed the test on day 4 p.i., when there were still higher numbers of non-lethal parasites in the spleens of infected mice (13.83 ± 1.64% for 17X and 9.90 ± 0.19% for 17XL; $P = 0.0160$). Phenotypic analysis of splenocytes revealed higher proportions of $F4/80^+GFP^+$ cells in animals infected with 17XL than in those infected with 17X (Fig. 2A), even though the non-lethal strain had higher numbers of parasites and $F4/80^+$ macrophages in infections (12.5 ± 1.99% of spleen cells for 17X and 6.64 ± 1.46% of spleen cells for 17XL; $P = 0.0452$). Of note, there was a pool of unidentified $F4/80^-GFP^+$ phagocytic cells in both parasite lines; because there were no

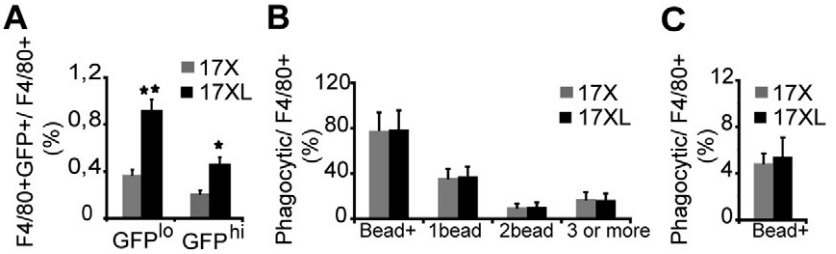

Fig. 2. Flow cytometry analysis of red pulp macrophage activity on day 4 p.i.
A. Splenocytes of mice infected with 17X and 17XL GFP transgenic parasites were labelled with an Alexa Fluor 647 conjugated antibody against F4/80 and analysed in a FacsCANTO flow cytometer. The gate was set to exclude debris and pRBCs. Percentages of $F4/80^-/GFP^+$ cells were 1.75 ± 0.26 for 17XL and 1.62 ± 0.29 in the 17X. No statistically significant differences were found between the two groups ($n = 7$ per group) (Student's *t*-test). $F4/80^+GFP^+$ cells were gated into two populations according to differences in GFP intensity. The mean ± SEM of GFP fluorescence of GFP^{lo}/GFP^{hi} populations was 1480.39 ± 36.52/13 961.70 ± 66 for 17X and 1503.86 ± 48.17/12 730.85 ± 407.79 for 17XL. Quantification of the percentage of $F4/80^+GFP^{lo}$ and $F4/80^+GFP^{hi}$ cells is expressed as the mean ± SEM of six independent experiments (analysed with Student's *t*-test). Differences are statistically significant (*$P < 0.05$, **$P < 0.01$).
B, C. Phagocytic activity measurements using fluorescent beads in $F4/80^+$ spleen cells of mice infected with 17XL and 17X wild-type parasites.
B. The percentage of macrophages obtained from infected spleens that had ingested *in vitro* one, two or three or more beads was calculated as a function of $F4/80^+$ cells. After 1 h, around 78% of macrophages in both groups had ingested the fluorescent beads.
C. Percentage of F4/80 cells that had incorporated fluorescent beads after *in vivo* i.v. injection.
B, C. Mean ± SEM is shown ($n = 6$–7). No significant differences were observed between the lethal and non-lethal groups.

significant differences in numbers with respect to total spleen cells, we did not investigate these further.

To evaluate the possibility that the differences detected might have been due to distinct phagocytic capacities of F4/80 cells, we determined the uptake of fluorescent beads by these cells. We demonstrated that the phagocytic capacity of spleen macrophages obtained from infections with 17X and 17XL was not significantly different either *in vitro* (Fig. 2C) or *in vivo* (Fig. 2D). These results exclude differences in engulfment by macrophages as the cause of the higher numbers of 17X parasites observed in the red pulp of the spleen.

Spleen closure and spleen blood flow are similar in infections with 17X and 17XL

Differences in spleen closure and blood flow could have also been responsible for differential input of pRBCs to the red pulp and for altering the chances of interaction with spleen cells. To determine whether the higher retention of parasites in the spleen of Balb/c mice infected with 17X was due to differences in spleen closure, we analysed the uptake capacity *in vivo* of 3 μm fluorescent beads. No differences were observed in the trapping capacity of the spleen of mice infected with either 17X or 17XL parasites at this early time p.i. (Fig. S3). To discard differences in spleen blood flow, we implemented intravital imaging of the spleen in malaria. Thus, mice were anaesthetized and their spleens exposed and visualized under a high-speed multiphoton confocal microscope fitted with an inverted 63x glycerol objective (Movie S1). Intravital microscopy of spleen vessels with different diameters (6–17 μm) was optimized to perform a line-scan image of the centre of the vessels (Fig. 3A and B). Volumetric blood flow was calculated from pRBC and RBC velocity based on the slope of fluorescent streaks (Zhong *et al.*, 2008). No differences in spleen blood flow were observed between 17X- and 17XL-infected mice (Fig. 3C). In addition, the values were not significantly different from spleen blood flow in uninfected mice injected with FITC-labelled RBCs (28.4 ± 4.5 μl s^{-1}, ANOVA $P = 0.2625$).

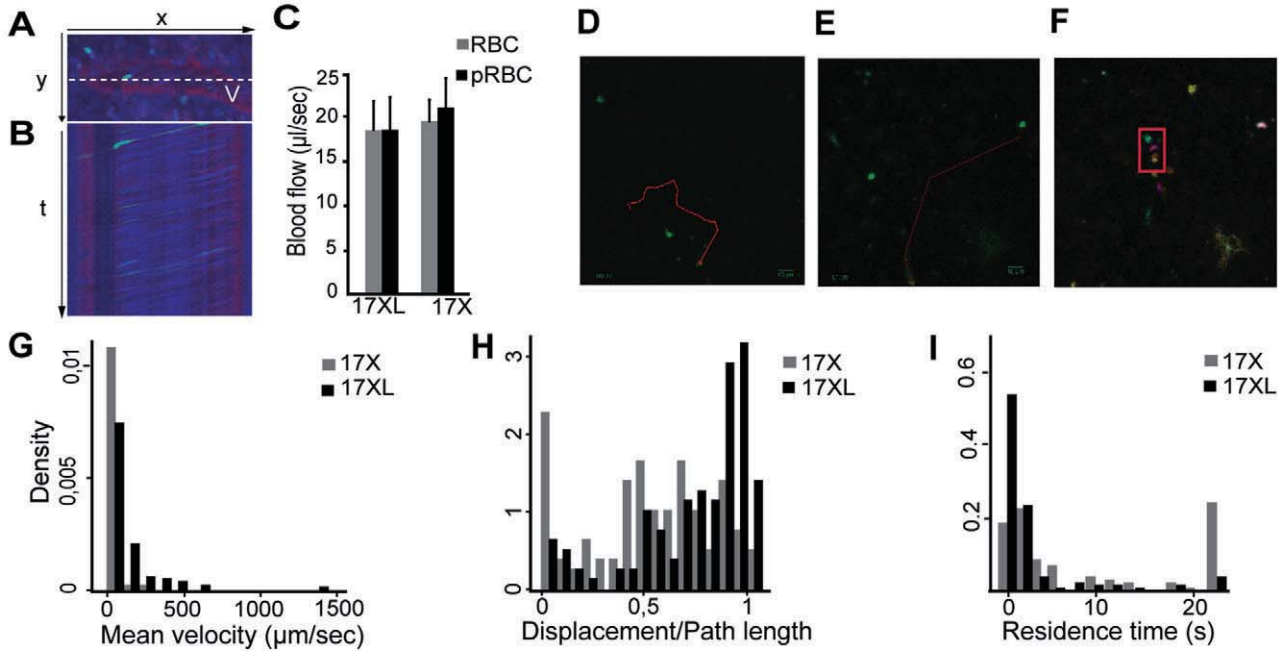

Fig. 3. Intravital imaging of GFP parasites in the spleen.
A, B, C. Spleen blood flow measurements. Representation of xy image (A) and xt image (B) from a line-scan of the central lumen of the same vessel (white line). Spleen vessel (V) showing plasma with 70 kDa dextran (red), pRBC (green) and erythrocyte reflection (blue).
C. Volumetric blood flow quantification from pRBCs and surrounding RBCs in spleens infected with both lines. Data are expressed as the mean ± SEM (μl s^{-1}) of three mice infected with each line at 1% parasitaemia (day 3 p.i.), considering vessels of different sizes (6–17 μm diameter) at different phases of the cardiac cycle. No significant differences were observed.
D, E, F. Images representing maximum intensity projection of five different depths (Z) at one time point. Red line represents 4D manual tracking of particles of 17X (11.8 s) (D) and 17XL (2.2 s) (E) GFP parasites using MTrackJ. Tracking was performed with the depth information from Z-coded colour stacks (F). Depth code: yellow (0 μm), orange (2 μm), pink (4 μm), blue (6 μm), green (8 μm). The box shows movement in z-axis of the same particle. Distribution of GFP particles by mean velocity (G), directionality (H) and residence time (I). Data correspond to 120 particles of each line from three independent experiments analysed with the equality-of-medians test. The 17X/17XL medians are 22.58/103.95 μm s^{-1} (G), 0.53/0.75 (H) and 4.61/0.67 s (I). Differences between the two lines in (G) (H) and (I) are statistically significant ($P < 0.001$). The location of the particles quantified is comparable in both lines: 52.5% of 17X and 51.67% of 17XL outside vessels, 17.5% of 17X and 15.83% of 17XL in vessels with a diameter < 10 μm and 29.17% of 17X and 32.5% of 17XL in vessels with a diameter > 10 μm.

Intravital imaging of the spleen revealed adherence of the P. yoelii *17X line*

Having excluded differences in engulfment by macrophages, spleen closure and spleen blood flow as reasonable explanations for the significantly higher numbers of 17X than 17XL parasites observed in the red pulp of the spleen, we aimed to characterize the dynamic behaviour of these parasites and to quantify their mobility within the spleen. These parameters have been recently used to demonstrate *in vivo* adherence, as opposed to mechanical trapping, of lymphocytes entering lymph nodes. To detect GFP parasites, images at five different depths per stack were acquired during 1.5 min with a velocity of 0.3 s per stack in spleens from mice with 17X and 17XL infections at 1% and 10% parasitaemia representing, respectively, days 3 and 4 p.i. (Movies S2 and S3). Moreover, control animals injected with FITC-labelled RBCs were used to characterize the movement of these cells in normal spleens. Different parameters to describe particle movement were quantified by 3D manual tracking with the help of Z-coded colour stacks to provide depth information (Fig. 3D–F and Movie S4). Quantitative analysis was performed using images from mice infected with both lines of parasites on day 3 p.i, corresponding to 1% parasitaemia. Under these conditions, individual particles are easily followed. Uninfected mice were injected with the necessary amount of labelled RBCs to achieve the same percentage of fluorescent cells. Noticeably, the mean velocity of 17X parasites was significantly lower than that of 17XL parasites ($P < 0.001$) (Fig. 3G). Moreover, pRBCs in the vessels had the same velocity as surrounding RBCs visualized by reflection (Fig. 3C), suggesting differences in velocity of movement outside the vessels. In addition, 17X parasites showed a loss of directionality with respect to 17XL parasites, as evidenced by the distribution of particle population by distance versus path length ($P < 0.001$) (Fig. 3H). The lack of directionality was accompanied by an increase in the residence time of parasites in a given area of the spleen. Indeed, the median time in which a parasite appeared was 6.83 times higher for non-lethal parasites than for lethal parasites ($P < 0.001$) (Fig. 3I). Of note, the number of parasites from the non-lethal strain that remained in the spleen for more than 20 s was 6.4 times higher than that of lethal parasites. When we analysed the same parameters for FITC-labelled RBCs, we found no significant differences to those obtained for particles from the 17XL *P. yoelii* parasites ($P > 0.05$) (Fig. S4). Of importance, *in vivo* images of the passage of the non-lethal strain showed an adhesive, rolling-circle behaviour of pRBCs in real time, further suggesting that these changes in motility were due to adherence and not to retention by spleen cells (Movies S5 and S6).

In vitro *adherence of pRBCs to spleen-derived fibrocytic cells and transmission electron microscopy further indicate adherence to the spleen*

To seek further evidence of adherence of pRBCs infected with 17X parasites in the spleen of Balb/c mice, we isolated splenocytes and cultured them in conditions where adherent cells were mostly fibrocytic splenocytes (Borrello and Phipps, 1996). Significantly, pRBCs infected with 17X on day 4 p.i. showed a 2.7-fold higher adhesion rate to fibrocytic splenocytes than those infected with 17XL ($P < 0.05$). Similar results (fourfold increase, $P < 0.05$) were obtained from adhesion assays using the immortalized cell line of fibroblastic origin 3T3/NIH, showing further evidence of the adherence capacity of RBCs infected with the *P. yoelii* 17X strain (Fig. 4A). Moreover, transmission electron microscope (TEM) images of spleens after infection with 17X showed pRBCs in close contact with longitudinal structures of fibroblastic cells that shared morphological features with those described in spleen barrier cells (Weiss *et al.*, 1986) (Fig. 4B and C). This

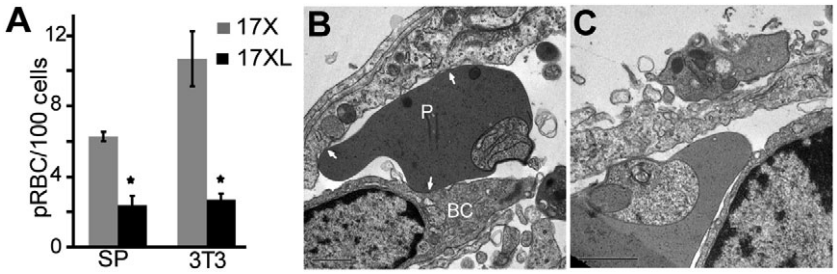

Fig. 4. Adhesion of *P. yoelii* 17X pRBCs to fibroblastic cells.
A. *In vitro* adhesion assays of 17X and 17XL pRBCs on cultured fibrocytic splenocytes (SP) and 3T3/NIH fibroblasts. Experiments were performed in duplicate and data expressed as the mean number of pRBC ± SEM per 100 cells. Differences are statistically significant (*$P < 0.05$).
B, C. Ultramicrographs of the spleen of mice infected with the non-lethal line at 1% parasitaemia. pRBCs (P) were found in close contact with elongated fibroblastic structures corresponding to barrier cells (BCs). Adhesion of pRBCs to tissue BCs was evidenced by points of P membrane deformability and close interaction with BC membrane, indicated by arrows. Scale bars represent 1 μm.

phenomenon was not observed in TEM analysis of spleens from animals infected with 17XL. Together, intravital imaging, *in vitro* adherence to fibrocytic cells and TEM results strongly suggest adherence of pRBCs to the spleen in this rodent malaria model.

Expression of fibroblast growth factor 8 (FGF8) associates with the formation of a spleen tissue barrier in infections with 17X parasites

The blood spleen barrier is formed by cells of fibroblastic origin (Weiss *et al*., 1986). We thus performed time-series global transcriptional analyses from spleens of mice infected with 17X and 17XL parasites on days 3, 4 and 5 p.i using commercially available arrays representing the complete mouse genome (Agilent Whole Mouse Genome G4122A). Initially, low-variance filtering of genes across each strain was performed and some relevant genes were identified and grouped into functional families, among which erythropoiesis, glycolysis and fibroblasts can be highlighted (all data deposited at GEO; accession number, GSE17603). Then, the five most variable fibroblast genes (from a total of 67 in this array) were extracted for each strain and between them. The most salient feature of gene expression values was that 17X had the largest variations throughout this time-course experiment (Fig. S5). Significantly, the gene encoding the mouse FGF8 was found to be the only gene in all three sets of genes with the largest variability (Fig. 5A). Accordingly, we decided to further analyse this particular gene and logFC values were validated by real-time polymerase chain reaction (PCR) analysis (Fig. 5B).

To determine whether FGF8 might be a molecular marker to the spleen tissue barrier, we used an anti-FGF8 murine polyclonal antibody for immunohistofluorescence analysis. Quadruple labelling of GFP-expressing parasites, FGF8, F4/80 red pulp macrophage receptor and nucleic acids was performed on time-series cryosections of the spleens of uninfected and mice infected with the non-lethal and lethal lines. Visualization under laser confocal microscopy revealed the existence of distinct FGF8-stained longitudinal structures only in the spleens of animals infected with 17X (Figs 5D and S6). Quantitative data in stained areas reflected increased expression of FGF8 over days 3, 4 and 5 p.i., which correlated with the percentage of non-lethal parasites found in association with FGF8-stained structures in the red pulp (Fig. 5C and E). Remarkably, 25% of the non-lethal parasites are associated to the FGF8-stained structure representing *c*. 3% of red pulp at day 5 p.i. In contrast, spleens of mice infected with 17XL showed the presence of small structures that did not develop into barriers. No specific staining was detected in liver or kidney sections from the same animals (Fig. S6), further demonstrating that expression of FGF8 is only associated with formation of this organ-specific tissue barrier. Moreover, studies using correlative microscopy to localize FGF8 at the ultrastructural level showed specific staining in the intercellular spaces surrounding barrier cells of spleen micrographs (Fig. 5F and G).

MRI confirms remodelling of the spleen in the 17X strain

Magnetic resonance imaging is a non-invasive technique that allows the study of the structural and functional features of tissues and organs. To determine whether or not MRI might also be of value in detecting structural differences in the spleens of mice infected with lethal and non-lethal lines of parasites, we measured spleen T2 relaxation times, which can provide accurate quantitative measurements to differentiate between normal and pathological tissues as well as information on cellularity and oedema (Oh *et al*., 2006). Noticeably, MRI of Balb/c spleens demonstrated a significant increase in T2 relaxation times in mice infected with the 17X strain compared with uninfected mice ($P < 0.05$) (Fig. 6A and B). In addition, the standard deviation of T2 relaxation times measured in the red and white pulp of mice infected with the 17X strain was almost twice as high as that of control mice and mice infected with the 17XL strain ($P < 0.01$), further indicating enhanced structural heterogeneity after infection with the non-lethal strain (Fig. 6C). None of these differences were observed in similar measurements of selected areas of muscle or kidney from the same animals (Fig. S7). These findings corroborate that only the *P. yoelii* 17X strain induces spleen remodelling.

Discussion

The spleen is exquisitely adapted to selectively clearing abnormal RBCs, particles from the blood and infectious agents including malaria. Because of ethical and technical constraints, however, functional studies of the spleen are very limited and none to date has addressed the dynamic features of the passage of the malaria parasite through this organ *in vivo*. In here, we used the Balb/c *P. yoelii* rodent malaria model to study the function and structure of the spleen using different techniques including intravital and MRI. Our findings support a model in which the reticulocyte-prone non-lethal *P. yoelii* 17X strain induces remodelling of the Balb/c spleen through the formation of a spleen blood barrier of fibroblastic origin where infected RBCs adhere and where macrophage-clearance escape is facilitated (Fig. 7, Movie S7).

The different phenotypes of the *P. yoelii* reticulocyte-prone non-lethal versus normocyte-prone lethal lines are characterized by numerous differences including subcellular localization of parasite proteins, invasion mecha-

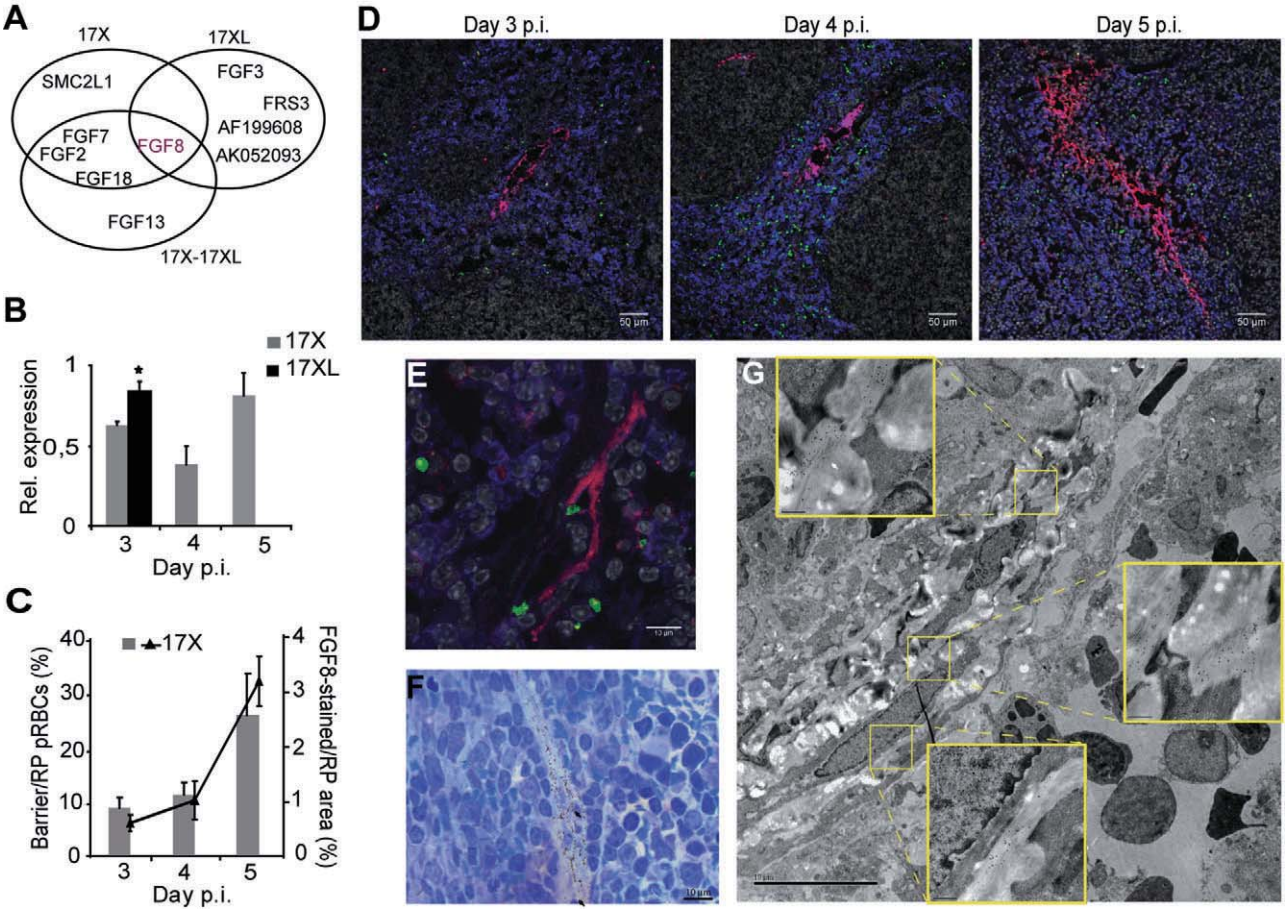

Fig. 5. Identification of FGF8 as barrier cell marker and histopathological analysis of infected spleens.
A. Venn diagram of the relations between the three sets of the five most variable genes in lines 17X (Cy3), 17XL (Cy5), and difference between lines (Cy3–Cy5), obtained from the microarray expression analysis of the spleen of Balb/c mice infected with 17X and 17XL at 3–5 days p.i.
B. Real-time PCR analysis of FGF8 expression in the spleen of mice infected with the two strains. Values are expressed as the mean ± SEM of two series of samples normalized to β-actin and expressed in relative amounts with respect to amplification in samples from uninfected spleens. Differences between the two lines are statistically significant $^*P < 0.05$.
C. (Right axis, lines) Quantification of FGF8-stained area on immunostained spleen cryosections, normalized to the red pulp area of the tissue section measured and expressed in percentage. (Left axis, bars) Quantification of the numbers of parasites within the FGF8-positive stained area expressed as a percentage of the number of parasites within the red pulp. Data correspond to the mean ± SEM of three images of the spleens from two series of mice infected with 17X line on days 3, 4 and 5 p.i.
D. Time-series immunohistofluorescence of spleens of mice infected with 17X parasites on days 3 to 5 p.i. Staining for FGF8 (red), F4/80 macrophages (blue), GFP (green) and DNA (gray) is shown. Scale bars represent 50 µm.
E, F, G. Microscopic visualization of FGF8 expression in spleens infected with the non-lethal strain of *P. yoelii.*
E. Immunohistofluorescence of spleen infected with 17X at day 3 p.i. visualized by confocal microscopy at 63× magnification.
F. Silver enhanced image of a FGF8 immunogold stained semithin section showing FGF8 (arrows).
G. Immunoelectron microscopic analysis of FGF8 expression in the spleen of mice infected with 17X at 1% parasitaemia with blow-ups of selected areas in yellow boxes (scale bar 3.5 µm). Scale bar represents 10 µm (E, F, G).

nisms, parasite growth rates and induction/suppression of immune responses (Pattaradilokrat *et al.*, 2008; 2009; Otsuki *et al.*, 2009). In our studies, we decided to examine the phagocytic activity of macrophages within the red pulp as this is where infected RBCs are destroyed (Yadava *et al.*, 1996) and also because other studies have shown the importance of spleen macrophages in parasite control during the early phase of infection in both lethal and non-lethal strains of *P. yoelii* (Couper *et al.*, 2007). In addition, several *in vitro* studies evaluating macrophage activity have shown that macrophages from animals infected with different non-lethal malaria parasites have a greater capacity to generate O_2 metabolites and greater cytotoxic activity than macrophages obtained from mice infected with lethal species (Brinkmann *et al.*, 1984; Taverne *et al.*, 1986). We observed lower numbers of parasites within macrophages in infections with 17X than in infections with 17XL. However, because these numbers

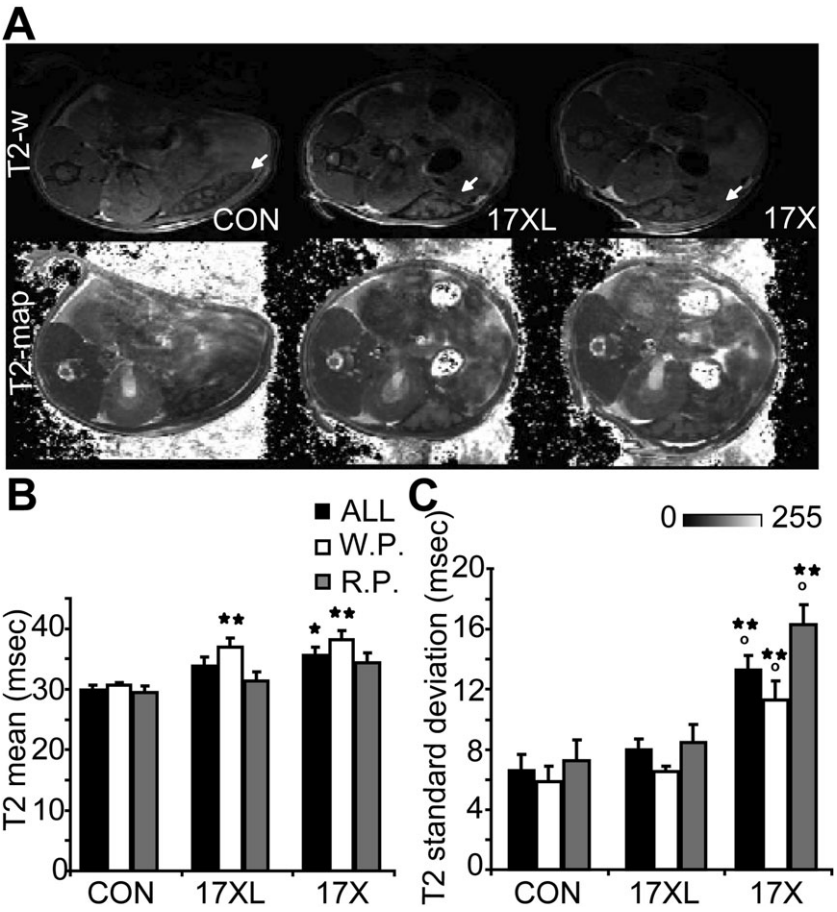

Fig. 6. MRI of the spleen using T2 relaxometry.
A. Coronal T2-weighted images (top) and T2 maps (bottom) showing the spleen (arrows), right kidney and back muscle from an uninfected mouse (CON), a mouse infected with the lethal line and a mouse infected with the non-lethal line on day 4 p.i. Gray-scale bar in T2 map represents intensity-related T2 values from 0 to 255 msec.
B. Measures for mean T2 relaxation time were evaluated in the white pulp (W.P.), red pulp (R.P.) or total area of the spleen, as well as in the muscle and kidney (Fig. S8).
C. Variance of T2 values in the selected areas. T2 times are expressed in milliseconds (msec) as the mean ± SEM of 4 to 5 mice from each group; data were evaluated by analysis of variance versus uninfected (*$P < 0.05$ and **$P < 0.01$) and versus lethal ($P < 0.01$) (Tukey *post hoc* test).

were observed together with larger numbers of parasites in spleens infected with 17X and no differences were observed in either *in vitro* or *in vivo* phagocytic activity measured using fluorescent beads between the two infections, it can be assumed that the differences in the numbers of parasites within the macrophages are not due to an increased ability of macrophages to kill parasites during non-lethal infections. This provides yet further evidence of different spleen compartmentalization in animals infected with non-lethal strains.

Cytoadherence of infected RBCs to the endothelium of venular capillaries in the deep vascular bed of inner organs is considered a fundamental aspect in the pathology of malaria and a major mechanism to escape spleen clearance (Miller *et al.*, 1994). Remarkably, in our study 27% of the parasites from the non-lethal line remained in the spleen for more than 20 s, lost directionality, reduced their velocity and showed rolling-circle behaviour, all parameters associated with adherence (Grayson *et al.*, 2003; Khandoga *et al.*, 2009). Adherence of 17X parasites was also demonstrated *in vitro* using spleen-derived fibrocytic cells and immortalized fibroblast cells, as well as by TEM analysis demonstrating physical contact of pRBCs to barrier cells. Noticeably, in all these experi-

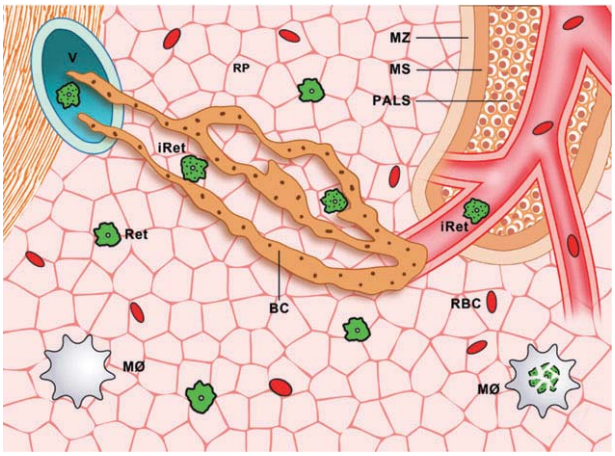

Fig. 7. Model of spleen-clearance evasion mechanism in reticulocyte-prone non-lethal malaria. Infection of Balb/c mice with the reticulocyte-prone non-lethal *P. yoelii* 17X strain induces remodelling of the spleen through the formation of a spleen tissue barrier of fibroblastic origin characterized by a syncitium of cells. Such barrier facilitates the channelling of blood from arterioles to venules and the adherence of infected reticulocytes to it thus physically protecting them from destruction by macrophages. V, venous lumen; Ret, reticulocytes; iRet, infected reticulocytes; RP, red pulp; PALS, periarteriolar lymphoid tissue; MS, marginal sinus; MZ, marginal zone; MØ, macrophages; BC, barrier cells.

ments, 17XL parasites served as a stringent control for specificity of such adherence. Thus, even though we have not formally proven the existence of ligand-receptors in this adherence, mechanical retention is difficult to accept as the sole explanation of our results, particularly if we consider that the spleen of mice is non-sinusoidal and the pore size of the reticular mesh in the red pulp is several times that of the diameter of pRBCs (Groom *et al*., 2002). We thus believe that our findings provide, to our knowledge, the first strong evidence of adherence of malaria parasites to the spleen opening new avenues for the investigation of host–parasite interactions in this lymphoid organ.

A question that remains to be answered is what role, if any, FGF8 plays in the formation of the spleen barrier. Fibroblast growth factors are peptides involved in signalling for correct vertebrate development *in vivo* and determining their function has presented major difficulties as many knock-out studies are lethal in embryonic stages or do not cause any particular phenotype as a result of the redundancy of this family (Itoh, 2007). It is tempting to speculate that the initial adherence of infected RBCs to individual spleen barrier cells transduces a signalling pathway via its specific FGF nuclear receptors to express FGF8, which, in turn, would induce autocrine activation and proliferation to create the barrier. To explore this possibility, we treated mice with PD 173074, an inhibitor of the FGFR3 receptor, known to be activated by FGF8 (Eswarakumar *et al*., 2005), using a regimen of 25 mg kg^{-1} of PD29447 (Sigma) from day −1 to day 14 p.i. Immunostaining for FGF8 of treated mouse spleens revealed that the tissue barrier developed in the non-lethal line, suggesting that a more complex mechanism is involved (not shown). Further studies are required to establish the role of FGF8 and other factors in the formation of this blood spleen barrier.

The spleen appears to have a dual role in malaria infections as it destroys pRBCs but also appears to modulate parasite biology as splenectomy has a major effect on the parasite phenotype (Engwerda *et al*., 2005). Strikingly, retention of *Plasmodium falciparum* RBCs containing ring stages by the human spleen was recently demonstrated in an *ex vivo* model system (Safeukui *et al*., 2008). Moreover, the same authors postulated that retention of rings in the spleen reduces the risk of cerebral malaria while increasing the risk of severe malarial anaemia (Buffet *et al*., 2009). The results presented here reveal remodelling of the spleen and adherence to this organ in Balb/c mice infected with the *P. yoelii* 17X strain. Moreover, they suggest that structural remodelling of the spleen might have a role in chronic infection as it is somehow related to delay in the onset of precrisis and prevention of host death. Noticeably, injection of splenocytes from *P. yoelii* 17X-infected mice that had cleared parasitaemia for over 3 months into naïve recipient mice resulted in infection in one of three mice (data not shown). While further experimentation is required to support this single observation, it indicates that in this rodent model, *P. yoelii* can establish sub-patent chronic infections as has been previously observed in CBA mice (Jayawardena *et al*., 1975). It will be interesting to determine the intercellular communication signals that induce this remodelling process and the ligand-receptors involved in adherence. Importantly, remodelling was also evidenced using MRI, a non-invasive technique widely used in human diagnostics. Finally, we postulate that a similar mechanism occurs in *Plasmodium vivax*, a reticulocyte-prone non-lethal human malaria parasite, as cytoadhesion has been recently reported to occur in cells expressing endothelial receptors (Carvalho *et al*., 2010).

Experimental procedures

Mice and parasites

All the animal studies were performed at the animal facilities of Hospital Clinic in Barcelona in accordance with guidelines and protocols approved by the Ethics Committee for Animal Experimentation of the University of Barcelona CEEA-UB (Protocol No DMAH: 3968). Female Balb/c mice, 6–8 weeks of age, were obtained from Charles River Laboratories. The original *P. yoelii yoelii* lethal (17XL) and non-lethal (17X) strains were obtained from MR4 (http://www.mr4.org/). *P. yoelii*–GFP transgenic lines of 17XL and 17X were generated using the same vectors, targeting strategy and protocols described elsewhere for *P. berghei* (Franke-Fayard *et al*., 2004). Infections were induced by the i.p. injection of 5×10^5 pRBCs obtained from the tail blood of donor mice at 5–10% parasitaemia. Parasitaemia was monitored daily by Giemsa staining of blood smears calculating the percentage of pRBCs over total RBCs in three optical fields of approximately 300 RBCs. Brilliant Cresyl Blue-Giemsa staining was used to detect reticulocytes (Taylor-Robinson and Phillips, 1994). Briefly, 5 μl of mouse blood was mixed with an equal volume of 1% Brilliant Cresyl Blue in 0.65% sodium chloride and incubated at room temperature (RT) for 20 min. After incubation, smears were prepared and left to air dry. After fixation with methanol, the smears were counterstained with Giemsa. Infected and uninfected reticulocytes were counted in different optical fields with, at least, 1500 RBCs.

Tissue preparation

Spleens, livers and kidneys from infected (17XL and 17X) and uninfected mice were aseptically removed on days 1 to 5 p.i. Tissues were fixed in 4% paraformaldehyde at 4°C for 2 h and cryoprotected in 30% sucrose at 4°C overnight before inclusion in Optimum Cutting Temperature compound (O.C.T. Tissue-Tek) and storage at −80°C. Cryosections of 7 μm were cut and processed for histopathological analysis.

Immunofluorescence assays

Tissue sections were thawed at RT for 30 min and fixed in cold acetone for 5 min. Fixed sections were treated with 100 mM

NH_4Cl PBS for 5 min and 100 mM Glycine PBS for 10 min to reduce autofluorescence. After blocking with 1% BSA PBS at RT for 1 h, sections were incubated at 4°C overnight with primary antibodies diluted in 0.5% BSA and 0.05% Tween-20 PBS. The primary antibodies used were rabbit anti-GFP antibody (Invitrogen, dilution 1/100), rat anti-F4/80 antibody (Abcam, dilution 1/100) and goat anti-FGF8b antibody (R&D Systems, dilution 1/7). After incubation, tissue sections were washed in 0.05% Tween-20 PBS and incubated with secondary antibodies at RT for 1.5 h. The corresponding secondary antibodies were conjugated to Alexa Fluor 488, 647 and 546 (Invitrogen, dilution 1/200). After washing, nuclei were stained with 4,6-diamidino-2-phenylindole (Invitrogen, 5 mg ml^{-1}) at RT for 7 min. Sections were mounted in Vectashield mounting media.

Images were obtained using a Leica TCS-SP5 microscope at a magnification of 20x (0.7 NA) and 63x (1.4 NA, oil objective). Five Z-stacks covering a depth of 7 μm were acquired and images were processed using ImageJ software (version 1.39o, Wayne Rasband, NIH, http://www.macbiophotonics.ca). Z-maximum projection and filtering of Gaussian Blur = 1 was performed for all images. For each day p.i., the FGF8-stained area over the red pulp area was quantified using ImageJ software. A threshold was set for positive staining and values averaged over three images obtained at 20× magnification representing different areas of the immunostained section.

Tissue Giemsa staining

Fixed spleen cryosections were stained in 20% Giemsa solution, 0.1% acetic acid and 96% ethanol and finally dehydrated and mounted in Depex-Polystyrene dissolved in xylene mountant for microscopy (Sigma-Aldrich). To determine the red pulp to white pulp ratio, those two regions were manually defined on images representing the whole Giemsa-stained tissue sections, considering the differential histopathological and Giemsa staining patterns between the red and white pulp. The area of the regions was then calculated using ImageJ software.

Quantification of number of parasites in spleens

Fluorescence wide-field microscopy was used to acquire images of the spleen and liver sections immunostained with anti-GFP antibody. Giemsa-stained sections were visualized under polarized light microscopy at 20× magnification. For parasite quantification, images were thresholded and automatic particle counting was used in ImageJ software, with a particle size of > 2 μm and circularity values of 0–1. The number of particles in the red pulp of the spleen was normalized for the manually defined tissue area. To determine the number of GFP parasites that were associated with the tissue barrier, Z-projections of the confocal images were used to define a second region of interest based on the FGF8-stained area within the red pulp. This selection was dilated two times to ensure inclusion of all associated pRBCs and number of parasites calculated as above.

Flow cytometry analysis of macrophage activity

Splenocytes were prepared from the spleens of mice infected with 17X and 17XL GFP transgenic parasites on day 4 p.i. Briefly, the spleens were homogenized and passed through a nylon mesh to create a single-cell suspension. Before addition of specific fluorescently labelled antibodies, the cells were pre-incubated with Seroblock anti-Fc receptor antibody (Abcam, dilution 1/100) for 10 min. Splenocytes were incubated with an antibody against murine F4/80 receptor conjugated to Alexa Fluor 647 (Invitrogen, dilution 1/10) at 4°C for 30 min. Cells were washed twice with 5 mM EDTA, 1% BSA PBS. Samples were incubated with the viability dye propidium iodide (Sigma, 1 mg ml^{-1}) before data acquisition. The data were collected and analysed using a FacsCANTO flow cytometer (BD Biosciences) and CELLQuest software. GFP^+ cells in these spleens were gated with respect to splenocytes obtained from infections with non-transgenic lines of *P. yoelii*. Data for $F4/80^-/GFP^+$, parasites and F4/80 macrophages in the spleen are representative of 200 000 events collected. For $F4/80^+/GFP^+$cell analysis, 1000 events of that population were collected.

Analysis of the phagocytic capacity of $F4/80^+$ cells using fluorescent beads was performed using Balb/c mice infected with wild-type 17XL and 17X strains. *In vitro* phagocytic activity was evaluated as the capacity of macrophages to incorporate 1 μm yellow-green fluorescent beads (Molecular Probes). Splenocytes of mice infected with the two lines of parasites were resuspended to 1×10^8 cells ml^{-1} in DMEM containing 5% heat-inactivated FBS and seeded on a 24-well plate. Plates were incubated at 37°C, 5% CO_2, 100% humidity for 1 h. They were then incubated with 100 beads per cell in 500 ml medium at 37°C for 1 h. Cells were then washed three times with cold PBS to remove any free beads and scraped from the plate. Cells samples were labelled with an anti-F4/80 antibody conjugated to Alexa Fluor 647 and analysed on a FacsCANTO flow cytometer. The acquisition threshold was set to include cells but to exclude debris and remaining unbound beads. For *in vivo* analysis of $F4/80^+$ macrophage activity, mice were anaesthetized before intravenous (i.v.) injection of 200 μl of PBS with 1.7×10^8 3 μm yellow-green fluorescent beads (Polysciences). After 30 min, the mice were killed by cervical dislocation and the spleen was removed and processed as described above. Splenocytes were incubated with an anti-F4/80 antibody conjugated to Alexa Fluor 647 and 10^6 cells per sample were analysed on a FacsCANTO flow cytometer. The percentage of phagocytic cells (macrophages that had ingested beads) was calculated as a function of $F4/80^+$ cells.

Parasite in vivo *imaging and mobility analysis*

In vivo imaging of the spleen was performed on mice infected with the 17XL or 17X GFP transgenic lines at 1% (day 3 p.i.) and 10% (day 4 p.i.) parasitaemia. Briefly, the spleen of anaesthetized mice (100 mg kg^{-1} ketamine and 5 mg kg^{-1} midazolam i.p.) was surgically exposed as described elsewhere (Thiberge *et al.*, 2007). Imaging of living parasites within the intact spleen was achieved by placing the mice on a stage of a Leica TCS-SP5 microscope fitted with an inverted 63x (1.3 NA) glycerol objective, which permits a working distance of 0.28 mm. Movies of 1.5 min were recorded through five Z-stacks covering a depth of 8 μm at a speed of 8 kHz. Fluorescence was recorded on two different channels (excitation/emission wavelength 488/505–580 nm for GFP and of 570–630 nm for tissue autofluorescence) with the pinhole set to 3.0 Airy units. RBC reflection (488/480–495 nm) was used in some experiments to obtain additional information on

the zone being imaged and in the blood flow experiments described below.

Quantization of parasite mobility parameters was achieved using movies of the spleen of infected mice at 1% parasitaemia and of FITC-RBC injected control mice using ImageJ software. To this end, 4D (x, y, z, t) manual tracking of green fluorescent particles was performed using the MTrackJ plugin (written by E. Meijering) with the help of Z-coded colour stacks to facilitate single-particle identification and tracking over time. Particles representing pRBCs from each strain were tracked in different areas of the spleen of mice at 1% parasitaemia. In total, 120 particles from three mice infected with each parasite line were tracked. Tracking was performed in a maximum of 100 frames for each particle. Z movement was considered only if displacement was higher than 6 μm (average diameter for an infected particle). For each particle, measures for directionality, defined as the quotient of displacement versus path length (Miller *et al.*, 2002), mean velocity and residence time were calculated and plotted as density distributions. Differences between the two lines were assessed using the equality-of-medians test in STATA (IC10).

Spleen blood flow measurements

After exposing spleens as described above, 50 μg of 70 kDa Dextran labelled with Texas Red (Invitrogen) dialysed through a 0.2 μm membrane and diluted in 100 μl of saline buffer were injected i.v. Image was further acquired using xy and xt line-scanning modes in the central lumen of the vessel as previously described (Molitoris and Sandoval, 2005; Zhong *et al.*, 2008). Vessels were set horizontally, in the direction of laser scanning, by optical field rotation (not affecting speed). Bidirectional scanning with a line average of 32 was used at a speed of 8 kHz and an image of 512 pixels × 512 lines was obtained. In these images, the streaks resulting from moving cells were used to quantify blood flow as described (Zhong *et al.*, 2008).

Microarray global expression analysis

Spleens of mice infected with 17XL and 17X parasites were aseptically removed and snap-frozen in liquid nitrogen between days 3 and 5 p.i. Tissues were homogenized individually and RNA was extracted using the TrizolR reagent (Invitrogen). Total RNA was labelled using an Agilent Low RNA Input Fluorescent Linear Amplification Kit. mRNA from the spleen of each mouse infected with either the 17X or 17XL lines on days 3, 4, and 5 p.i. was labelled with Cy3 and Cy5 respectively. Dual hybridizations were performed using the Agilent Whole Mouse Genome G4122A microarray according to the manufacturer's protocol. Microarray images were obtained using the GenePix 4000B scanner. Data were processed with the Bioconductor limma package, using background correction ('normexp') and 'quantile' normalization between arrays for final values (Cy3 and Cy5 signal intensities were separately normalized as one-colour arrays).

Real-time PCR analysis

Total RNA from spleen cells was retro-transcribed and cDNA was subjected to real-time PCR using specific primers for FGF8 and β-actin with the use of ABI-Prism 7500 (AME Bioscience). PCR was performed using the following cycling parameters: activation at 95°C for 10 min; PCR cycling, 40 cycles at 95°C for 15 s, and 60°C for 1 min. The primers used were the following: TTCCT CAACTACCCGCCCTTCA and GCCCCTCCCCTTTGCTGTGC for FGF8 and GCGGGCGACGATGCT and AGGGCGGCCCAC GAT for β-actin, which hybridize to the corresponding murine cDNAs. Experiments were performed in triplicate. The PCR arbitrary units of each gene were defined as the mRNA levels normalized to the β-actin expression level in each sample.

Electron microscopy

For ultrastructural analysis, the spleens of uninfected mice and mice infected with 17XL and 17X strains at 1% parasitaemia were aseptically removed and immediately fixed with Karnovsky's fixative. Small pieces of 1 mm^2 were fixed in the same fixative at 4°C for at least 24 h, post-fixed in 1% osmium tetroxide and dehydrated in acetones before embedding in Spurr resin. Semithin (0.5 μm) and ultrathin (70–90 nm) sections of the spleen were obtained on an ultramicrotom Ultracut E (Reichert-Jung) equipped with a diamond knife (Diatome). Semithin sections were stained with methylene blue and optical microscopy was used to locate red pulp area. Serial ultrathin sections from the same region were cut and stained with 2% uranyl acetate and lead citrate (Reynolds, 1963) to allow high-contrast imaging. Image acquisition was performed using a JEOL 1010 TEM operating at 80 kV with a Bioscan 792 camera (Gatan MultiScan cameras).

Correlative light electron microscopy

Correlative light electron microscopy was used to detect FGF8 expression at the ultrastructural level. Briefly, the spleens of infected mice were fixed in 4% paraformaldehyde and 0.1% glutaraldehyde phosphate buffer. Pieces of 0.5 cm were cut, dehydrated in ethanols by progressive lowering of the temperature to –35°C and embedded in Lowicryl K4M (Carlemalm *et al.*, 1982; 1985). Immunogold assays were performed on semithin sections from different blocks of the spleen covered with a blocking buffer of 1% BSA (Sigma), 20 mM glycine in 0.1M PBS, pH 7.4 at RT for 30 min in a moist chamber. After blotting off excess buffer, sections were incubated in primary anti-FGF-8b antibody diluted 1/3 with blocking buffer at RT for 2 h. Sections were washed and incubated in 10 nm protein A gold conjugate (Utrecht University) for 1 h. After washing with PBS and deionized water, the sections were silver-enhanced using a SEKL 15 silver enhancing kit (BBInternational) according to the manufacturer's instructions, with progress being periodically monitored using a light microscope. Silver enhancement was reached at between 8 and 10 min. The sections were then washed in several changes of distilled water. Next, serial ultrathin sections obtained from the blocks that revealed FGF8-specific staining were immunolabelled and prepared for TEM as above.

In vitro *adhesion assays*

Spleen-derived fibroblasts were obtained from long-term splenocyte culture with slight modifications (Borrello and Phipps, 1996). Briefly, a single-cell suspension of the spleen from a control

Balb/c mouse was obtained and cells cultured in RPMI complete medium [RPMI1640 with L-glutamine (Sigma) containing 10% fetal bovine serum (Invitrogen), 5×10^{-5} M 2-ME (Invitrogen), 10 mM Hepes (Sigma), 50 μg ml^{-1} gentamicin (Invitrogen), 1% Penicillin/Streptomycin (Invitrogen) and 25 mM sodium bicarbonate (Sigma)] using an incubator with 5% CO_2 at 37°C. After 2 weeks, adherent cells were dissociated with a 0.05% trypsin-EDTA solution, seeded in 8-well chambered slides (Lab-Tek II) at 10^5 cells well^{-1} in 300 μl well^{-1} of RPMI complete medium and incubated in 5% CO_2 at 37°C for 2 days before adhesion assays were performed.

Murine fibroblasts of the 3T3/NIH cell line were originally obtained from ATCC (http://www.atcc.org) and maintained in culture following standard methodologies. For adhesion assays, 10^4 cells well^{-1} were seeded in 8-well chambered slides and incubated for 2 days in 5% CO_2 at 37°C.

For parasite preparation, total peripheral blood was collected in EDTA/PBS through intracardiac puncture from 17X- or 17XL-infected mice on day 4 p.i. The blood pellet was washed three times in RPMI adhesion media (RPMI 1640 with L-Glutamine containing 20 mM Hepes and 50 μg ml^{-1} Gentamicin at pH 6.8) and pRBCs were enriched for mature stages using a 55% Histodenz (Sigma)/PBS gradient as described (Mota *et al*., 2001). The adhesion assays were performed in duplicates, incubating the cells with 10^5 pRBC well^{-1} in 300 μl well^{-1} of adhesion media at 37°C for 1 h. Slides were washed by immersion 10 times in adhesion media, air-dried, fixed with methanol and stained with Giemsa. The number of pRBCs was averaged from 150 optical fields of each well using an optical microscope with a 100x objective.

In vivo *MRI*

A high-field magnetic resonance system was used for non-invasive imaging of the spleen of anaesthetized mice infected with either the 17XL or 17X line on day 4 p.i. MRI scans were performed under isoflurane anaesthesia using a BioSpec 70/30 horizontal animal scanner (Bruker BioSpin) equipped with a 12 cm inner diameter actively shielded gradient system (400 mT m^{-1}). Coil configuration consisted of a surface transceiver coil for cardiac and abdominal imaging. The animals were placed in a prone position in the holder with a nose cone for administering anaesthetic gases and fixed using adhesive tape. Tripilot scans were used for accurate positioning of the animals' spleen inside the isocentre of the magnet. As a reference to select the same slices in the T2 transversal relaxation maps, T1-weighted 3D coronal images were acquired using a FISP (Fast Imaging Steady State Precession) sequence with the following parameters: echo times = 2.2 msec, repetition time = 14 msec, field of view = $35 \times 35 \times 17$ mm, matrix = $256 \times 256 \times 50$ pixels, resulting in a spatial resolution of $0.137 \times 0.137 \times 0.340$ mm. Indeed, T2 mapping of one abdominal coronal section containing the spleen, the kidney at the level of the renal artery and the back muscle was acquired using an MSME sequence with the following parameters: 16 different echo times, repetition time = 2.5 s, field of view = $30 \times 30 \times 1$ mm, matrix = $256 \times 256 \times 50$ pixels resulting, in a spatial resolution of $0.117 \times 0.117 \times 1.00$ mm.

T2 maps were constructed and analysed with Paravision 5.0 (Bruker BioSpin). Measurements of T2 relaxation times were performed by manually drawing the red and white pulp of the spleen. Three different blinded experimenters repeated this process, and an average of the three measurements was obtained. T2 values from muscle and the renal cortex were measured in independent circular regions of interest.

Acknowledgements

We are grateful to Ricardo NZ Venzio for his initial input into global transcriptional analysis and to Anna Bosch for assistance in image analysis and quantification. MF is a recipient of a graduate fellowship from the Generalitat de Catalonia. JB – NIH. Work in the laboratory of HAP is funded by the Ministerio Español de Ciencia e Innovación (SAF2009-07760) and by the Fundación Privada CELLEX (Catalonia, Spain).

References

Amino, R., Thiberge, S., Martin, B., Celli, S., Shorte, S., Frischknecht, F., and Menard, R. (2006) Quantitative imaging of Plasmodium transmission from mosquito to mammal. *Nat Med* **12:** 220–224.

Borrello, M.A., and Phipps, R.P. (1996) Differential Thy-1 expression by splenic fibroblasts defines functionally distinct subsets. *Cell Immunol* **173:** 198–206.

Bowdler, A.J. (2002) *The Complete Spleen*. Totowa: Humana Press.

Brinkmann, V., Kaufmann, S.H., Simon, M.M., and Fischer, H. (1984) Role of macrophages in malaria: O2 metabolite production and phagocytosis by splenic macrophages during lethal *Plasmodium berghei* and self-limiting *Plasmodium yoelii* infection in mice. *Infect Immun* **44:** 743–746.

Buffet, P.A., Safeukui, I., Milon, G., Mercereau-Puijalon, O., and David, P.H. (2009) Retention of erythrocytes in the spleen: a double-edged process in human malaria. *Curr Opin Hematol* **16:** 157–164.

Carlemalm, E., Acetarin, J.D., Villiger, W., Colliex, C., and Kellenberger, E. (1982) Heavy metal-containing surroundings provide much more 'negative' contrast by Z-imaging in STEM than with conventional modes. *J Ultrastruct Res* **80:** 339–343.

Carlemalm, E., Villiger, W., Hobot, J.A., Acetarin, J.D., and Kellenberger, E. (1985) Low temperature embedding with Lowicryl resins: two new formulations and some applications. *J Microsc* **140:** 55–63.

Carvalho, B.O., Lopes, S.C., Nogueira, P.A., Orlandi, P.P., Bargieri, D.Y., Blanco, Y.C., *et al*. (2010) On the cytoadhesion of plasmodium vivax-infected erythrocytes. *J Infect Dis* **202:** 638–647.

Couper, K.N., Blount, D.G., Hafalla, J.C., van Rooijen, N., de Souza, J.B., and Riley, E.M. (2007) Macrophage-mediated but gamma interferon-independent innate immune responses control the primary wave of *Plasmodium yoelii* parasitemia. *Infect Immun* **75:** 5806–5818.

Engwerda, C.R., Beattie, L., and Amante, F.H. (2005) The importance of the spleen in malaria. *Trends Parasitol* **21:** 75–80.

Eswarakumar, V.P., Lax, I., and Schlessinger, J. (2005) Cellular signaling by fibroblast growth factor receptors. *Cytokine Growth Factor Rev* **16:** 139–149.

Franke-Fayard, B., Trueman, H., Ramesar, J., Mendoza, J., van der Keur, M., van der Linden, R., *et al*. (2004) A

Plasmodium berghei reference line that constitutively expresses GFP at a high level throughout the complete life cycle. *Mol Biochem Parasitol* **137:** 23–33.

Grayson, M.H., Hotchkiss, R.S., Karl, I.E., Holtzman, M.J., and Chaplin, D.D. (2003) Intravital microscopy comparing T lymphocyte trafficking to the spleen and the mesenteric lymph node. *Am J Physiol Heart Circ Physiol* **284:** H2213–H2226.

Groom, A.C., MacDonald, I.C., and Schmid, E.E. (2002) Splenic microcirculatory blood flow and function with respect to blood cells. In *The Complete Spleen*. Bowdler, A.J. (ed.). Totowa: Humana Press Inc, pp. 23–50.

Heussler, V., and Doerig, C. (2006) *In vivo* imaging enters parasitology. *Trends Parasitol* **22:** 192–195. Discussion 195–196.

Itoh, N. (2007) The Fgf families in humans, mice, and zebrafish: their evolutional processes and roles in development, metabolism, and disease. *Biol Pharm Bull* **30:** 1819–1825.

Jayawardena, A.N., Targett, G.A., Davies, A.J., Leuchars, E., and Carter, R. (1975) Proceedings: the passive transfer of immunity to *Plasmodium berghei yoelii*. *Trans R Soc Trop Med Hyg* **69:** 426.

Khandoga, A.G., Khandoga, A., Reichel, C.A., Bihari, P., Rehberg, M., and Krombach, F. (2009) *In vivo* imaging and quantitative analysis of leukocyte directional migration and polarization in inflamed tissue. *PLoS One* **4:** e4693.

Miller, L.H., Good, M.F., and Milon, G. (1994) Malaria pathogenesis. *Science* **264:** 1878–1883.

Miller, M.J., Wei, S.H., Parker, I., and Cahalan, M.D. (2002) Two-photon imaging of lymphocyte motility and antigen response in intact lymph node. *Science* **296:** 1869–1873.

Molitoris, B.A., and Sandoval, R.M. (2005) Intravital multiphoton microscopy of dynamic renal processes. *Am J Physiol Renal Physiol* **288:** F1084–F1089.

Mota, M.M., Thathy, V., Nussenzweig, R.S., and Nussenzweig, V. (2001) Gene targeting in the rodent malaria parasite *Plasmodium yoelii*. *Mol Biochem Parasitol* **113:** 271–278.

Oh, J., Han, E.T., Pelletier, D., and Nelson, S.J. (2006) Measurement of *in vivo* multi-component T2 relaxation times for brain tissue using multi-slice T2 prep at 1.5 and 3 T. *Magn Reson Imaging* **24:** 33–43.

Otsuki, H., Kaneko, O., Thongkukiatkul, A., Tachibana, M., Iriko, H., Takeo, S., *et al.* (2009) Single amino acid substitution in *Plasmodium yoelii* erythrocyte ligand determines its localization and controls parasite virulence. *Proc Natl Acad Sci USA* **106:** 7167–7172.

Pattaradilokrat, S., Cheesman, S.J., and Carter, R. (2008) Congenicity and genetic polymorphism in cloned lines derived from a single isolate of a rodent malaria parasite. *Mol Biochem Parasitol* **157:** 244–247.

Pattaradilokrat, S., Culleton, R.L., Cheesman, S.J., and Carter, R. (2009) Gene encoding erythrocyte binding ligand linked to blood stage multiplication rate phenotype in *Plasmodium yoelii yoelii*. *Proc Natl Acad Sci USA* **106:** 7161–7166.

Penet, M.F., Kober, F., Confort-Gouny, S., Le Fur, Y., Dalmasso, C., Coltel, N., *et al.* (2007) Magnetic resonance spectroscopy reveals an impaired brain metabolic profile in mice resistant to cerebral malaria infected with *Plasmodium berghei* ANKA. *J Biol Chem* **282:** 14505–14514.

Reynolds, E.S. (1963) The use of lead citrate at high pH as an electron-opaque stain in electron microscopy. *J Cell Biol* **17:** 208–212.

Safeukui, I., Correas, J.M., Brousse, V., Hirt, D., Deplaine, G., Mulé, S., *et al.* (2008) Retention of Plasmodium falciparum ring-infected erythrocytes in the slow, open microcirculation of the human spleen. *Blood* **112:** 2520–2528.

Sturm, A., Amino, R., van de Sand, C., Regen, T., Retzlaff, S., Rennenberg, A., *et al.* (2006) Manipulation of host hepatocytes by the malaria parasite for delivery into liver sinusoids. *Science* **313:** 1287–1290.

Taverne, J., Treagust, J.D., and Playfair, J.H. (1986) Macrophage cytotoxicity in lethal and non-lethal murine malaria and the effect of vaccination. *Clin Exp Immunol* **66:** 44–51.

Taylor-Robinson, A.W., and Phillips, R.S. (1994) Predominance of infected reticulocytes in the peripheral blood of CD4+ T-cell-depleted mice chronically infected with *Plasmodium chabaudi chabaudi*. *Parasitol Res* **80:** 614–619.

Thiberge, S., Blazquez, S., Baldacci, P., Renaud, O., Shorte, S., Ménard, R., and Amino, R. (2007) *In vivo* imaging of malaria parasites in the murine liver. *Nat Protoc* **2:** 1811–1818.

Weiss, L., Geduldig, U., and Weidanz, W. (1986) Mechanisms of splenic control of murine malaria: reticular cell activation and the development of a blood-spleen barrier. *Am J Anat* **176:** 251–285.

Yadava, A., Kumar, S., Dvorak, J.A., Milon, G., and Miller, L.H. (1996) Trafficking of *Plasmodium chabaudi* adami-infected erythrocytes within the mouse spleen. *Proc Natl Acad Sci USA* **93:** 4595–4599.

Zhong, Z., Petrig, B.L., Qi, X., and Burns, S.A. (2008) *In vivo* measurement of erythrocyte velocity and retinal blood flow using adaptive optics scanning laser ophthalmoscopy. *Opt Express* **16:** 12746–12756.

Supporting information

Additional Supporting Information may be found in the online version of this article:

Fig. S1. Characterization of the Balb/c-GFP *P. yoelii* murine malaria model (A) Transgenic *P. yoelii* parasites express GFP at all asexual blood stages (rings, trophozoites, schizonts and merozoites). (B) Time-course parasitemia in experimental infections of 6–8 week-old female Balb/c mice with the 17XL and the 17X lines. Curves were calculated from the mean of five mice injected with 5×10^5 pRBCs from each line of the wild-type or GFP transgenic parasites. Time-course reticulocytemia (number of reticulocytes/number of RBCs $\times$ 100) (C) and percentage of infected reticulocytes (number of reticulocytes/number of infected RBCs $\times$ 100) (D) in GFP transgenic *P. yoelii* 17X and 17XL infections. Results are based on BCB-Giemsa staining of infected blood smears. Curves were calculated from the mean of at least six mice per group injected with 5×10^5 pRBCs from each line of the GFP transgenic parasites. (E) Brilliant Cresyl Blue

(BCB)-Giemsa staining images of blood smears from the transgenic 17X and 17XL infected mice on days 3, 4, 5 and 10 p.i.

Fig. S2. Retention of *P. yoelii* 17X and 17XL parasites in the murine spleen. (Upper panel) Visualization under polarized light microscopy of Giemsa-stained cryosections of the spleens from mice infected with the 17X line (A) and the 17XL line (B) at 1% peripheral parasitemia (day 3 p.i.). (Lower panel) Thresholded images (142–255 threshold level) used for parasite quantification, showing distribution of parasitized red blood cells in the red pulp of the spleen. N = numbers of parasites in spleen. Scale bars represent 50 μm.

Fig. S3. Analysis of spleen closure four days after *P. yoelii* infection. 1.68×10^8 3 μm yellow-green fluorescent beads were injected i.v. into uninfected mice (Con) and mice infected with 17X and 17XL wild-type parasites on day 4 p.i. Five minutes after injection, splenic uptake of beads was analyzed by flow cytometry (A) and fluorescence microscopy (B). (A) 10^6 spleen cells were analyzed by FACS and the numbers of beads was quantified. The percentage of the number of beads per spleen cell is expressed as the mean ± SEM of six different mice (ANOVA). No significant differences were observed between the groups. (B) The uptake of beads per spleen area was quantified using ImageJ software in six to ten confocal images per mouse with six mice per group after injection of fluorescent beads. Each bar indicates the mean, and each error bar the SEM. No significant differences were observed between the groups after ANOVA analysis.

Fig. S4. Analysis of FITC-labeled RBC movement. Density distribution of FITC-labeled RBCs in the spleen of control mice (N = 3) by mean velocity (A), directionality (B) and residence time (C). In total, 100 particles were tracked using the same methodology described for GFP-pRBCs in infected mice and compared to 17X and 17XL parasites with equality-of-medians test. The median value for mean velocity is 103.66 μm/sec, for directionality 0.852 and for residence time 0.9 sec. Particles quantified were moving outside vessels (49.52%) and through vessels with a diameter of less than 10 μm (16.19%) and greater than 10 μm (32.38%).

Fig. S5. Microarray analysis. Heatmaps and plotted values of the logFC values on days 3, 4 and 5 p.i. (with respect to time 0) for unsupervised selection of fibroblast-related genes with the largest variability on spleen samples of mice infected with 17X(Cy3) (A); 17XL (Cy5) (B) and 17X-17XL differences (Cy3–Cy5) (C) together with a housekeeping gene (GAPDH) with small variability.

Fig. S6. Strain and tissue specificity of the *P. yoelii* 17X-induced barrier. Time-series immunohistofluorescence of tissue sections. (A) Sections of spleen and liver of mice infected with *P. yoelii* 17XL lethal strain. No specific staining for FGF8 was observed in cryosections of infected mice on days 3 to 5 p.i. (B) Immunofluorescence of liver and kidney cryosections in 17X infected mice was also negative for FGF8. Staining for FGF8 (red), GFP (green), F4/80 macrophage receptor in the spleen (blue) and nucleic acids (gray) was performed. Scale bars represent 50 μm.

Fig. S7. MRI analysis of the muscle and kidney. (A) T2 mean relaxation times quantified in circular regions of the back muscle and the outer part of kidney from T2 maps of coronal T2-weighted images containing the spleen (Figure 6). (B) Variance of T2 values in the selected areas of muscle and kidney. T2 times (msec) are expressed as the mean ± SEM of four to five mice from each group (control, lethal and non-lethal). No significant differences were observed.

Movie S1. IVM movie of a representative dextran-labeled (red) spleen vessel (10.4 μm lumen diameter) in a mouse infected with the 17X GFP line (green) at 1% parasitemia used for blood flow analysis. Scale bars represent 10 μm. Quick-time. S1 (4.6 MB, 9 sec).

Movie S2. Time-lapse intravital microscopy images of the murine spleen infected with 17XL GFP-transgenic parasites at 10% parasitemia (Z-maximum projection). Parasite and tissue autofluorescence are shown in green and red respectively. Scale bars represent 10 μm and the time interval is in sec. Quick-time. S2 (4.1 MB, 10 sec).

Movie S3. Time-lapse intravital microscopy images of the murine spleen infected with 17X GFP parasites at 10% parasitemia (Z-maximum projection). Parasite and tissue autofluorescence are shown in green and red respectively. Scale bars represent 10 μm and the time interval is in sec. Quick-time. S3 (2.6 MB, 10 sec).

Movie S4. IVM Z-coded color video of the murine spleen infected with 17XL showing three-dimensional movement of parasites. These videos were used as a tool to follow single-particle movement over time. Each time point is the result of a projection from 5 different depths (Z) with a Z-delay of approximatively 0.06 sec. Depth code: yellow (0 μm), orange (2 μm), pink (4 μm), blue (6 μm), green (8 μm). Quick-time. S4 (0.9 MB, 3 sec).

Movie S5. IVM video of representative area of the spleen of mice infected with 17X at 1% peripheral parasitemia. Selected area focus on an example of the dynamic adherence of pRBCs to spleen cells. Twenty-seven percent of the parasites from the non-lethal line remained in the spleen for more than 20 sec, compared to 4% in the lethal line. Quick-time. S5 (0.7 MB, 6 sec).

Movie S6. IVM video of representative area of the spleen of mice infected with the 17X at 1% peripheral parasitemia. Selected area focus on examples of the dynamic adherence of pRBCs to spleen cells. Quick-time. S6 (0.6 MB, 6 sec).

Movie S7. Animation illustrating our present model of *P. yoelii* 17X line-induced spleen remodeling, infected RBC adherence to the tissue barrier and macrophage-clearance evasion. Quick-time. S7 (1.1 MB, 11 sec).

Supporting Information

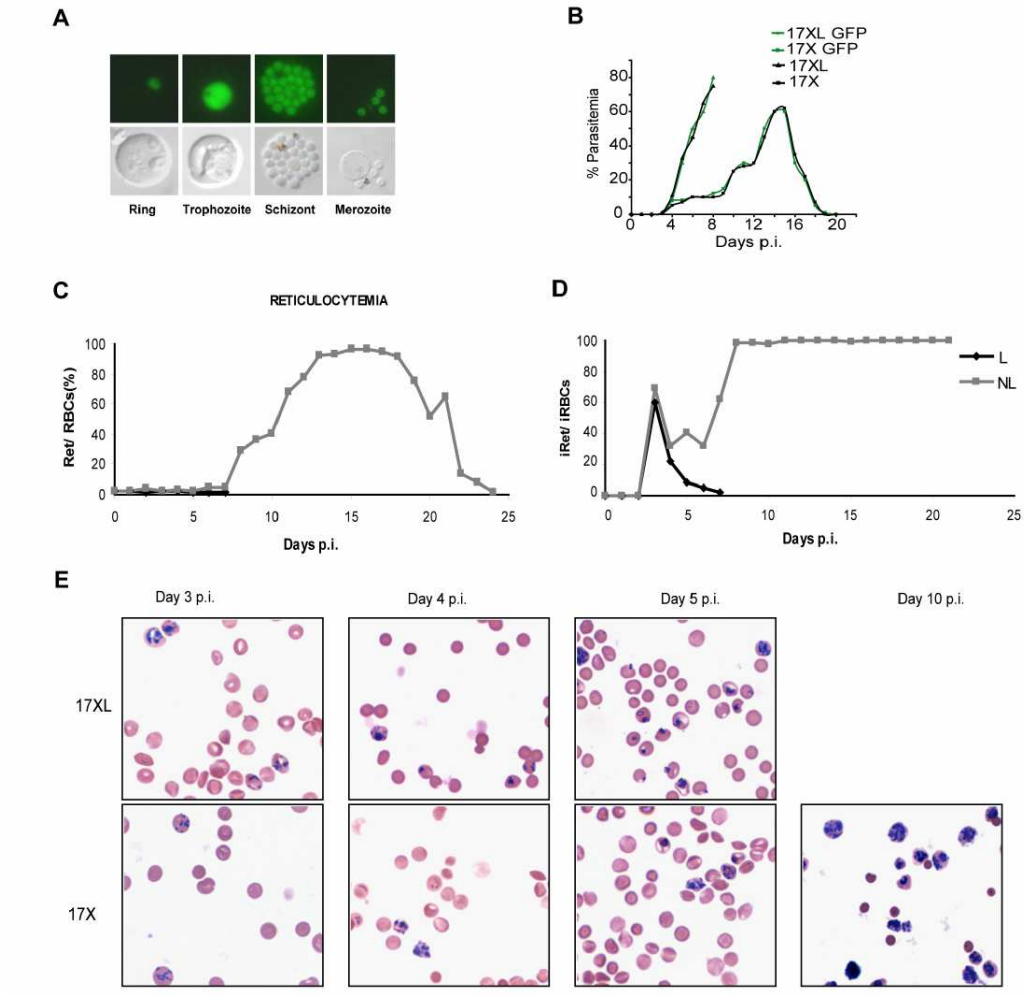

Fig. S1. Characterization of the Balb/c-GFP *P. yoelii* murine malaria model (A) Transgenic *P. yoelii* parasites express GFP at all asexual blood stages (rings, trophozoites, schizonts and merozoites). (B) Time-course parasitemia in experimental infections of 6–8 week-old female Balb/c mice with the 17XL and the 17X lines. Curves were calculated from the mean of five mice injected with 5×10^5 pRBCs from each line of the wild-type or GFP transgenic parasites. Time-course reticulocytemia (number of reticulocytes/number of RBCs × 100) (C) and percentage of infected reticulocytes (number of reticulocytes/number of infected RBCs × 100) (D) in GFP transgenic *P. yoelii* 17X and 17XL infections. Results are based on BCB-Giemsa staining of infected blood smears. Curves were calculated from the mean of at least six mice per group injected with 5×10^5 pRBCs from each line of the GFP transgenic parasites. (E) Brilliant Cresyl Blue (BCB)-Giemsa staining images of blood smears from the transgenic 17X and 17XL infected mice on days 3, 4, 5 and 10 p.i.

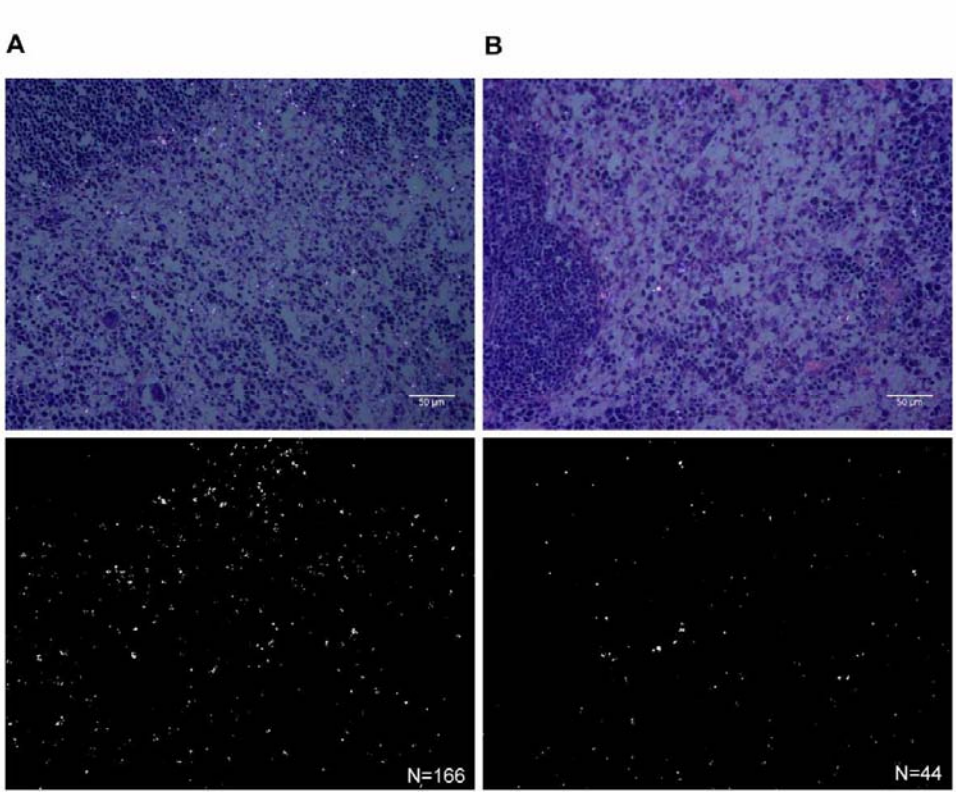

Fig. S2. Retention of *P. yoelii* 17X and 17XL parasites in the murine spleen. (Upper panel) Visualization under polarized light microscopy of Giemsa-stained cryosections of the spleens from mice infected with the 17X line (A) and the 17XL line (B) at 1% peripheral parasitemia (day 3 p.i.). (Lower panel) Thresholded images (142–255 threshold level) used for parasite quantification, showing distribution of parasitized red blood cells in the red pulp of the spleen. N = numbers of parasites in spleen. Scale bars represent 50 µm.

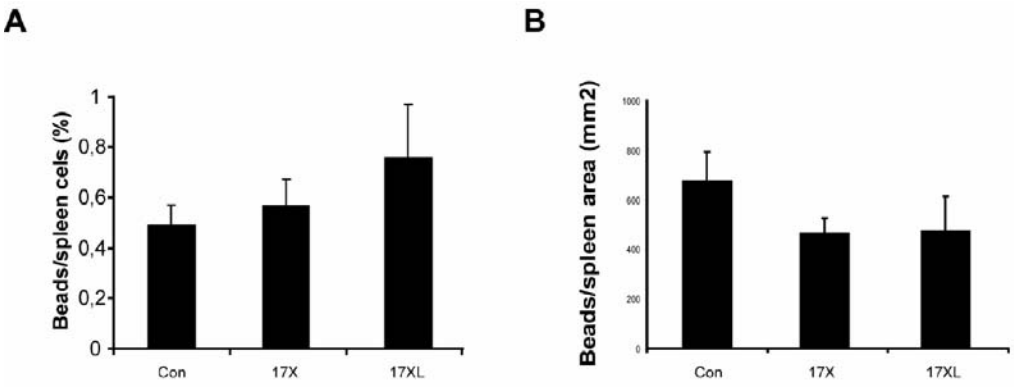

Fig. S3. Analysis of spleen closure four days after *P. yoelii* infection. 1.68×10^8 3 µm yellow-green fluorescent beads were injected i.v. into uninfected mice (Con) and mice infected with 17X and 17XL wild-type parasites on day 4 p.i. Five minutes after injection, splenic uptake of beads was analyzed by flow cytometry (A) and fluorescence microscopy (B). (A) 10^6 spleen cells were analyzed by FACS and the numbers of beads was quantified. The percentage of the number of beads per spleen cell is expressed as the mean ± SEM of six different mice (ANOVA). No significant differences were observed between the groups. (B) The uptake of beads per spleen area was quantified using ImageJ software in six to ten confocal images per mouse with six mice per group after injection of fluorescent beads. Each bar indicates the mean, and each error bar the SEM. No significant differences were observed between the groups after ANOVA analysis.

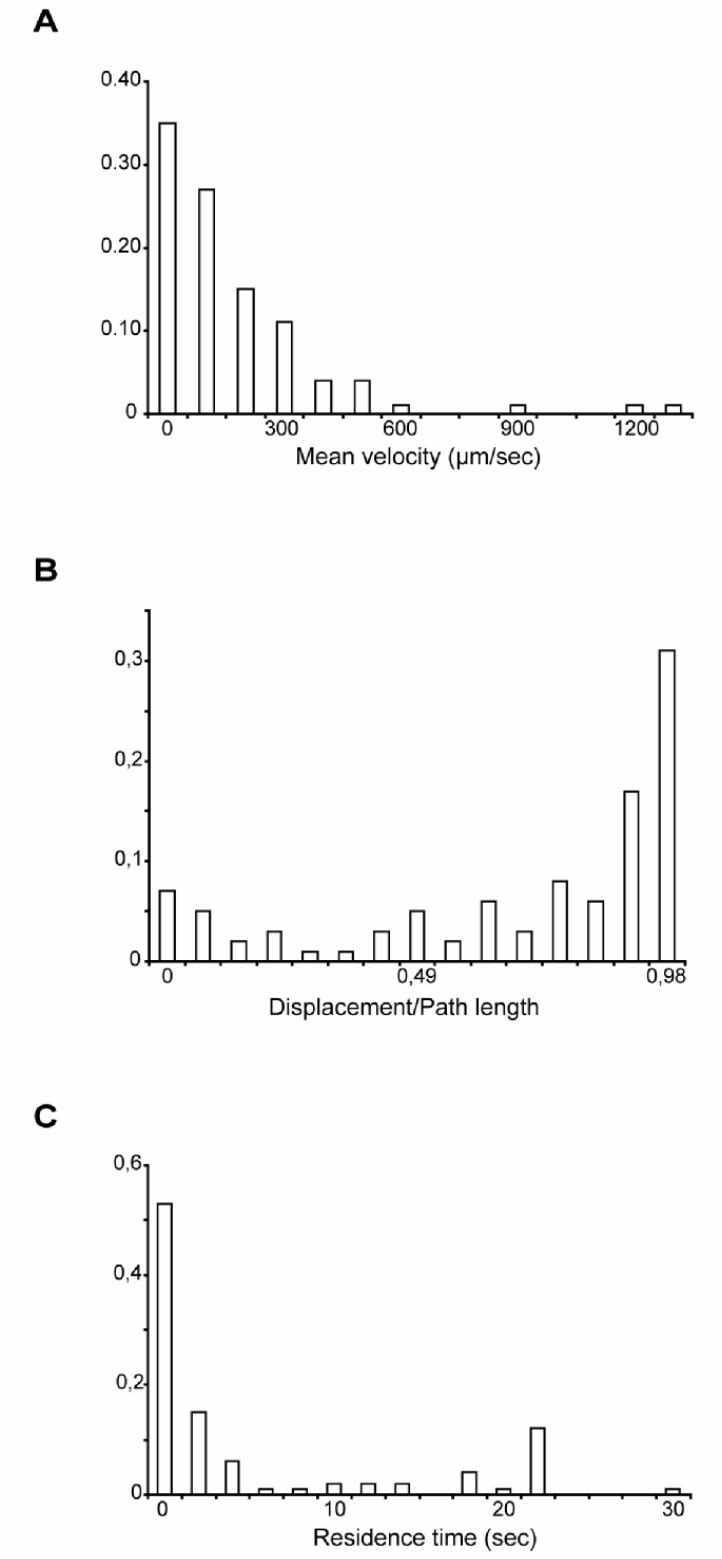

Fig. S4. Analysis of FITC-labeled RBC movement. Density distribution of FITC-labeled RBCs in the spleen of control mice (N = 3) by mean velocity (A), directionality (B) and residence time (C). In total, 100 particles were tracked using the same methodology described for GFP-pRBCs in infected mice and compared to 17X and 17XL parasites with equality-of-medians test. The median value for mean velocity is 103.66 µm/sec, for directionality 0.852 and for residence time 0.9 sec. Particles quantified were moving outside vessels (49.52%) and through vessels with a diameter of less than 10 µm (16.19%) and greater than 10 µm (32.38%).

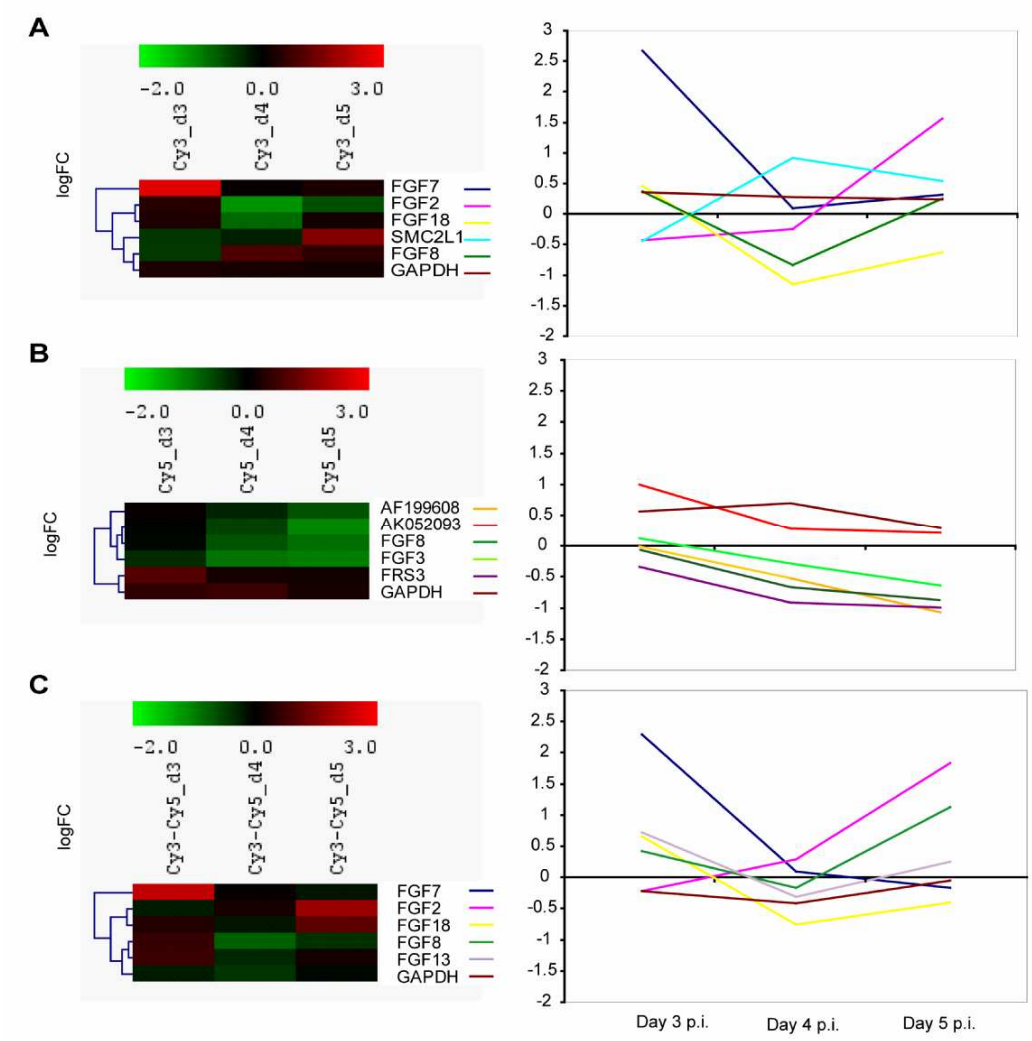

Fig. S5. Microarray analysis. Heatmaps and plotted values of the logFC values on days 3, 4 and 5 p.i. (with respect to time 0) for unsupervised selection of fibroblast-related genes with the largest variability on spleen samples of mice infected with 17X(Cy3) (A); 17XL (Cy5) (B) and 17X-17XL differences (Cy3–Cy5) (C) together with a housekeeping gene (GAPDH) with small variability.

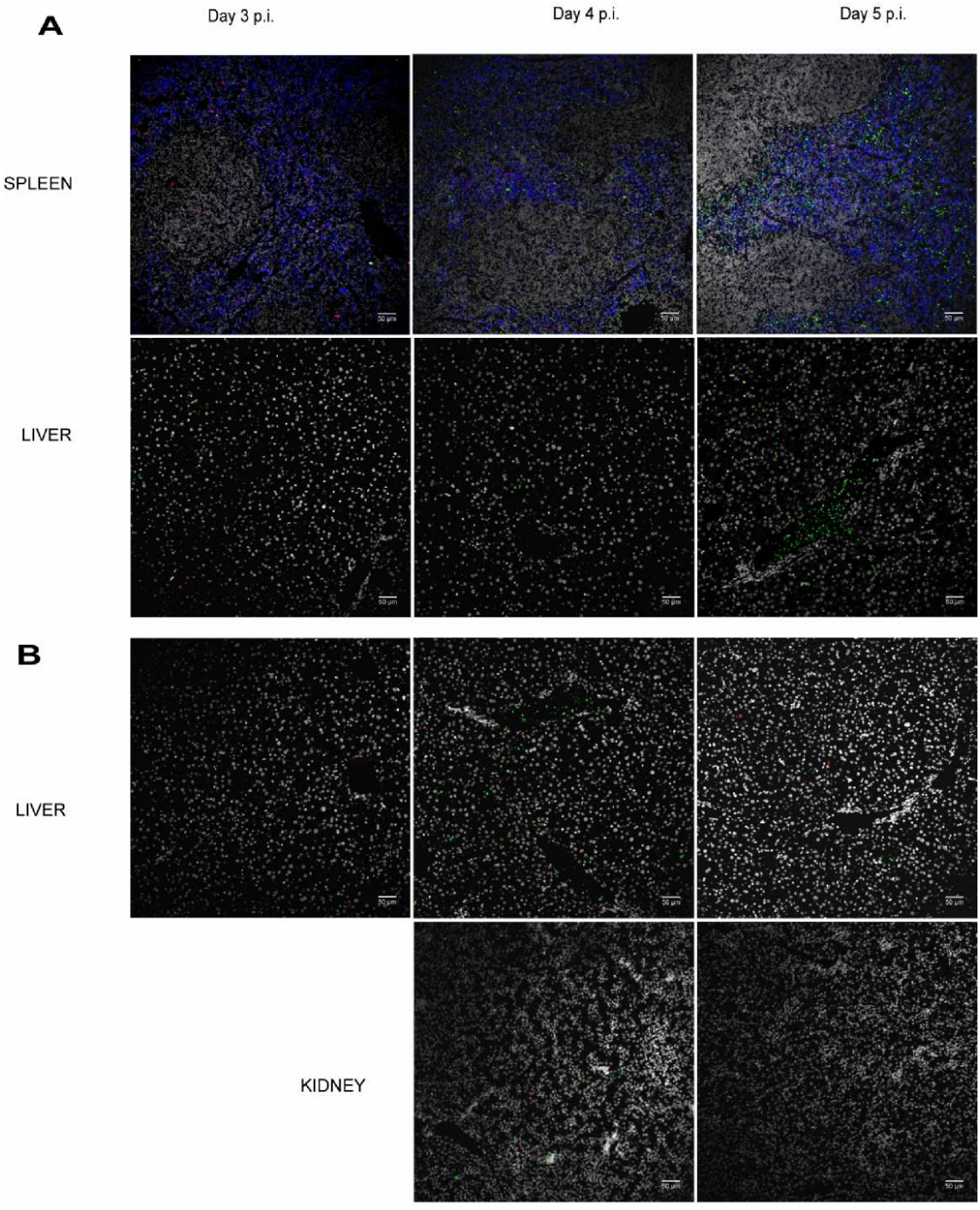

Fig. S6. Strain and tissue specificity of the *P. yoelii* 17X-induced barrier. Time-series immunohistofluorescence of tissue sections. (A) Sections of spleen and liver of mice infected with *P. yoelii* 17XL lethal strain. No specific staining for FGF8 was observed in cryosections of infected mice on days 3 to 5 p.i. (B) Immunofluorescence of liver and kidney cryosections in 17X infected mice was also negative for FGF8. Staining for FGF8 (red), GFP (green), F4/80 macrophage receptor in the spleen (blue) and nucleic acids (gray) was performed. Scale bars represent 50 µm.

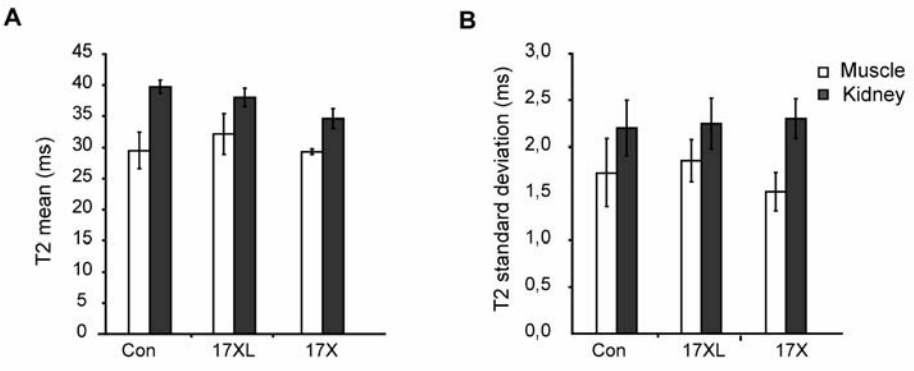

Fig. S7. MRI analysis of the muscle and kidney. (A) T2 mean relaxation times quantified in circular regions of the back muscle and the outer part of kidney from T2 maps of coronal T2-weighted images containing the spleen (Figure 6). (B) Variance of T2 values in the selected areas of muscle and kidney. T2 times (msec) are expressed as the mean ± SEM of four to five mice from each group (control, lethal and non-lethal). No significant differences were observed.

Movies

Movie S1. IVM movie of a representative dextran-labeled (red) spleen vessel (10.4 µm lumen diameter) in a mouse infected with the 17X GFP line (green) at 1% parasitemia used for blood flow analysis. Scale bars represent 10 µm. Quick-time. S1 (4.6 MB, 9 sec).

Movie S2. Time-lapse intravital microscopy images of the murine spleen infected with 17XL GFP-transgenic parasites at 10% parasitemia (Z-maximum projection). Parasite and tissue autofluorescence are shown in green and red respectively. Scale bars represent 10 µm and the time interval is in sec. Quick-time. S2 (4.1 MB, 10 sec).

Movie S3. Time-lapse intravital microscopy images of the murine spleen infected with 17X GFP parasites at 10% parasitemia (Z-maximum projection). Parasite and tissue autofluorescence are shown in green and red respectively. Scale bars represent 10 µm and the time interval is in sec. Quick-time. S3 (2.6 MB, 10 sec).

Movie S4. IVM Z-coded color video of the murine spleen infected with 17XL showing three-dimensional movement of parasites. These videos were used as a tool to follow single-particle movement over time. Each time point is the result of a projection from 5 different depths (Z) with a Z-delay of approximatively 0.06 sec. Depth code: yellow (0 µm), orange (2 µm), pink (4 µm), blue (6 µm), green (8 µm). Quick-time. S4 (0.9 MB, 3 sec).

Movie S5. IVM video of representative area of the spleen of mice infected with 17X at 1% peripheral parasitemia. Selected area focus on an example of the dynamic adherence of pRBCs to spleen cells. Twenty-seven percent of the parasites from the non-lethal line remained in the spleen for more than 20 sec, compared to 4% in the lethal line. Quick-time. S5 (0.7 MB, 6 sec).

Movie S6. IVM video of representative area of the spleen of mice infected with the 17X at 1% peripheral parasitemia. Selected area focus on examples of the dynamic adherence of pRBCs to spleen cells. Quick-time. S6 (0.6 MB, 6 sec).

Movie S7. Animation illustrating our present model of *P. yoelii* 17X line-induced spleen remodeling, infected RBC adherence to the tissue barrier and macrophage-clearance evasion. Quick-time. S7 (1.1 MB, 11 sec).

6.3 *Adherence of* Plasmodium vivax *infected reticulocytes to the human spleen*

6.3.1 Summary

Objectives

To study the adherence of *P. vivax* infected reticulocytes to the human spleen and to investigate whether VIR proteins are involved in this process.

Results

1. We report adhesion of *P. vivax*-infected reticulocytes obtained from the blood of infected patients to cryosections of normal human spleens.
2. pRBCs adhered to fibroblast and endothelial cell lines with similar intensity.
3. We observed a trend in inhibition of such adherence when using antibodies against VIR proteins suggesting a role of these variant proteins in such adhesion.

6.3.2 Report 3

Adherence of *Plasmodium vivax*-infected reticulocytes to the human spleen

Mireia Ferrer[1]
Hernando A. del Portillo[1,5]

Coinvestigators
Fabio T. M. Costa[2]
Paulo Nogueira[3]
Marcus V. G. Lacerda[4]

Institutions
[1]Barcelona Centre for International Health Research (CRESIB), Barcelona, Spain
[2]Departamento de Genética, Evoluçao e Bioagentes, Instituto de Biologia, Universidade Estadual de Campinas (UNICAMP), Campinas, Brazil
[3]Centro Leonidas e Maria Deane, Fiocruz, Manaus, Brazil
[4]Fundaçao de Medicina Tropical do Amazonas (FMT-HVD), Decepen, Gerência de Malária, Manaus, Brazil
[5]Institució Catalana de Recerca i Estudis Avançats (ICREA), Barcelona, Spain

SUMMARY

This scientific report summarizes the work performed in collaboration with the laboratories of Dr. Fabio T.M. Costa (UNICAMP, Campinas, Brazil), Dr. Paulo A. Nogueira (Fiocruz, Manaus, Brazil) and Dr. Marcus V. Lacerda (FMT-HVD, Manaus, Brazil) during the months of November 2009 and November 2010 which main objective was to study the cytoadherence of *Plasmodium vivax* infected reticulocytes to the human spleen. *Plasmodium vivax* is a parasite that causes malaria with high incidence in Latin America and Asia where it contributes to the morbidity of the inhabitants. In previous studies using the Plasmodium yoelii mouse model, we discovered the importance of the spleen to infection by this parasite. To extrapolate the results obtained in the mouse model of malaria, we performed in vitro adhesion assays using blood from infected patients on human spleen cryosections. Significantly, our results demonstrated adherence of infected reticulocytes to the red pulp of the spleen, with variable intensity depending on the isolate and section used. Moreover, inhibition assays were performed to explore the role of VIR proteins in adhesion. Despite the inherent variability when working with field isolates, a trend in inhibition was observed that may suggest involvement of these proteins in parasite adhesion. In the future, additional experiments including immunofluorescence assays will be performed to complement the results obtained in Brazil.

1. INTRODUCTION

Plasmodium vivax is the most widely distributed human malaria parasite and responsible each year for 100-300 million clinical cases including severe disease manifestations and death. The technological advances enabling the sequencing of the *P. vivax* genome and a recent call for global malaria eradication together have placed new emphasis on the potential and importance of addressing *P. vivax* as a major public health problem. Pathology in malaria is associated with the capacity of infected red blood cells to escape immune responses and establish chronic infections. In the case of *P. falciparum*, cytoadherence of infected red blood cells containing mature stages of the parasite in the deep capillaries of internal organs avoids passage through the spleen, where these cells would be targeted for destruction. Notably, cytoadherence is mediated by the *var* multigene family. *P. vivax* invades predominantly, if not exclusively, reticulocytes and it is amply accepted that infected-reticulocytes do not cytoadhere in the deep capillaries of inner organs having an obligate passage through the spleen. Contrary to this view, it has been recently shown that *P. vivax* infected reticulocytes adhere to endothelial receptors of lung and placental tissues (Carvalho, B., et al., 2010, J Infect Dis 202(4):638-47). The question remains as to how *P. vivax* is able to escape spleen clearance to establish chronic infections and whether VIR proteins have a role in such an escape.

Based on work of L. Weiss and collaborators (Weiss, L., 1991, Imm Today 12:24), we have advanced a hypothesis postulating that this parasite induces the formation of spleen barrier cells where infected reticulocytes specifically cytoadhere through variant VIR proteins or other ligand(s) yet to be identified. This way, infected reticulocytes are physically protected from direct contact with spleen macrophages and consequently escape spleen clearance. Moreover, free vivax merozoites readily encounter reticulocytes, their specific host-cell for invasion, as spleen erythropoiesis is induced by infections. In doing so, *Plasmodium*-harboring reticulocytes prolong parasitism and establish chronic infections.

To advance this hypothesis, we have used the rodent malaria model of Balb/c mice infected with the reticulocyte-prone non-lethal *P. yoelii* 17X strain, resembling *P. vivax*, and the normocyte-prone lethal *P. yoelii* 17XL strain, resembling *P. falciparum*. We have implemented intravital microscopy and magnetic resonance imaging of the mouse spleen in experimental infections. Notably, there was higher parasite accumulation, reduced motility, loss of directionality, and altered magnetic resonance features only in spleens of mice infected with the 17X strain. Moreover, these differences were associated with the formation of a strain-specific induced spleen tissue barrier, with macrophage-clearance escape, and with cytoadherence of infected reticulocytes to this barrier. Thus, reticulocyte-prone non-lethal malaria parasites appear to induce remodelling of the spleen to both evade the immune response and to establish chronic infections (Martin-Jaular, L., et al., 2011, Cell Microbiol 13(1):109-22). Together, this data suggests that adherence to the spleen by malaria parasites is directly correlated with malaria pathogenesis. It will be interesting to determine the inter-cellular communication signals that induce this remodelling of the spleen and the ligand-receptors involved in cytoadherence. In addition, we postulate that a similar mechanism occurs in *P. vivax*, a reticulocyte-prone non-lethal human malaria parasite.

Demonstrating cytoadherence of *P. vivax*-infected reticulocytes to the human spleen is a rather

difficult objective as biopsies are unethically doable and obtaining spleens from *P. vivax* patients with spleen rupture or sudden death are difficult to obtain due to the low casuistic numbers. Nevertheless, these studies remain of fundamental value to understand the pathophysiology of *P. vivax* and thus we have started pioneer ex-vivo studies on spleen cytoadherence of *P. vivax*-infected reticulocytes. To do so, serial cuts of spleens from human patients undergoing splenectomy at the Hospital Clinic in Barcelona were placed in microscope slides and transported to Manaus, Brazil. *P. vivax*-infected reticulocytes were incubated in such slides for 1h at 37oC and after extensive washing the slides were stained with Giemsa.

2. OBJECTIVES

The purpose of this work is to study the cytoadherence of *P.vivax* infected reticulocytes (pRBCs) to the human spleen and to investigate whether VIR proteins are involved in this process.

Main Objective:

- To study the cytoadherence properties of *P. vivax* parasites to the human spleen

Specific Objectives:

- To perform cytoadherence experiments of *P. vivax* parasites on cultured fibroblast and endothelial cells
- To determine if VIR proteins play a role in such adherence

Ethics statement

All the studies involving *P. vivax* infected blood had received the oral informed consent of their donors. Human spleen biopsies received multiorgan donation agreement.

3. METHODOLOGY

Human biopsies

Uninfected control spleens were obtained from patients suffering from spleen-unrelated pathologies and submitted to splenectomy at the Hospital Clínic de Barcelona, Spain. Other organs such as lung and placenta were also collected from Hospital Clínic to provide control samples for our studies. All samples available had been snap-frozen in liquid nitrogen and stored frozen until cryosectioning and were obtained according to ethical guidelines from the hospital. 5 um cryosections of spleens were placed on 4-well printed Superfrost slides for static adhesion assays.

Parasites

P. vivax-infected reticulocytes were obtained from patients presenting to Fundaçao de Medicina Tropical do Amazonas (FMT-HVD), Brazil, in collaboration with Dr. M. Lacerda, after their informed consent. Blood from patients with confirmed *P. vivax* parasitemia was collected and enriched for mature stages using 45% Percoll gradient as described (Carvalho, B., et al., 2010, J Infect Dis 202(4):638-47). Mature enriched infected RBC (pRBC) were collected from the brownish interphase, washed and resuspended in adhesion media (RPMI1640, pH 6.8). Number of pRBC/ml were calculated as

%parasitemiaxnºcells/ml.

P. falciparum parasites of the line FCR3 panned for CSA were obtained from synchronized continuous *in vitro* culture. To concentrate for mature pRBCs, culture was let stand in a solution of Voluven 1h at 37ºC. After that time, supernatant was recovered and washed as described above.

Cells

Human fibroblast cell lines HLEC (human lung endothelial cells), MCF-7 (mammal carcinoma fibroblasts) and WI-38 (human fetal lung fibroblast) were originally purchased from ATCC (www.atcc.org). Cells were maintained in culture with DMEM media supplemented with 10% FBS and 1% PenStrep in a humidified incubator at 37ºC, 5% CO_2. Spleen-derived fibroblasts were originally obtained from primary cultures of human spleen tissue and maintained in culture with RPMI media supplemented with 15% FBS and 40mg/L Gentamycin in a humidified incubator at 37ºC, 5% CO_2. For adhesion experiments, $5 \cdot 10^4$ cells/well (300ul/well) were plated in 8-well chambered slides (LabtekII) and incubated for 48h at 37ºC, 5% CO_2.

Cytoadherence

To study the adhesive behaviour of *P. vivax* infected reticulocytes, static adhesion assays were performed on cells and tissue cryosections using the methodology described by our collaborators (Carvalho, B., et al., 2010, J Infect Dis 202(4):638-47). Briefly, spleen cryosections were thawed, washed in adhesion media and incubated with 10^5 pRBCs/tissue in 20ul of adhesion media. When using cell cultures for adhesion experiments, cells grown to 60-80% confluence in 8-well chambered slides were washed three times in adhesion media and incubated with 10^5 pRBCs/well in 300ul of adhesion media. After incubating for 1 hour at 37ºC, 5% CO2, slides were extensively washed in the same media, air-dried and stained with Panotico Rapido kit for enumeration of adherent parasites under a light microscope. To allow for immunohistofluorescence assays, in some experiments slides were fixed with cold methanol and stored frozen.

Inhibition assays

Two different sera obtained in guinea pig and raised against VIR peptides (M6 and M7) were tested for inhibition of adhesion of P.vivax infected reticulocytes to the spleen. A serum reacting against the merozoite surface protein MSP1 19 (M5) and a preimmune serum (M3) were also used in inhibition assays. Inhibition of adhesion was performed by preincubating the parasites in adhesion media containing a ¼ dilution of the sera for 30 minutes at RT before incubating with the cells/tissues as described above.

Quantitative analysis

Stained slides were visualized using a Zeiss Axiostar plus light microscope fitted with a 100x oil objective. For quantification of adherent pRBC, each section was divided into four areas and pRBCs enumerated in 10 optical fields over each area. Numbers of pRBC were normalized by the area estimated.

4. RESULTS AND DISCUSSION

4.1. Collection and enrichment of P. vivax *infected blood*

After their informed consent, peripheral blood (2-4 ml) was collected from 18 patients presenting at the FMT-HVD with confirmed parasitemia for *P. vivax*. All the patients suffered from non-severe malaria and were in age between 20-40 years old. Parasitaemia and parasite species were determined by expert microscopists at the FMT-HVD through the examination of thick blood smears. The table below contains some relevant information on the patients' blood used for the study and on the parasite enrichment yield.

Period	Patient id. number	Parasitemia (crosses)	Previous malarias	% enrichment post-percoll			Number of total pRBC ($x10^5$)
				pRBC	uRBC	WBC	
November 2009	132	2	nd	100	nd	nd	170
	133	2	nd	100	nd	nd	17
	147	2	nd	100	nd	nd	15
	155	2	0	100	nd	nd	38
	156	2	1	100	nd	nd	36
	159	2	4	90	nd	nd	16
	160	2	7	80	nd	nd	31
November 2010	205	1	2	45	10	45	1,4
	206	2	nd	44	44,16	12	12
	207	3	1	97	3	0	870
	208	2	0	15	nd	nd	3,4
	211	2	nd	60	nd	nd	24
	214	2	2	71	11	17	16
	215	2	nd	23	37	44	3,4
	218	2	2*	95	3	2	150
	220	2	2	33	44	22	37
	221	1	2	26	54	20	5,2
	224	1	2*	25	50	25	15
	225	2	nd	40	56	4	20
	226	2	0	45	27	27	50
	227	1/2	0	30	50	20	10
	228	2	2*	53	44	3	640
	230	1/2	0	30	42	25	11
	232	1/2	1	65	25	10	8,1
	234	2	4*	43	15	40	3,5

Table 1. Patients recluted and results of parasite enrichment. Parasitemia varied between ½ and 3 crosses (0,4 and 200 parasites/field respectively). Percentage of parasitized red blood cells (pRBC), uninfected red blood cells (uRBC) and white blood cells (WBC), were determined on smears from the enriched fraction. nd: not determined. (*): Last malaria within the past 4 months.

After parasite enrichment, contamination of *P. vivax* isolates with host leukocytes was due to the similar density of these cells, which concentrated into the same interphase. Though some methods are described for the removal of leukocytes from peripheral blood, we decided not to include any extra step as it diminishes the yield of pRBC enrichment. Some samples presented high numbers of uRBCs that aggregated to pRBCs. The percentage of pRBCs over these cells was used to calculate the number of cells in order to dispense 10^5 pRBC for each adhesion assay.

4.2. Adhesion of P. vivax *to endothelial and fibroblast cells*

Adhesion of *P. vivax* parasites obtained from fresh isolates was performed in HLEC (human lung endothelial cells), MCF-7 (human breast cancer fibroblast cells) and WI-38 (human embryonic lung fibroblast cells) cell monolayers. FCR3CSA parasites were included as control of adhesion. The number of pRBC per area (mm^2) were determined and values normalized with respect to FCR3CSA.
The adhesive profile of *P. vivax* isolates was 10 to 100-fold lower than for FCR3CSA parasites, with MCF-7 showing 4-fold higher adhesion than WI-38 cells (figure 1). FCR3CSA adhesion was similar in both lung cell lines (HLEC and WI-38) and 1.3-fold lower in the breast cancer cell line MCF-7 when compared to the lung cells (not shown).

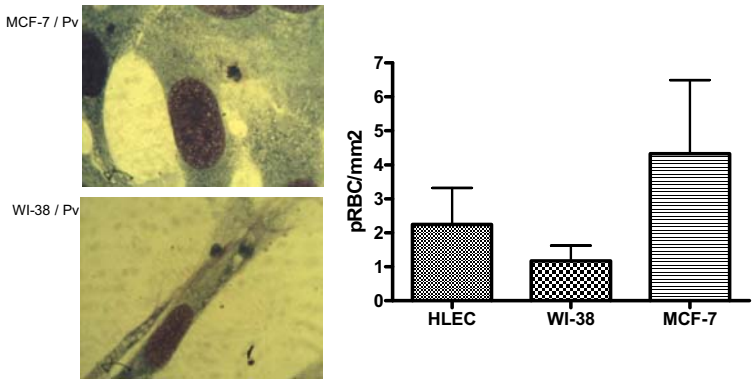

Figure 1- Adhesion of *P. vivax*-pRBCs to endothelial and fibroblast cells.
Representative images of Giemsa stained cells are shown. Results are shown as the mean +/- s.e.m. from 4 patients (November 2009).

To explore the adhesive behaviour of *P. vivax* infected reticulocytes to spleen fibroblasts, a fibroblast-like cell culture was derived from primary culture of spleen explants and used for cytoadherence experiments. However, we could not fully accomplish this objective due to contamination of the cell culture with bacteria, and the only two isolates that were tested gave low adhesion (<1parasite/100cells).

4.3. Adhesion of P.vivax to spleen cryosections

A preliminary study on *P. vivax* adhesion to spleen, placenta and lung tissue was performed in November 2009. Of interest, FCR3CSA parasites showed similar adhesion to all the organs whereas *P. vivax* isolates had preferred adhesion for either lung (132, 133, 147) or spleen (155, 159, 160) cryosections (figure 2).

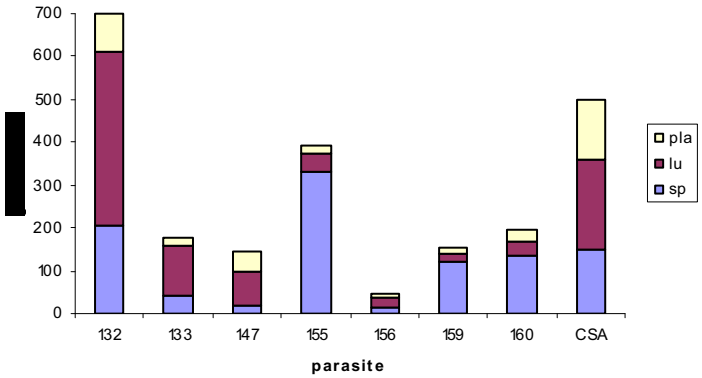

Figure 2- Representation of the adhesion assays of Pv and FCR3CSA parasites to spleen, placenta and lung cryosections. Values are shown in cumulative bars for each isolate.

Based on the results obtained, adhesion assays were performed in November 2010 using cryosections of different "normal" spleen biopsies (C1 to C3). An "immunoactivated" spleen biopsy from a patient with lupus disease (L1), where we had previously observed high adhesion of pRBCs, was included as control for adhesion. Noticeably, a total of 18 *P. vivax* and 1 *P. falciparum* isolates (November 2010) were tested in single adhesion experiments, with a few performed in duplicate because of the scarcity of material. Results from quantification of adherent pRBC are presented in figure 3.

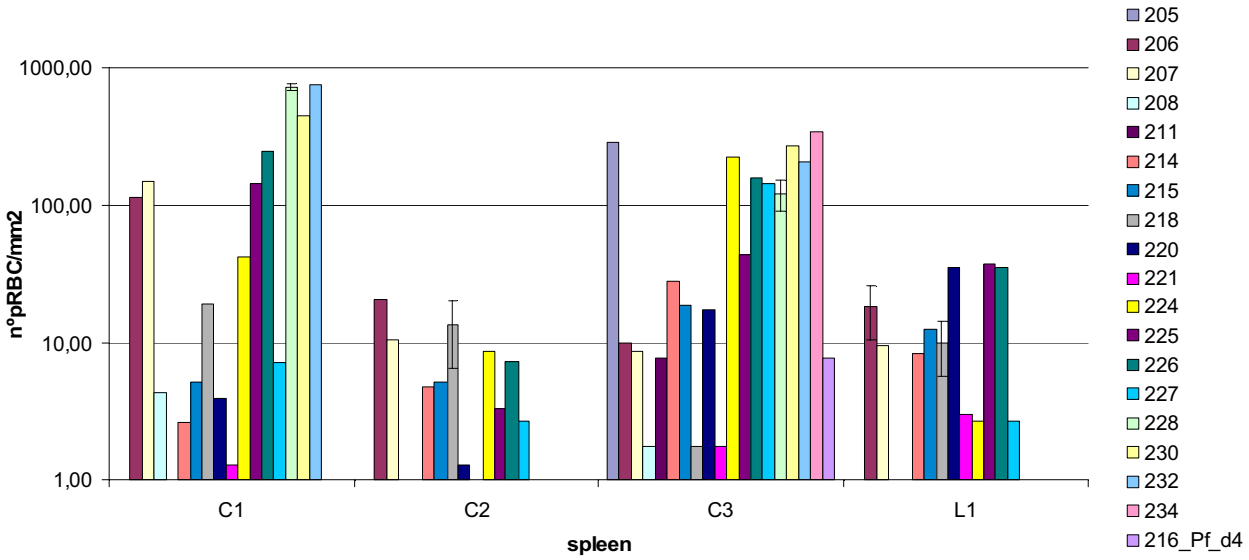

Figure 3- Cytoadherence of *P.vivax* isolates to normal (C1-C3) and immunoactivated (L1) spleen sections. Number of pRBC per area (nºpRBC/mm^2) is presented for each parasite in y-axis, with logarithmic scale. In duplicate experiments, results are expressed as the mean +/- s.e.m.

Results demonstrated the adhesion capacity of *P.vivax* infected reticulocytes to the human spleen (figures 3 and 4). Adhesion to the red pulp of the spleen was observed for all the parasites tested, with spleens C1 and C3 showing the highest adhesion profile, though, as expected, high variability between isolates was observed. An isolate of *P. falciparum* that was maintained for 4 days in culture (216_Pf_d4) was included as a specificity control for adhesion. Of importance, adhesion to the immunoactivated

spleen L1 occurred preferentially at the lumen of vessels and tissue borders, whereas in control spleens parasites accumulated in the red pulp. The high adhesiveness of these spleens could be attributed to differences in red pulp area represented in the sections.

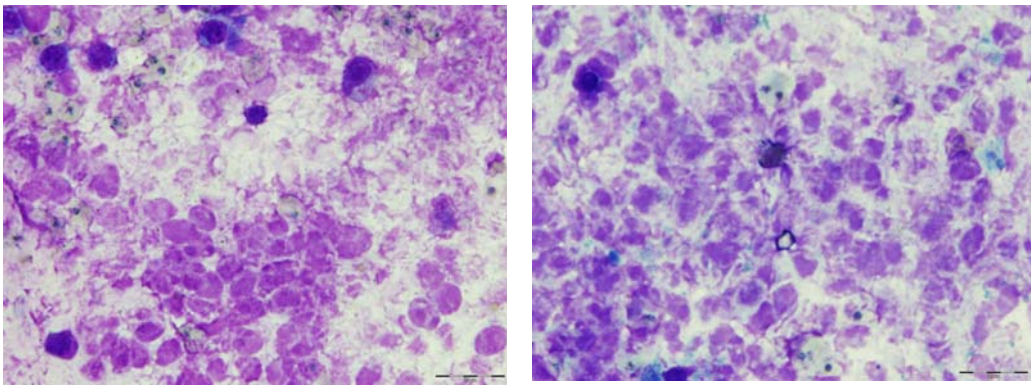

Figure 4- Images of adherent pRBCs to the spleen. Representative images of stained slides were obtained under a light microscope equipped wih a 60x oil objective.

Moreover, quantitative analysis of each adherent cell type is shown in figure 5, where differences in leukocyte affinity and pRBC-uRBC aggregates can be observed between tissues and isolates.

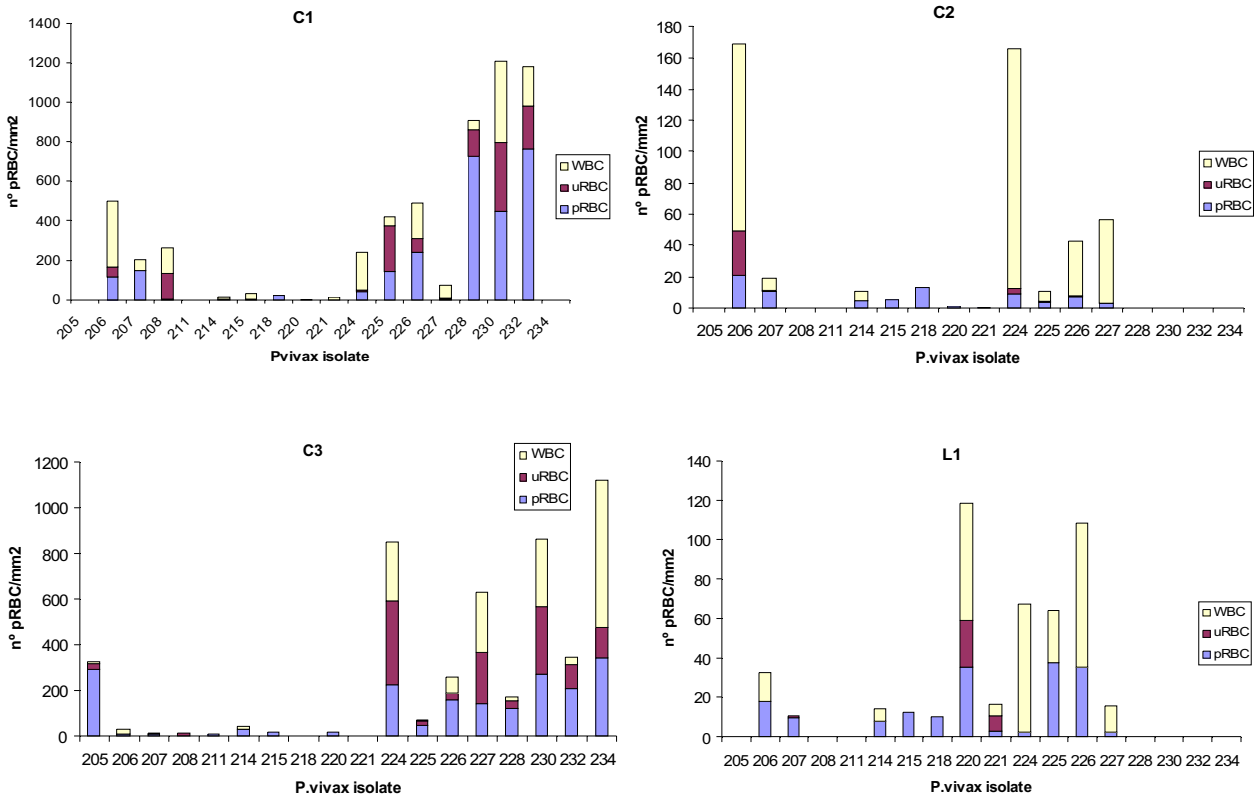

Figure 5- Cytoadherence of different cell types. All adherent cells were quantified and represented in cumulative bars.

4.4.Role of VIR proteins in mediating adhesion

We aimed to study if VIR proteins might play a role in mediating adhesion of infected reticulocytes to the spleen. Therefore, inhibition adhesion assays were performed with 11 *P. vivax* isolates in the presence of sera reacting against two different VIR peptides (M6 and M7). A serum reacting against the MSP1 of *P. vivax*, which is known to be exported at the surface of the reticulocyte at late stages, was also included. Results are shown in figure 6.

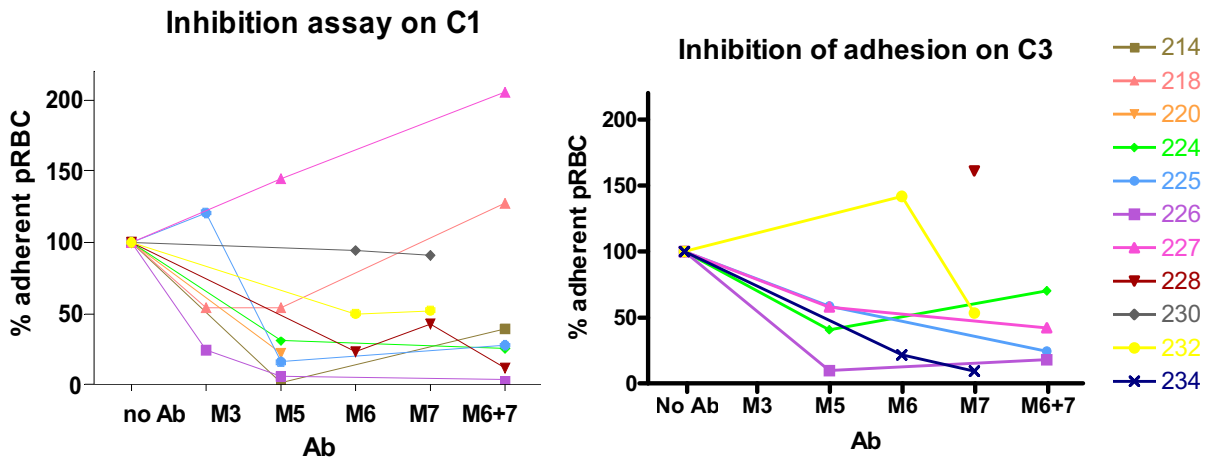

Figure 6- Inhibition adhesion assays of P.vivax to the spleen using anti-VIR sera. Adhesion assays with different P.vivax isolates were performed on sections of spleens C1 and C3 in the presence of preimmune sera (M3), anti-MSP1 sera (M5), or anti-VIR sera (M6 and M7). Results are expressed in percentage with respect to adhesion values in the absence of antibodies.

We performed the inhibition assays on spleens C1 and C3 as they were where highest adherence was reported. As shown in the graphs, most isolates were inhibited by the presence of immune sera. These results will be complemented through immunofluorescence analysis of the isolates used for inhibition to detect VIR and MSP1 expression. However, the inhibitory effect obtained with preimmune sera in two out of three isolates make it difficult to conclude whether this inhibition might be specific.

5. CONCLUSIONS AND FUTURE

Studying adhesion of *P. vivax* to the human spleen is a complex objective with several limitations due to the difficulty in obtaining human biopsies and the lack of a continuous in vitro culture of the parasite. We reported adhesion of several *P. vivax* isolates to three different control spleens and one immunoactivated spleen. We observed a broad range of adhesion intensity between isolates, with spleens C1 and C3 showing the highest number of adherent parasites. Finally, in an attempt to study if VIR proteins may play a role in such adhesion, we performed inhibition adhesion assays where we observed a trend in inhibition. In conclusion, to the best of our knowledge, this is the first report showing adherence of *P. vivax* to the spleen, opening new avenues for studying the physiopathology of this organ in malaria and the ligand-receptors involved in adherence.

To complement the results obtained, nested PCR of blood samples will be performed for each isolate to confirm *P. vivax* specificity and immunofluorescence assays of blood smears will provide information on

the expression of VIR and MSP1 proteins in infected cells. Moreover, characterization of spleen tissues through immunohistofluorescence for different fibrotic markers will be performed.

6. AKNOWLEDGEMENTS

We are very grateful to Stefanie Lopes for all the logistic, technical and experimental support and contribution in this work; to Juliana Leite, Bruna Carvalho and Wanessa Neiras for helping in parasite processing; to Erecilda Araujo for helping in the obtention of blood samples; to the Malaria Diagnostic Unit at FMT-HVD for microscopy; to Jaume Ordi and Angel Ruiz for providing tissue cryosections; to Carmen Fernandez and Lorena Martin for anti-VIR and anti-MSP1 antibody production; and to all the patients involved in this work.

Funding

Work in the laboratory of HAP is funded by the European Community's Seventh Framework Programme (FP7/2007-2013) under grant agreement Nº 242095, by the Private Foundation CELLEX (Catalonia, Spain), and by the Spanish Ministery of Science and Innovation (SAF2009-07760). The stage of MFA was funded by a grant from AGAUR/Generalitat de Catalunya.

6.4 *Spleen rupture reveals intense plasmablastic proliferation in subcapsular and perivascular spaces in a case of untreated* Plasmodium vivax *infection*

6.4.1 Summary

Objectives

To study the immunohistopathology of the spleen in the course of a *P. vivax*-infection and determine if pRBCs are sequestered in the tissue.

Results

1. The spleen of a 19-year old man undergoing splenectomy due to traumatic splenic rupture was obtained and preserved for histopathological analysis.
2. Nested-PCR analysis of peripheral blood and splenic tissue revealed a subpatent non-treated *P. vivax*-infection and excluded *P. falciparum* coinfection.
3. Immunohistofluorescence analysis of spleen sections using anti-VIR antibodies showed the presence of pRBCs in the red pulp, mostly outside CD68 macrophages.
4. Morphological analysis reported white pulp expansion and a diffuse hipercellularity in the splenic red pulp, as compared to uninfected spleens. As well, infiltration by immunoblasts and plasma cells was observed in the cords.
5. Immunohistochemical characterization of the tissue was performed using an array of antibodies against different immunological markers. Importantly, double immunostaining with CD138 and the Ki-67 proliferation marker revealed a plasmablast expansion and proliferation in subcapsular and perivascular compartments.

6.4.2 Article 4

Spleen rupture reveals intense plasmablastic proliferation in subcapsular and perivascular spaces in a case of untreated non-severe *Plasmodium vivax* infection

Marcus Lacerda, M.D., Ph.D., André M. Siqueira, M.D., Belisa Magalhães, M.Sc., Gisely Melo M.Sc., Paola Castillo, M.D., Mireia Ferrer, M.Sc., Lorena Martin-Jaular, Ph.D., Carmen Fernandez-Becerra, Ph.D., Jaume Ordi, M.D., Antonio Martinez, M.D., Ph.D., and Hernando del Portillo, Ph.D.

From the Fundação de Medicina Tropical Dr. Heitor Vieira Dourado (FMT-HVD) and Universidade do Estado do Amazonas (UEA), Manaus, Brasil (ML, AMS, BM, GM), the Barcelona Centre for International Health Research (CRESIB) (MF, LM-J, CF-B, HP), the Laboratory of Pathology, Hospital Clínic, Barcelona (PC, JO, AM), and the Institució Catalana de Recerca I Estudis Avançats (ICREA) (HAP), Barcelona, Spain.

Correspondence

ML (marcuslacerda.br@gmail.com) Fundação de Medicina Tropical Dr. Heitor Vieira Dourado, Av. Pedro Teixeira 25, 69040-000, Manaus, Brazil and HAP (hernandoa.delportillo@cresib.cat) Barcelona Centre for International Health Research (CRESIB), Hospital Clinic/IDIBAPS, Universitat de Barcelona, Centre Esther Koplowitz Roselló 153, 1a planta, 08036, Barcelona, Spain.

SUMMARY

We report the unique case of a 19-year old non-immune patient with *P. vivax* monoinfection confirmed by PCR in the peripheral blood and in the spleen section, who was splenectomized due to spleen rupture two days prior to the diagnosis and treatment of the malarial infection. Microscopic analyses evidenced white pulp expansion and a diffuse hypercellularity in the splenic red pulp, with intense proliferating plasmablasts in the subcapsular and perivascular compartments as well as *P. vivax*-infected reticulocytes in the cords, in the absence of other concomitant infectious diseases. To our knowledge, this is the first full detailed immuno-histopathological characterization of a non-treated *P. vivax*-infected spleen.

For a long time *Plasmodium vivax* infection has been associated with a benign course, leading to an unjustified neglect of its importance.[1] However, the recent call for malaria eradication has strongly pointed the need for a more prominent position for this parasite in the research agenda.[2] *P. vivax* is the most widely distributed *Plasmodium* species infecting humans, with around 2.85 billion people living at risk of infection,[3] and 300 million annual cases.[4] Based on some of its biological particularities and historical malaria control program reports, experts agree that the current control tools will not suffice for *P. vivax* elimination, requiring the development of specific control measures.[5] Regarding clinical manifestations of severity of *P. vivax* infection, the attention has always been directed to spleen-related complications such as splenic hematoma and specially spleen rupture.[6] In the last decade, however, there have been numerous reports from distinct areas of severe manifestations associated with exclusive *P. vivax* infection, including anemia, thrombocytopenia, acute respiratory distress syndrome and death,[7-10] further contributing to deconstruct the benignity attributed to *P. vivax* and to highlight gaps in knowledge of clinical aspects of severe disease in this infection.[5]

The spleen is a complex organ involved in both the removal of damaged and parasitized red blood cells and in the generation of immunity, consequently having a pivotal role in malaria.[11] Enlargement of the spleen is a well-known clinical feature of malaria and it is estimated to occur in 70-80% of cases, with its size normalizing after successful treatment.[12] In areas of intense transmission, the spleen is palpable in 50-80% of individuals, being directly associated with immunity acquisition, as shown by its higher prevalence in children and correlation with both antibody levels and host genetics.[13,14] In addition, the population prevalence of palpable spleens (the spleen rate) has been widely adopted as a measurement tool of malaria transmission.[15]

The real incidence of splenic complications is unknown as there is substantial underreport of mild, asymptomatic and non-complicated cases. An extensive review of published cases of splenic rupture demonstrated that it is most commonly observed during the primary attack in non-immune individuals and that the conservative treatment seems to be appropriate in most cases.[16] The essential role of the spleen in the control of parasite loads is also reinforced by higher parasitemias and increased clinical severity in patients who suffered splenectomy.[17] Furthermore it has been shown that individuals with chronic *Plasmodium* carriage can present symptomatic malarial episodes 3-8 weeks after splenectomy,[17] mostly seen in hyperendemic areas affecting individuals who have suffered several malaria attacks.

Notwithstanding the critical role of the spleen in malarial infection, the understanding of the spleen architecture and dynamics is mostly restricted to experimental studies and pathological analysis of already treated splenectomized patients with *P. falciparum*.[17] Not a single case was ever reported addressing the full morphological and immunohistochemical characterization of the spleen in patients with *P. vivax* monoinfection.

CASE REPORT

A 19-year-old man was admitted in a general hospital in the city of Manaus, located in the Western Brazilian Amazon, after having an accidental blunt abdominal trauma. He was diagnosed with spleen rupture and intra-abdominal hemorrhage, which prompted immediate splenectomy. In the previous two days before surgery, the patient had begun to develop intermittent low-grade fever associated with chills, headache and generalized asthenia. The initial routine investigation performed by the Surgery Department did not reach any diagnosis and in the eighth day post-surgery the patient was transferred to infectious diseases specialized care at the Fundação de Medicina Tropical Dr. Heitor Vieira Dourado, a tertiary care hospital which hospitalizes patients with vivax malaria in a 10-bed ward for investigational purposes.

The only laboratory abnormalities were mild anemia (Hb 8.7 g/dL) and thrombocytopenia (66,000 platelets/mm^3). Blood biochemical analysis was in the normal range. A thick blood smear disclosed *P. vivax* infection with a semi-quantitative parasitemia between 10.000 and 100.000 parasites/mm^3. Real-time polymerase chain reaction (PCR) confirmed *P. vivax* monoinfection in the peripheral blood in the day of the diagnosis. The patient lived in an urban area of Manaus where there is no malaria transmission and had no previous history of malaria infection. He referred having gone to a rural region close to the city 20 days before the accident, when supposedly infection occurred. Treatment was initiated with chloroquine (1,500 mg divided in three days) and primaquine (30mg/day during 7 days), according to the National Program for Malaria Control guidelines. Both fever and parasitemia were cleared within 48 hours. The patient was discharged in the third day of treatment and he did not develop any relapse nor had any other complications through a one-year follow-up. An extensive histopathological exploration of the surgically removed spleen was performed in

order to provide a thorough characterization of the effects of *P. vivax* infection in this organ during an active and untreated infection.

METHODS

Tissue preparation

After surgery, a large spleen of 1,300 grams with a capsule rupture in the colic surface was obtained from this patient and a portion of it was fixed in 10% buffered formalin for routine histopathological analysis. As control, a spleen from a normal individual who suffered a trauma forcing splenectomy was sampled and fixed as above. Tissue sections were embedded in paraffin blocks and 4 µm sections were routinely used for immuno-histopathological analyses.

Extraction of parasite DNA from formalin-fixed paraffin-embedded tissue

Twenty paraffin tissue sections of 10 µm were used for DNA extraction. Tissue sections contained in a 1,5 ml tube were dewaxed in two changes of 1ml xylene for 5min at RT, washed in two changes of ethanol 100% for 5min at room temperature (RT) and air-dried for 30 min at RT. Tissue lysis was performed by incubating at 52^{o}C overnight in 500 µl of lysis buffer containing Proteinase K (10mg/ml), TrisHCl (pH8, 1M), EDTA (pH 8.0, 0,5M) and SDS (10%) in distilled water. In some tissues, additional proteinase K was used to complete lysis. DNA was extracted with phenol/chloroform/isoamyl alcohol and precipitated in cold ethanol and sodium acetate (pH 5.2, 3M).

Nested-PCR

Nested PCR using 200 ng of DNA was performed as previously described [18] to confirm *P. vivax* infection and exclude *P. falciparum* infection. Fragments were resolved and visualized on 2% agarose gels stained with sybr green.

Immunohistochemistry of formalin-fixed paraffin-embedded tissues

Immunohistochemistry was performed on 4 µm sections of formalin fixed, paraffin embedded tissue using the automated immunohistochemical system AUtostainer ik 48 (Dako Co., Carpinteria, CA, USA).[19] Briefly, sections were dewaxed, and antigen retrieval was carried out by treating the slides with EnvisionTM FlexTarget Retrieval Solution Low pH (Dako®), using a PTLink (Dako®). Hereafter, an automated immunostainer device Autostainer Link 48 (Dako®) was used. Sections were incubated with a primary mouse monoclonal or rabbit polyclonal antibodies against human antigens. Cell markers, clones, sources and dilutions are summarized in supplemental Table S1. The immunostaining was performed at room temperature using the following protocol: (1) blocking of endogenous peroxidase for 5 min (EnVision™ FLEX Peroxidase-Blocking Reagent); (2) incubation with the primary antibody for 90 minutes; (3) detection using Envision® Mouse LINKER for 15 min (Dako®) followed by EnVision™ FLEX+ Mouse (Dako®) for 20 min. We used 3-3'diamonibenzidine as chromogen for 10 minutes and hematoxylin as the counterstain.

Immunohistofluorescence of formalin-fixed paraffin-embedded tissues

5 µm paraffin tissue sections were used for immunofluorescence assays. Sections were dewaxed in two changes of Xylene for 10 min and rehydrated through alcohol gradient at 100%, 80%, 70% and distilled water. Slides were then heated in a microwave for 10 min in citrate buffer (pH 6.0) at 700W for antigen retrieval and cooled for 30 min at RT. After that time, slides were washed in distilled water and PBS, and fixed for 2 min in cold methanol. Tissues were incubated with blocking solution of BSA 5% in PBS for 1 hour at RT. After blocking, sections were incubated at 4^{o}C overnight with anti-Vir antibodies produced against long synthetic peptides representing conserved Vir motifs (CF-B and HP, unpublished). After incubation, tissue sections were washed in 0.05% Tween-20 PBS and incubated with secondary antibodies for 1.5 h at RT. The corresponding secondary antibodies were conjugated to Alexa Fluor 488 (Invitrogen®, dilution 1/200). After washing, nuclei were stained with DAPI

(Invitrogen®, 5 mg/mL) for 7 min at RT. Sections were mounted in Vectashield® mounting media.

RESULTS

Nested PCR performed in the spleen sections demonstrated the presence of *P. vivax* and excluded coinfection with *P. falciparum* (Figure S1). Infections by HIV, EBV, CMV and HHV8 were discarded through immunohistochemistry and *in situ* hybridization (Table S2). This data thus indicates that the only detectable pathology in this patient prior to the accident was *P. vivax* infection.

Histologically, HE-staining revealed that, compared to a normal spleen, the most significant changes in the *P. vivax*-infected spleen were a white pulp expansion and a diffuse hipercellularity in the splenic red pulp (Figure 1A and 1B). The periarteriolar lymphoid sheets of the white pulp were enlarged and well-developed secondary lymphoid follicles were easily found. A prominent infiltration by immunoblasts and plasma cells was observed in the cords, as well as a striking intrasinusoidal histiocytosis

A series of cell markers were used to determine the effects of *P. vivax* infection in this organ (Table 1). Noticeably, a mild follicular hyperplasia (CD20, CD10), mild red cord hyperplasia (CD2, CD3, CD5, CD7), expansion of monocytes-macrophages (CD68), and plasmablast expansion and proliferation (CD138, MUM-1, Ki 67) in subcapsular and perivascular areas, as well as large expression of B-cell and antibody markers (IgM, IgG, IgD, Lambda and Kappa light chains) were observed when compared to sections from the spleen of a normal individual who suffered a trauma forcing splenectomy. In contrast, none of the other markers used to identify T-cells (Granzyme B, CD4, CD8, CD57, FOXP3, TCRbeta), dendritic cells (CD123), natural killer cells (CD56), NK cells and histiocytes (CD16), endothelial cells (CD31, CD34), myeloid and monocytic cells (CD33), neutrophil granulocytes/monocytes (myeloperoxidase), normal erythroid cells at all stages of differentiation (glycophorin A), or

megakaryocytes (CD61), showed a difference in location or expression of these receptors in the spleen from the *P. vivax* patient as compared to the normal spleen (Table 1). Worth highlighting, in the *P. vivax*-infected spleen, CD138 positive plasma cells were located in the subcapsular and perivascular compartments although a marked increase in CD138 positive plasma cells was observed (Figure 1C) as compared to the normal spleen (Fig 1D). Moreover, abundant mitotic figures were found in the *P. vivax* infected spleen (Figure 1D inset) while only very rare CD138 positive cells were in mitosis in the normal spleen. A double immunostaining with CD138 and the Ki-67 proliferation marker confirmed the plasmablastic expansion of double Ki-67 and CD138 positive cells in the *P. vivax* infected spleen in the subcapsular and perivascular compartments (Figure 1E,F).

Immunofluorescence assays of spleen sections were performed using antibodies raised against conserved motifs of *P. vivax* Vir proteins, previously shown to specifically recognize *P. vivax*-infected reticulocytes from human patients (CF-B and HP, unpublished), to determine the presence of parasites. Results demonstrated the presence of large numbers of parasites in the red pulp (Fig 2A) and specificity was demonstrated using pre-immune sera (Fig 2B). Noticeably, confocal images using anti-*P. vivax* Vir antibodies and CD68 (a marker of macrophages) revealed intact *P. vivax*-infected reticulocytes characterized by dotted structures[20] mostly outside macrophages (Fig 2C and inset) and the presence of large amounts of parasite pigment as revealed by reflection contrast (Fig 2D).

DISCUSSION

Here, we performed a histopathological and immunohistochemical analysis of the spleen of a 19-years old man who was submitted to splenectomy, due to a traumatic accident, in the course of an acute untreated non-severe infection with *P. vivax*. This unique case thus allowed us to determine the histopathological effects of an active *P. vivax* in the spleen of a

non-immune individual. Our findings revealed that in addition to well-described splenomegaly and diffuse cellular hyperplasia associated with malaria infections, there were intense proliferating plasmablasts in the subcapsular and perivascular compartments as well as *P. vivax*-infected reticulocytes in the cords.

Histopathological analyses of the spleen in natural malaria infections have been limited to snap-shots of *post-mortem* specimens in patients mostly having received antimalarial therapy.[17] In an extensive histological and immunohistochemical study of the spleen from Vietnamese patients who died from late complications of *P. falciparum* infection in the course of a clinical trial, attention was drawn to a marked architectural disorganization and loss of B cells from the marginal zone.[21] However, as the authors emphasize, these alterations are very unlikely to reflect what occurs in the majority of patients who are able to control the infection.[21] The review of spleen rupture from *P. vivax*-infected patients published by Lubitz in 1949 remains the most complete description of the alterations in the acute infection by this parasite.[22] In this study, attention was drawn to where most cases had acute infection and showed follicle hyperplasia with active germinal centers and stretching of splenic parenchyma and capsule. Similar observations were made microscopically in two other cases of spleen rupture due to *P. vivax*.[23] Our results also showed white pulp expansion and a diffuse hipercellularity. Moreover, the use of different cellular markers, allowed to identify an increase in B-cells, plasmablasts and plasma cells, all implicated in production of humoral antibody responses.

B-cells and antibodies play a prominent role in the development of immunity against asexual infections in human malaria.[24,25] Fast production of antibodies is elicited by B-cells which after antigen encounter migrate to T-cell rich zones of secondary lymphoid organs, including the spleen. From there, independently of whether B-cells encounter T-cell dependent or T-cell independent antigens, B-cells become plasmablasts for subsequent

differentiation of plasma cells.[26] Noticeably, in experimental infections of C56BL/6 mice with the *P. chabaudi chabaudi* AS non-lethal strain, remodeling of the spleen and induction of plasmablasts in extra-follicular compartments have been described.[27] In addition, similar results have been obtained in experimental infections of Balb/c mice with the *P. yoelii* 17X reticulocyte-prone non-lethal strain (data not shown). Interestingly, a population of extrafollicular splenic plasmablasts responsible for T-cell independent antibody responses has also been described in mice infected with the intracellular bacterial pathogen *Erlichia muris* [28] In humans, this infection causes a disease known as ehrlichioses which is characterized by splenomegaly, lymphopenia and thrombocytopenia thus resembling the clinical symptoms of the *P. vivax* patient reported here. In striking contrast, no extra-follicular plasmablast proliferation was observed in histopathological examinations of the spleen of patients dying of severe falciparum malaria.[29] It is thus tempting to speculate that *P. vivax* infections elicit extrafollicular plamablastic proliferation and a large T-cell independent immune response.

In spite of an intense B-cell antibody plasmablastic response and expanded number of intrasinusoidal macrophages in the cords, immunofluorescece analysis revealed the presence of large numbers of *P. vivax*-infected reticulocytes in the cords (Fig 2). Although it is plausible that some of these parasites were simply detected in their passage through the spleen, it is difficult to reconcile this sole explanation with the large numbers detected. Noticeably, cytoadherence of the reticulocyte-prone non-lethal *P. yoelii* 17X strain to a spleen blood barrier of fibroblastic origin has been recently demonstrated.[30] Most important, cytoadherence of *P. vivax*-infected reticulocytes to different endothelial receptors have been also recently demonstrated.[31] Whether the large numbers of *P. vivax*-infected reticulocytes observed in the cords are due to cytoadherence, remains to be determined.

In conclusion, the misfortune of our patient provided the unique opportunity of performing , to the best of our knowledge, the first detailed immuno-histopathological study

of a human spleen from a *P. vivax* patient having an active infection with no other clinical confounding effects and that had not been drug-treated before splenectomy. Similar to *P. falciparum*, *P. vivax* infections induced white pulp expansion and a diffuse hypercellularity in the splenic red pulp. In contrast to *P. falciparum*, however, and similar to experimental infections in rodent malaria models, *P. vivax* induced a striking proliferation of plasmablasts in extrafollicular compartments of the spleen. Whether antibody responses elicited by these cells are T-cell independent and protective remains to be determined.

Supported by the Brazilian Council for Scientific and Technological Development (CNPq) and by the European Community's Seventh Framework Programme (grant agreement N° 242095), by Fundación Privada CELLEX (Catalonia, Spain), and by the Ministerio Español de Ciencia e Innovación (SAF2009-07760), Spain,

Conflict of interest

The authors declare no conflict of interest.

Authors' contribution

Clinical aspects of the patient were studied by ML and AMS.

Histological and immunihistochemical aspects were analyzed by PC, JO and AM.

Molecular data were produced and analyzed by GM, MF, LM-J and CF-B.

AMS and HP drafted the manuscript

ML and HP idealized this work

References

1. Carlton JM, Sina BJ, Adams JH. Why Is Plasmodium vivax a Neglected Tropical Disease? PLoS Negl Trop Dis 2011;5:e1160.

2. Alonso PL, Brown G, Arevalo-Herrera M, et al. A research agenda to underpin malaria eradication. PLoS medicine 2011;8:e1000406.

3. Guerra CA, Howes RE, Patil AP, et al. he International Limits and Population at Risk of Plasmodium vivax Transmission in 2009. PLoS Negl Trop Dis 2010;4:e774.

4. Hay SI, Guerra CA, Tatem AJ, Noor AM, Snow RW. The global distribution and population at risk of malaria: past, present, and future. The Lancet infectious diseases 2004;4:327-36.

5. Mueller I, Galinski MR, Baird JK, et al. Key gaps in the knowledge of *Plasmodium vivax*, a neglected human malaria parasite. Lancet Infect Dis 2009;9:555-66.

6. Baird JK. Neglect of Plasmodium vivax malaria. Trends Parasitol 2007;23:533-9.

7. Kochar DK, Das A, Kochar SK, et al. Severe Plasmodium vivax malaria: a report on serial cases from Bikaner in northwestern India. The American journal of tropical medicine and hygiene 2009;80:194-8.

8. Alexandre MA. Severe Plasmodium vivax Malaria, Brazilian Amazon. Emerg Infect Dis 2010.

9. Poespoprodjo JR, Fobia W, Kenangalem E, et al. Vivax malaria: a major cause of morbidity in early infancy. Clin Infect Dis 2009;48:1704-12.

10. Tjitra E, Anstey NM, Sugiarto P, et al. Multidrug-resistant Plasmodium vivax associated with severe and fatal malaria: a prospective study in Papua, Indonesia. PLoS Med 2008;5:e128.

11. Engwerda C, Beattie L, Amante F. The importance of the spleen in malaria. Trends Parasitol 2005;21:75-80.

12. Neva FA, Sheagren JN, Shulman NR, Canfield CJ. Malaria: host-defense mechanisms and complications. Ann Intern Med 1970;73:295-306.

13. Thomas V, Hock SK, Leng YP. Seroepidemiology of malaria: age-specific pattern of Plasmodium falciparum antibody, parasite and spleen rates among children in an endemic area in peninsular Malaysia. Trop Doct 1981;11:149-54.

14. Brabin L, Brabin BJ, van der Kaay HJ. High and low spleen rates distinguish two populations of women living under the same malaria endemic conditions in Madang, Papua, New Guinea. Trans R Soc Trop Med Hyg 1988;82:671-6.

15. Chaves LF, Taleo G, Kalkoa M, Kaneko A. Spleen rates in children: an old and new surveillance tool for malaria elimination initiatives in island settings. Trans R Soc Trop Med Hyg 2011;105:226-31.

16. Imbert P, Rapp C, Buffet PA. Pathological rupture of the spleen in malaria: analysis of 55 cases (1958-2008). Travel Med Infect Dis 2009;7:147-59.

17. Buffet PA, Safeukui I, Deplaine G, et al. The pathogenesis of Plasmodium falciparum malaria in humans: insights from splenic physiology. Blood 2011;117:381-92.

18. Snounou G, Singh B. Nested PCR analysis of Plasmodium parasites. Methods in molecular medicine 2002;72:189-203.

19. Garcia-Herrera A, Song JY, Chuang SS, et al. Nonhepatosplenic gammadelta T-cell lymphomas represent a spectrum of aggressive cytotoxic T-cell lymphomas with a mainly extranodal presentation. Am J Surg Pathol 2011;35:1214-25.

20. Fernandez-Becerra C, Pein O, de Oliveira TR, et al. Variant proteins of Plasmodium vivax are not clonally expressed in natural infections. Molecular microbiology 2005;58:648-58.

21. Urban BC, Hien TT, Day NP, et al. Fatal Plasmodium falciparum malaria causes specific patterns of splenic architectural disorganization. Infect Immun 2005;73:1986-94.

22. Lubitz JM. Pathology of the ruptured spleen in acute vivax malaria. Blood 1949;4:1168-76.

23. Mokashi AJ, Shirahatti RG, Prabhu SK, Vagholkar KR. Pathological rupture of malarial spleen. J Postgrad Med 1992;38:141-2.

24. Cohen S, Mc GI, Carrington S. Gamma-globulin and acquired immunity to human malaria. Nature 1961;192:733-7.

25. Sabchareon A, Burnouf T, Ouattara D, et al. Parasitologic and clinical human response to immunoglobulin administration in falciparum malaria. The American journal of tropical medicine and hygiene 1991;45:297-308.

26. MacLennan IC, Toellner KM, Cunningham AF, et al. Extrafollicular antibody responses. Immunol Rev 2003;194:8-18.

27. Achtman AH, Khan M, MacLennan IC, Langhorne J. Plasmodium chabaudi chabaudi infection in mice induces strong B cell responses and striking but temporary changes in splenic cell distribution. J Immunol 2003;171:317-24.

28. Racine R, Chatterjee M, Winslow GM. CD11c expression identifies a population of extrafollicular antigen-specific splenic plasmablasts responsible for CD4 T-independent antibody responses during intracellular bacterial infection. J Immunol 2008;181:1375-85.

29. Urban BC, Hien TT, Day NP, et al. Fatal Plasmodium falciparum malaria causes specific patterns of splenic architectural disorganization. Infection and immunity 2005;73:1986-94.

30. Martin-Jaular L, Ferrer M, Calvo M, et al. Strain-specific spleen remodelling in Plasmodium yoelii infections in Balb/c mice facilitates adherence and spleen macrophage-clearance escape. Cell Microbiol 2011;13:109-22.

31. Carvalho BO, Lopes SC, Nogueira PA, et al. On the cytoadhesion of Plasmodium vivax-infected erythrocytes. The Journal of infectious diseases 2010;202:638-47.

Table 1. Markers, application and findings used in the phenotypic in situ characterization and distribution of cells in the spleen of the *P. vivax* patient.

MARKER	APPLICATION	MAIN FINDINGS
CD20, CD79a	B-cell lineage	Mild follicular hyperplasia
CD10, bcl-6	Follicular center cells	Mild follicular hyperplasia
CD68 KP1	Monocytes, macrophages and myeloid cells	Expansion monocytes and macrophages
CD138	Plasma cells	Plasma cells and plasmablasts expansion in subcapsular and perivascular areas
MUM-1	Plasma cells and activated T-cells	Plasma cells and plasmablasts expansion in subcapsular and perivascular areas
Ki67	Proliferating cells	Expression in subcapsular and perivascular areas
IgD	Delta-chains of human IgD	Main expression in B-cells
IgA	Alpha-chains of human IgA	No expression
IgM	Mu-chains of human IgM	Main expression in B-cells
IgG	Gamma-chain of human IgG	Main expression in plasma cells
Lambda-light chains	Lambda light chain	Polytipic expression in plasma cells
Kappa-light chains	Lambda light chain	Polytipic expression in plasma cells
Granzyme B	Cytotoxic granules	No significant changes
CD2,CD3,CD5,CD7	T-cell lineage	No significant changes
CD4	T-helper cells and antigen presenting cells	No significant changes
CD8	T-cytotoxic cells, littoral cells of the spleen	No significant changes
CD16	NK cells, histiocytes	No significant changes
CD31	Endothelial cells	No significant changes
CD33	Myeloid and monocytic cells	No significant changes
CD34	Endothelial cells, stem cells	No significant changes
CD56	Natural killer (NK) cells	No significant changes

CD57	T follicular helper cells	No significant changes
CD123	Plasmocytoid dendritic cells	No significant changes
FOX P3	T-regulatory cells	No significant changes
TCR beta	Alpha-beta T-cells	No significant changes
Myeloperoxidase	Neutrophil granulocytes and monocytes	No positive cells
CD235a, glycophorin A	Normal erythroid cells at all differentiation stages	No positive erythroid precursors

Table S1. Immunohistochemical study: antibodies and conditions of use

Antibody	Clone	Dilution	Source
CD20	L26	1:80	Dako, Glostrup, DK
CD79a	JCB117	1:80	Dako
CD2	AB75	1:50	Dako
CD3	PS1	1:30	Novocastra, Newcastle upon Tyne, UK
CD5	4C7	1:25	Novocastra
CD7	CBC.37	1:10	Dako
CD4	4B12	1:200	Dako
CD8	C8/144B	1:600	Dako
CD56	123C2	1;15	Novocastra
CD138	B-B4	1:10	Dako
IRF4	MUM1p	1:2	Dako
Kappa chain	Polyclonal	1:32000	Dako
Lambda chain	Polyclonal	1:32000	Dako
IgG	Polyclonal	1:16000	Dako
IgM	Polyclonal	1:1500	Dako
IgD	Polyclonal	1:800	Dako
IgA	Polyclonal	1:8000	Dako
CD56	123C3	1:15	Dako
Ki67	Mib1	1:10	Dako
Granzyme B	GrB-7	1:10	Dako
TCR Beta	8A3,	1:5	Pierce Endogen, IL
FOXP3	236A/E7	1:10	eBioscience, Hatfield, UK
CD68	KP1	1:10	Dako
CD123	6H6	1:20	eBioscience
CD16	2H7	1:50	Novocastra
CD31	JC70a	1:25	Dako
CD33	PWS44	1:20	Novocastra
CD34	QBEnd10	1:50	Dako
CD61	Y2/51	1:25	Dako
CD235a	JC159	1:20	Dako
CD10	56C6	1:50	Dako
Bcl-6	PG-B6p	1:5	Dako
CMV	CCH2+DDG9	1:5	Dako
p24	Kal-1	1:10	Dako
LMP-1	CS1-4	1:100	Dako
HHV-8	13b10	1:50	Novocastra

Table S2. Viral infections investigated through immunohistochemistry

P24	24 kDa inner capsid protein of HIV	Negative
Epstein-Barr virus (EB ER)	Latent EBV infection by in situ hybridization	Negative
Virus Herpes 8	Virus herpes 8	Negative
Cytomegalovirus	Cytomegalovirus	Negative

Figure legends

Figure 1. **Immunohistochemical staining of *P. vivax*-infected and normal spleen sections**.

In panel A, HE staining of the normal and *P. vivax*-infected spleen sections evidencing, respectively, periarteriolar lymphoid cuffs and red pulp cords depleted of lymphoid cells (inset 20x normal) and a prominent white pulp expansion with hyperplastic germinal centers in secondary lymphoid follicles highlighting in the inset a striking red cord infiltration by immunoblasts and reactive plasma cells (20x *P. vivax*-infected). In panel B, the normal spleen reveals a scattered CD138 positive plasma cell distribution in the subcapsular and perivascular compartments (2x); higher magnification view showed in the inset (40x). In contrast, a marked increase of CD138 positive plasma cells is observed in the *P. vivax*-infected spleen (2x) including the detection of mitotic activity among several CD138 postive plasma cells shown in the inset (40x). In panel C, double immunostaining with CD138 (brown) and Ki-67 (red) demonstrated the lack of proliferation in plasma cells in the normal spleen (20X) whereas there is a significant increase in CD138 and Ki67 positive plasmablasts in the *P. vivax* infected spleen (20x).

Figure 2. **Immunohistofluorescence images of *P.vivax*-infected spleen sections.** In panel A, spleen section showing *P. vivax* parasites mostly in the cords of the red pulp as detected by polyclonal antibodies against Vir proteins. In panel B, negative control using preimmune sera. Nuclei are shown in blue and the bright field image of the tissue in gray. Scale bar is 20 µm. In panel C, double staining showing CD68 macrophages in red and parasites stained in green. Scale bar is 10 µm. In panel D, reflection contrast (magenta) was used to detect parasite pigment.

Figure S1. Nested PCR to identify *Plasmodium* species. Electrophoresis gel of 2% agarose showing the amplification of 200ng of genomic DNA obtained from 20 sections of formalin-fixed paraffin-embedded spleen (*Pv* sp) using specific *P. vivax* (v) and *P. falciparum* (f) primers. Positive controls of amplification were performed using 40 ng of DNA from *P. falciparum* 3D7 and *P. vivax* Sal I strain (Pv+). A negative control (C-) using water was also included. Molecular weight ladder (M) is of 100 bp. A positive reaction is noted when primers for *P. falciparum* and *P. vivax* produce amplification products of 205-bp and 120-bp, respectively.

Figure 1

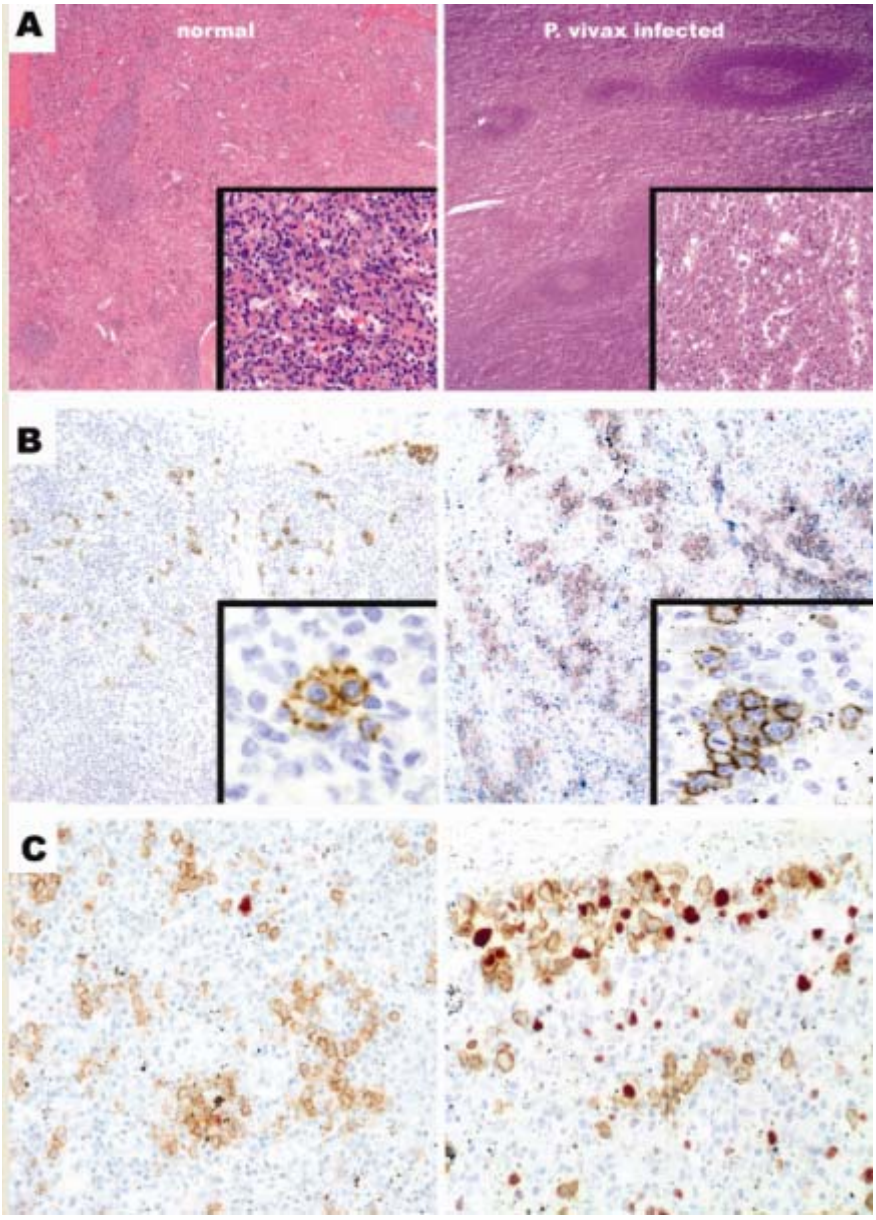

Figure 2

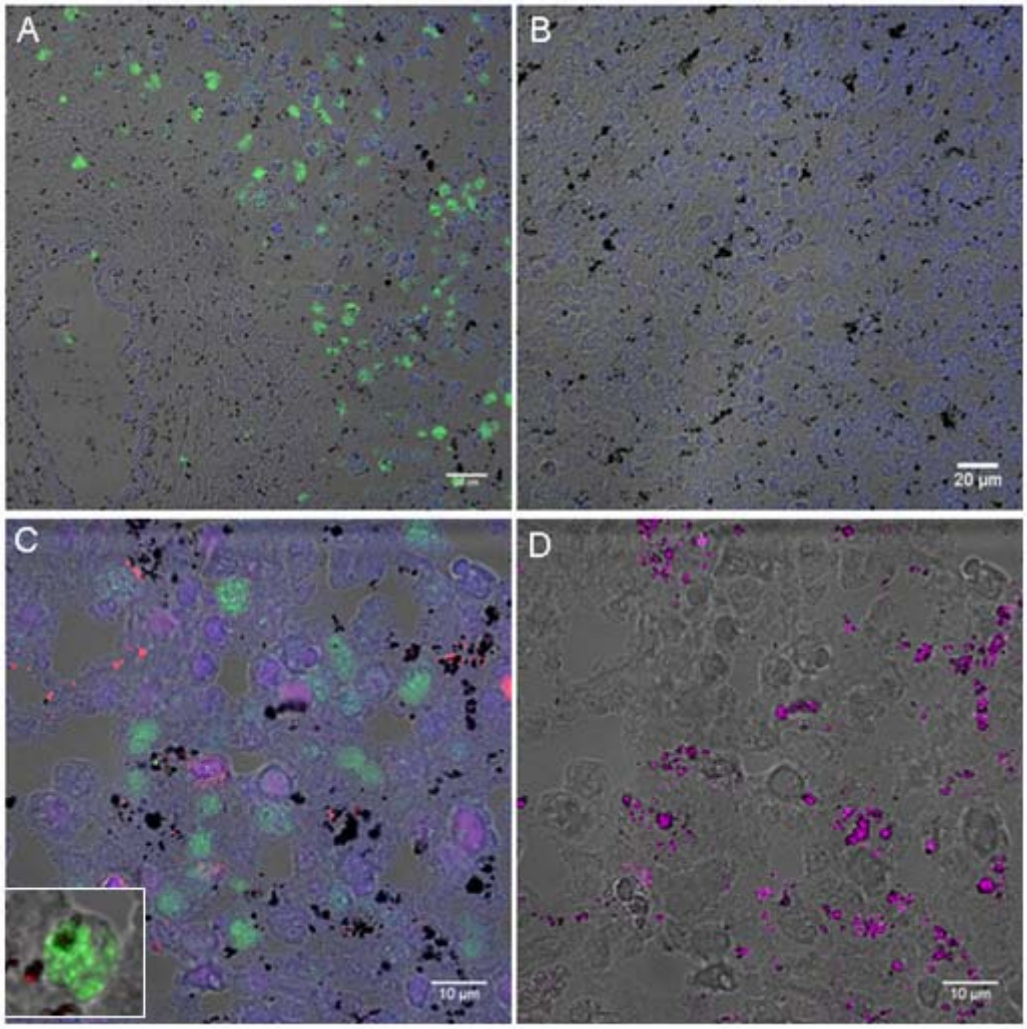

Figure S1

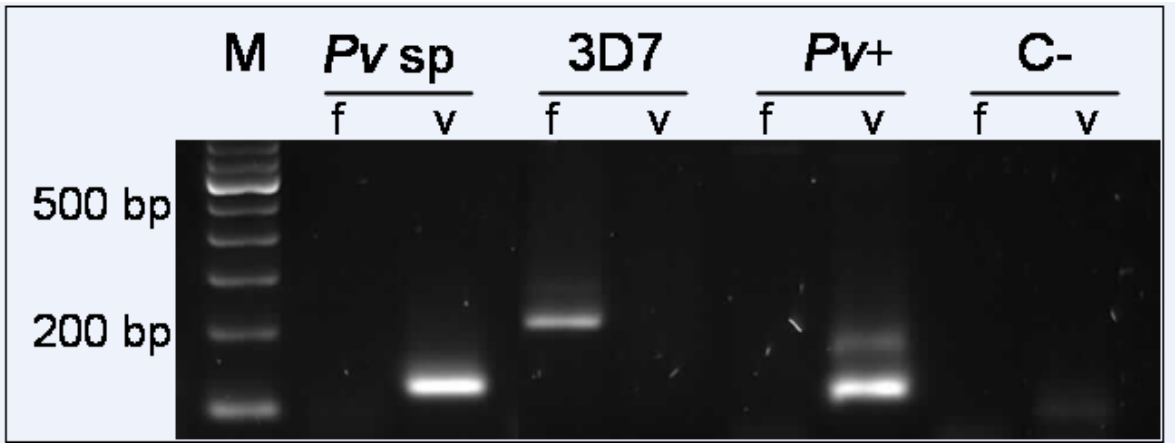

7 Discussion

P. vivax malaria has been long neglected due to its low severity and self-limiting infections, as opposed to *P. falciparum* malaria. However, it courses with chronic and reemergent infections that associate with high morbidity and impedance to socioeconomic growth in endemic areas. Further, severe clinical manifestations, including respiratory distress, anemia and splenic rupture, are incresingly being reported, questioning its benignity. The recent call for malaria eradication reinforces the need for understanding the unique biology, epidemiology and pathology of this neglected parasite (Mills *et al.*, 2008; Mueller *et al.*, 2009; Alonso *et al.*, 2011), as present tools against *P. falciparum* will not suffice to control *P. vivax.* Despite a major hinder for research with this parasite being the lack of a continuous *in vitro* culture, with the availability of the complete genome of *P. vivax* (Carlton *et al.*, 2008), a trail has been blazed to move forward on the knowledge of the parasite and reevaluate obsolete paradigms.

The spleen plays an important role in *Plasmodium* infections. Pioneering studies by Weiss and collaborators using a reticulocyte-prone non-lethal rodent model of malaria, a situation resembling *P. vivax* malaria, revealed a barrier cell dependent closure of the "open" circulation of the spleen to prevent newly formed reticulocytes from parasitation (Weiss, 1991). Based on this data, our group advanced a working hypothesis postulating that in *P. vivax* malaria, infected reticulocytes induce the formation of spleen barrier cells to actively and selectively cytoadhere, through parasite variant VIR proteins or unidentified ligands, to avoid macrophage clearance. This way, infected reticulocytes protected by these barriers prolong parasitism and establish chronic infections, as dismantling of barrier cells can take weeks (del Portillo *et al.*, 2004; Fernandez-Becerra *et al.*, 2009).

With the advent led by the cloning and expression of the jellyfish green fluorescent protein in different cells (Tsien, 1998), visualization of living protozoan parasites within their hosts, such as *Plasmodium berghei* (Franke-Fayard *et al.*, 2004)*, Leishmania major* (Peters *et al.*, 2008) *and Toxoplasma gondii* (Chtanova *et al.*, 2009)*,* is now feasible*.* In malaria, implementation of imaging technology has provided knowledge of the mechanisms of parasite invasion, dissemination and tissue distribution at different stages of the life cycle, including the mosquito and mammal hosts (Frischknecht *et al.*, 2004; Amino *et al.*, 2005; Frevert *et al.*, 2005; Franke-Fayard *et al.*, 2006; Heussler and Doerig, 2006). In spite of the enormous contributions of imaging to our understanding of host-parasite interactions, implementation of intravital microscopy to blood stages still encounters some drawbacks. First, infected erythrocytes circulate at high speeds within blood vessels and have altered surface rigidity and deformability that modulate rheological properties. Second, focusing on single cell events may lead to isolated observations that are not representative of the whole population. Third, there is still little knowledge of the three-dimensional structural organization and cellular composition of several organs.

In this study, we implemented intravital microscopy to the spleen to investigate the dynamics of parasite-spleen interplay in mice infected with two GFP-expressing *P. yoelii* strains causing either normocyte-prone lethal (17XL) or reticulocyte-prone non-lethal (17X) infections. In order to quantify and compare pRBC mobility, specific procedures

were developed to track individual particles in space and time (Ferrer *et al.*, 2011), where automatic softwares failed to follow fast moving particles over time. Comparative analysis between both strains and between uninfected mice injected with FITC-labelled RBCs revealed significant differences in the accumulation and dynamic behavior of parasite populations.

However, there exist several factors affecting cell mobility that must be taken into consideration. On the one hand, the rheological properties of red blood cells, the hematocrit or other hematologic parameters can affect blood flow and hence cell dynamics (Rogausch *et al.*, 2003). To avoid any confounding effects, we imaged parasites passing through the spleen at day 3 post-infection, when hematocrit, reticulocytemia, parasitemia and host cell invasion preference are comparable in both strains. Whether the adherent population in non-lethal infected mice corresponded to infected reticulocytes and the developmental stage of the parasites remains to be determined.

On the other hand, changes in the tissue architecture in response to infection with different *Plasmodium* strains can modify cell passage and interaction with the tissue (Weiss *et al.*, 1986). The structural remodeling of the spleen in non-lethal infection through the formation of barrier cells could account for the different mobility patterns observed between lethal and non-lethal infections. Actually, *P. yoelii* 17X pRBCs showed reduced velocity and lack of directionality, indicating restrained mobility due to the presence of physical or biological barriers (Grayson *et al.*, 2003; Khandoga *et al.*, 2009). At that time point, no closure of the circulation was observed and physical retention of pRBCs by mechanical trapping in the red pulp meshwork is difficult to be the sole explanation, as it was not accompanied by higher macrophage uptake when compared to 17XL strain, which provided a stringent control. Further, some non-lethal parasites displayed a rolling-circle like behavior accompanied by increased residence times in the spleen, similar to the process of lymphocyte adhesion to activated endothelium (Cahalan *et al.*, 2002; Miller *et al.*, 2003; Lindquist *et al.*, 2004; Roozendaal *et al.*, 2009). Overall, imaging pRBC passage through the spleen and detailed analysis of mobility parameters at single and population level were used to describe adhesion of pRBC to spleen cells *in vivo* (Martin-Jaular *et al.*, 2011).

Thus, this methodology and parameters should be considered a new tool to the *in vivo* studies of adherence in malaria. In the future, we will use this technology to gain insight into the immunobiology and parasite-spleen cell interactions by imaging infection in transgenic mice expressing fluorescent reporter genes in different cells. Moreover, the generation of transgenic parasites expressing fluorescent markers other than GFP such as mCherry (annex 1) may be used in combination to image dual infections in this model and dissect physical and biological aspects from each infection.

The application of different technologies from the micro to the macro scale in our research sinergized to build a model of infection in *Balb/c* mice where the reticulocyte-prone non-lethal *P. yoelii* 17X strain induces remodelling of the spleen through the formation of a spleen tissue barrier (BC) that facilitates the channelling of blood from arterioles to venules (V) and the adherence of infected reticulocytes (iRet) to it thus physically protecting them from destruction by macrophages (MØ) and likely establishing chronic infections. These studies pave the way for the discovery of the parasite-spleen ligand-receptors involved in this rodent model and suggest that a similar mechanism occurs in *P. vivax*.

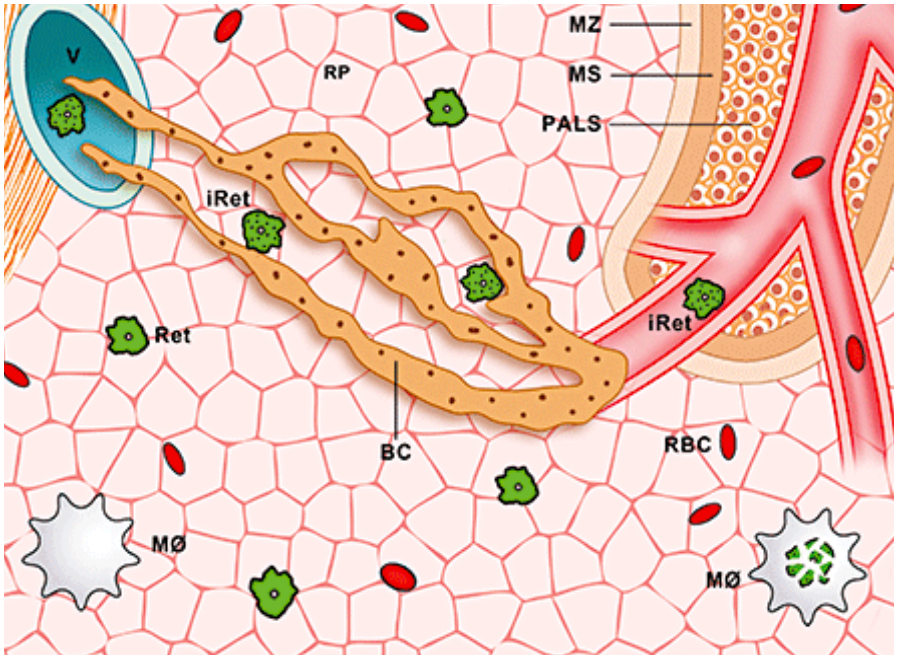

Model of spleen-clearance evasion mechanism in reticulocyte-prone non-lethal malaria. Ret, reticulocytes; RP, red pulp; PALS, periarteriolar lymphoid tissue; MS, marginal sinus; MZ, marginal zone.

Cytoadherence of *P. vivax* to host cells is a matter of debate as it is amply believed that sequestration does not occur in this species. Analysis of the literature, however, revealed that in spite of having different circulating parasite asexual blood stages in peripheral circulation, it is mostly young forms that circulate (Field *et al.*, 1963). Most important, with the contribution of our group, it has recently been shown that *P. vivax*-infected reticulocytes can adhere *in vitro* to endothelial receptors of human lung and placental tissues and that VIR proteins partly mediated such adherence (Carvalho *et al.*, 2010). Thus, using these same methodologies and together with the same collaborators, high numbers of mature-stage enriched pRBCs from non-severe *P. vivax* patients were found to adhere on spleen sections (report 3 of this thesis). These results could be somehow expected, as the presence of highly phagocytic cells and cells rich in extracellular matrix in the spleen confer a favorable surface for promiscuous entrapment of cells. However, under these conditions, RBCs obtained from healthy donors were not adherent, indicating a role for parasite proteins exposed at the surface of infection-derived red blood cells in mediating adhesion.

To identify ligands of *P. vivax*, we also reasoned that VIR proteins could play a role in such cytoadherence. Inhibition assays using antibodies raised against two peptides including conserved motifs among the VIR family abrogated adhesion of pRBCs, suggesting a role for these proteins in mediating adhesion (figure 5 in report 3). Noticeably, global transcription analysis of *P. vivax* parasites in the presence or absence of the spleen revealed VIR proteins whose expression is spleen-dependent (Fernandez-Becerra, C. and del Portillo, H.A., unpublished). In the absence of a continuous *in vitro* culture system for *P. vivax*, a 3D7 *P. falciparum* transgenic line expressing one of such VIR proteins was generated and unequivocally demonstrated VIR-mediated cytoadhrence to endothelial receptors (Bernabeu, M. and Fernandez-Becerra, C., unpublished). All together, these data further support our findings indicating that *P. vivax*-infected reticulocytes are able to cytoadhere to different endothelial receptors and to the spleen and that such adherence is at least partly and specifically mediated by VIR proteins opening avenues for developing subunit VIR protein vaccines. Moreover, understanding the molecular basis of adhesion and the changes induced by parasite-host intertalk will reveal key aspects of pathogenesis.

One major limitation of these spleen cytoadherence assays is its low reproduction of physiologic conditions, where spleen compartmentalization, three dimensionality and blood flow may compromise biologic observations, particularly in an organ where structure and function are intimately related. In fact, as revealed by leukocyte recruitment *in vivo* studies (Cahalan *et al.*, 2002), by flow adhesion assays of *P. falciparum* to vascular receptors *in vitro* (Ho and White, 1999) and by our own results of *P. yoelii* adhesion to the spleen *in vivo* (Ferrer *et al.*, 2011), the process of adhesion is dynamic, involving tethering, rolling and final adhesion, that comprise transient to stable interactions mediated by different molecules and deformability of the cell membrane. Thus, performance of these *P. vivax*-spleen adhesion assays under physiologic flow conditions remains of importance to resolve specific interactions. Of note, the strength of *P. vivax* adhesion to endothelial cells proved as comparable to that of *P. falciparum* when assayed under flow (Carvalho *et al.*, 2010).

A major advent in this line has been achieved by perfusing human spleens *ex vivo*, which maintains physiologic conditions during which parasites can be passed through to analyse splenic function, such as retention of ring-stage pRBCs infected with *P. falciparum* in the slow compartment of the red pulp (Safeukui *et al.*, 2008) and may help discern physical and biological aspects of disease. Usage of this model in *P. vivax*, will have to await the development of a continuous *in vitro culture* system for blood stages. In addition, with the advent of nanotechnologies and microfluidics, attempts to model tissue microenvironment, such as reproducing the minimal functional unit of the human spleen *in vitro*, may provide a system of study more adequate to the organ, in which synergy of diverse imaging techniques will help in the discovery of molecular and cellular aspects of infection (in collaboration with M. Calvo, N. Cortadellas, J. Samitier).

Finally, while single-organ studies may help in dissecting aspects of disease, integration into the host is ultimately required to validate the physiologic significance of these investigations in the context of infection. Notably, the misfortune of a 19-year old man undergoing splenectomy due to traumatic splenic rupture revealed a subpatent non-treated *P. vivax* mono-infection (Lacerda, M.V. and del Portillo, H. A., unpublished).

Immunohistofluorescence analyses of spleen sections using anti-VIR antibodies revealed large numbers of parasites in the red pulp, mostly outside macrophages. Whether such accumulation of *P. vivax*-infected reticulocytes observed in the cords are due to cytoadherence and whether a barrier cell-dependent mechanism is involved in this human malaria remains to be determined.

Though we are far from studying the dynamics of infection in this organ in humans, the advent of powerful non invasive imaging techniques and the development of specific probes offer promising for studying infection at adequate spatiotemporal resolution, not restricted to endpoint or snapshots of histopathological studies. In this line, based on the data obtained from MRI-T2 scans in the rodent model, we developed a protocol for abdominal scanning that is being performed to human volunteers with malaria arriving at Hospital Clinic (in collaboration with J. Gascón, C. Ayuso and J. Muñoz).

In conclusion, in this thesis, we refocus our attention to the neglected: *P. vivax* and the spleen. Despite technical, ethical and paradigmatic limitations having clouded the study of this organ in malaria pathogenesis, with the advent of imaging techniques and other biotechnological tools, the exploration of parasite-tissue interactions in the living host is now feasible and offers great potential for translational research from rodent models to human disease. Our data suggest that in reticulocyte-prone non-lethal malaria, passage through the spleen is different from what is known in other *Plasmodium* species and open new avenues for functional/structural studies of this lymphoid organ in malaria. Further, identification of the parasite ligands-host receptors involved will provide new targets for intervention.

8 References

Bibliography

Achtman, A. H., Khan, M., MacLennan, I. C. and Langhorne, J. (2003). "Plasmodium chabaudi chabaudi infection in mice induces strong B cell responses and striking but temporary changes in splenic cell distribution." J Immunol **171**(1): 317-24.

Aikawa, M. (1988). "Morphological changes in erythrocytes induced by malarial parasites." Biol Cell **64**(2): 173-81.

Alonso, P. L., Brown, G., Arevalo-Herrera, M., Binka, F., Chitnis, C., Collins, F., Doumbo, O. K., Greenwood, B., Hall, B. F., Levine, M. M., Mendis, K., Newman, R. D., Plowe, C. V., Rodriguez, M. H., Sinden, R., Slutsker, L. and Tanner, M. (2011). "A research agenda to underpin malaria eradication." PLoS Med **8**(1): e1000406.

Alves, H. J., Weidanz, W. and Weiss, L. (1996). "The spleen in murine Plasmodium chabaudi adami malaria: stromal cells, T lymphocytes, and hematopoiesis." Am J Trop Med Hyg **55**(4): 370-8.

Amino, R., Menard, R. and Frischknecht, F. (2005). "*In vivo* imaging of malaria parasites--recent advances and future directions." Curr Opin Microbiol **8**(4): 407-14.

Amino, R., Thiberge, S., Martin, B., Celli, S., Shorte, S., Frischknecht, F. and Menard, R. (2006). "Quantitative imaging of Plasmodium transmission from mosquito to mammal." Nat Med **12**(2): 220-4.

Aoshi, T., Zinselmeyer, B. H., Konjufca, V., Lynch, J. N., Zhang, X., Koide, Y. and Miller, M. J. (2008). "Bacterial entry to the splenic white pulp initiates antigen presentation to CD8+ T cells." Immunity **29**(3): 476-86.

Asami, M., Owhashi, M., Abe, T. and Nawa, Y. (1992). "A comparative study of the kinetic changes of hemopoietic stem cells in mice infected with lethal and non-lethal malaria." Int J Parasitol **22**(1): 43-7.

Bachmann, A., Esser, C., Petter, M., Predehl, S., von Kalckreuth, V., Schmiedel, S., Bruchhaus, I. and Tannich, E. (2009). "Absence of erythrocyte sequestration and lack of multicopy gene family expression in Plasmodium falciparum from a splenectomized malaria patient." PLoS One **4**(10): e7459.

Bae, K. and Jeon, K. N. (2006). "CT findings of malarial spleen." Br J Radiol **79**(946): e145-7.

Baer, K., Klotz, C., Kappe, S. H., Schnieder, T. and Frevert, U. (2007). "Release of hepatic Plasmodium yoelii merozoites into the pulmonary microvasculature." PLoS Pathog **3**(11): e171.

Baird, J. K. (2007). "Neglect of Plasmodium vivax malaria." Trends Parasitol **23**(11): 533-9.

Bajenoff, M., Glaichenhaus, N. and Germain, R. N. (2008). "Fibroblastic reticular cells guide T lymphocyte entry into and migration within the splenic T cell zone." J Immunol **181**(6): 3947-54.

Barnwell, J. W., Howard, R. J., Coon, H. G. and Miller, L. H. (1983). "Splenic requirement for antigenic variation and expression of the variant antigen on the erythrocyte membrane in cloned Plasmodium knowlesi malaria." Infect Immun **40**(3): 985-94.

Baruch, D. I., Pasloske, B. L., Singh, H. B., Bi, X., Ma, X. C., Feldman, M., Taraschi, T. F. and Howard, R. J. (1995). "Cloning the P. falciparum gene encoding PfEMP1, a malarial variant antigen and adherence receptor on the surface of parasitized human erythrocytes." Cell **82**(1): 77-87.

Batchelor, J. D., Zahm, J. A. and Tolia, N. H. (2011). "Dimerization of Plasmodium vivax DBP is induced upon receptor binding and drives recognition of DARC." Nat Struct Mol Biol **18**(8): 908-14.

Bignami, A. and Bastianelli, G. (1889). "Observations of estivo-autumnal malaria." Riforma Medica **6**: 1334-1335.

Bonnard, P., Guiard-Schmid, J. B., Develoux, M., Rozenbaum, W. and Pialoux, G. (2005). "Splenic infarction during acute malaria." Trans R Soc Trop Med Hyg **99**(1): 82-6.

Bowdler, A. J. (2002). "The Complete Spleen. Structure, Function and Clinical Disorders." Humana Press, New Jersey.

Boyd, M. F. and Kitchen, S. F. (1937). "On the infectiousness of patients infected with Plasmodium vivax and Plasmodium falciparum." Am J Trop Med Hyg **17**: 253-262.

Brown, K. N. and Brown, I. N. (1965). "Immunity to malaria: antigenic variation in chronic infections of Plasmodium knowlesi." Nature **208**(5017): 1286-8.

Buffet, P. A., Milon, G., Brousse, V., Correas, J. M., Dousset, B., Couvelard, A., Kianmanesh, R., Farges, O., Sauvanet, A., Paye, F., Ungeheuer, M. N., Ottone, C., Khun, H., Fiette, L., Guigon, G., Huerre, M., Mercereau-Puijalon, O. and David, P. H. (2006). "Ex vivo perfusion of human spleens maintains clearing and processing functions." Blood **107**(9): 3745-52.

Buffet, P. A., Safeukui, I., Deplaine, G., Brousse, V., Prendki, V., Thellier, M., Turner, G. D. and Mercereau-Puijalon, O. (2011). "The pathogenesis of Plasmodium falciparum malaria in humans: insights from splenic physiology." Blood **117**(2): 381-92.

Buffet, P. A., Safeukui, I., Milon, G., Mercereau-Puijalon, O. and David, P. H. (2009). "Retention of erythrocytes in the spleen: a double-edged process in human malaria." Curr Opin Hematol **16**(3): 157-64.

Cabrales, P. and Carvalho, L. J. (2010). "Intravital microscopy of the mouse brain microcirculation using a closed cranial window." J Vis Exp(45).

Cahalan, M. D., Parker, I., Wei, S. H. and Miller, M. J. (2002). "Two-photon tissue imaging: seeing the immune system in a fresh light." Nat Rev Immunol **2**(11): 872-80.

Carlton, J. M., Adams, J. H., Silva, J. C., Bidwell, S. L., Lorenzi, H., Caler, E., Crabtree, J., Angiuoli, S. V., Merino, E. F., Amedeo, P., Cheng, Q., Coulson, R. M., Crabb, B. S., Del Portillo, H. A., Essien, K., Feldblyum, T. V., Fernandez-Becerra, C., Gilson, P. R., Gueye, A. H., Guo, X., Kang'a, S., Kooij, T. W., Korsinczky, M., Meyer, E. V., Nene, V., Paulsen, I., White, O., Ralph, S. A., Ren, Q., Sargeant, T. J., Salzberg, S. L., Stoeckert, C. J., Sullivan, S. A., Yamamoto, M. M., Hoffman, S. L., Wortman, J. R., Gardner, M. J., Galinski, M. R., Barnwell, J. W. and Fraser-Liggett, C. M. (2008). "Comparative genomics of the neglected human malaria parasite Plasmodium vivax." Nature **455**(7214): 757-63.

Carvalho, B. O., Lopes, S. C., Nogueira, P. A., Orlandi, P. P., Bargieri, D. Y., Blanco, Y. C., Mamoni, R., Leite, J. A., Rodrigues, M. M., Soares, I. S., Oliveira, T. R., Wunderlich, G., Lacerda, M. V., del Portillo, H. A., Araujo, M. O., Russell, B., Suwanarusk, R., Snounou, G., Renia, L. and Costa, F. T. (2010). "On the cytoadhesion of Plasmodium vivax-infected erythrocytes." J Infect Dis **202**(4): 638-47.

Carvalho, L. J., Ferreira-da-Cruz, M. F., Daniel-Ribeiro, C. T., Pelajo-Machado, M. and Lenzi, H. L. (2007). "Germinal center architecture disturbance during Plasmodium berghei ANKA infection in CBA mice." Malar J **6**: 59.

Cavasini, C. E., Mattos, L. C., Couto, A. A., Bonini-Domingos, C. R., Valencia, S. H., Neiras, W. C., Alves, R. T., Rossit, A. R., Castilho, L. and Machado, R. L. (2007). "Plasmodium vivax infection among Duffy antigen-negative individuals from the Brazilian Amazon region: an exception?" Trans R Soc Trop Med Hyg **101**(10): 1042-4.

Cesta, M. F. (2006). "Normal structure, function, and histology of the spleen." Toxicol Pathol **34**(5): 455-65.

Coombes, J. L. and Robey, E. A. (2010). "Dynamic imaging of host-pathogen interactions *in vivo*." Nat Rev Immunol **10**(5): 353-64.

Cordoliani, Y. S., Sarrazin, J. L., Felten, D., Caumes, E., Leveque, C. and Fisch, A. (1998). "MR of cerebral malaria." AJNR Am J Neuroradiol **19**(5): 871-4.

Cox, F. E. (2010). "History of the discovery of the malaria parasites and their vectors." Parasit Vectors **3**(1): 5.

Chadburn, A. (2000). "The spleen: anatomy and anatomical function." Semin Hematol **37**(1 Suppl 1): 13-21.

Chakravarty, S., Cockburn, I. A., Kuk, S., Overstreet, M. G., Sacci, J. B. and Zavala, F. (2007). "CD8+ T lymphocytes protective against malaria liver stages are primed in skin-draining lymph nodes." Nat Med **13**(9): 1035-41.

Chang, W. L., Li, J., Sun, G., Chen, H. L., Specian, R. D., Berney, S. M., Granger, D. N. and van der Heyde, H. C. (2003). "P-selectin contributes to severe experimental malaria but is not required for leukocyte adhesion to brain microvasculature." Infect Immun **71**(4): 1911-8.

Charbord, P. (2003). "Stromal support of hematopoiesis. In "Stem Cell handbook". Edited by S. Sell." Humana Press, Totowa, NJ: 143-154.

Chotivanich, K., Udomsangpetch, R., Dondorp, A., Williams, T., Angus, B., Simpson, J. A., Pukrittayakamee, S., Looareesuwan, S., Newbold, C. I. and White, N. J. (2000). "The mechanisms of parasite clearance after antimalarial treatment of Plasmodium falciparum malaria." J Infect Dis **182**(2): 629-33.

Choudhury, J., Uttam, K. G. and Mukhopadhyay, M. (2008). "Spontaneous rupture of malarial spleen." Indian Pediatr **45**(4): 327-8.

Chtanova, T., Han, S. J., Schaeffer, M., van Dooren, G. G., Herzmark, P., Striepen, B. and Robey, E. A. (2009). "Dynamics of T cell, antigen-presenting cell, and pathogen interactions during recall responses in the lymph node." Immunity **31**(2): 342-55.

David, P. H., Handunnetti, S. M., Leech, J. H., Gamage, P. and Mendis, K. N. (1988). "Rosetting: a new cytoadherence property of malaria-infected erythrocytes." Am J Trop Med Hyg **38**(2): 289-97.

David, P. H., Hommel, M., Miller, L. H., Udeinya, I. J. and Oligino, L. D. (1983). "Parasite sequestration in Plasmodium falciparum malaria: spleen and antibody modulation of cytoadherence of infected erythrocytes." Proc Natl Acad Sci U S A **80**(16): 5075-9.

De Schepper, A. M., Vanhoenacker, F., Op de Beeck, B., Gielen, J. and Parizel, P. (2005). "Vascular pathology of the spleen, part I." Abdom Imaging **30**(1): 96-104.

del Portillo, H. A., Fernandez-Becerra, C., Bowman, S., Oliver, K., Preuss, M., Sanchez, C. P., Schneider, N. K., Villalobos, J. M., Rajandream, M. A., Harris, D., Pereira da Silva, L. H., Barrell, B. and Lanzer, M. (2001). "A superfamily of variant genes encoded in the subtelomeric region of Plasmodium vivax." Nature **410**(6830): 839-42.

del Portillo, H. A., Lanzer, M., Rodriguez-Malaga, S., Zavala, F. and Fernandez-Becerra, C. (2004). "Variant genes and the spleen in Plasmodium vivax malaria." Int J Parasitol **34**(13-14): 1547-54.

Demar, M., Legrand, E., Hommel, D., Esterre, P. and Carme, B. (2004). "Plasmodium falciparum malaria in splenectomized patients: two case reports in French Guiana and a literature review." Am J Trop Med Hyg **71**(3): 290-3.

Dijkstra, C. D., Van Vliet, E., Dopp, E. A., van der Lelij, A. A. and Kraal, G. (1985). "Marginal zone macrophages identified by a monoclonal antibody: characterization of immuno- and enzyme-histochemical properties and functional capacities." Immunology **55**(1): 23-30.

Elsayes, K. M., Narra, V. R., Mukundan, G., Lewis, J. S., Jr., Menias, C. O. and Heiken, J. P. (2005). "MR imaging of the spleen: spectrum of abnormalities." Radiographics **25**(4): 967-82.

Engwerda, C. R., Beattie, L. and Amante, F. H. (2005). "The importance of the spleen in malaria." Trends Parasitol **21**(2): 75-80.

Escalante, A. A. and Ayala, F. J. (1994). "Phylogeny of the malarial genus Plasmodium, derived from rRNA gene sequences." Proc Natl Acad Sci U S A **91**(24): 11373-7.

Fernandez-Becerra, C., Pein, O., de Oliveira, T. R., Yamamoto, M. M., Cassola, A. C., Rocha, C., Soares, I. S., de Braganca Pereira, C. A. and del Portillo, H. A. (2005).

"Variant proteins of Plasmodium vivax are not clonally expressed in natural infections." Mol Microbiol **58**(3): 648-58.

Fernandez-Becerra, C., Yamamoto, M. M., Vencio, R. Z., Lacerda, M., Rosanas-Urgell, A. and del Portillo, H. A. (2009). "Plasmodium vivax and the importance of the subtelomeric multigene vir superfamily." Trends Parasitol **25**(1): 44-51.

Ferrer, M., Martin-Jaular, L., Calvo, M. and del Portillo, H. A. (2011). "Intravital microscopy of the spleen in a rodent malaria model: quantitative analysis of parasite mobility and blood flow." Journal of Visualized Experiments.

Field, J. W., Sandosham, A. A. and Fong, Y. L. (1963). "The microscopial diagnosis of human malaria." The Government Press, Kuala Lampur: 20-117.

Franke-Fayard, B., Janse, C. J., Cunha-Rodrigues, M., Ramesar, J., Buscher, P., Que, I., Lowik, C., Voshol, P. J., den Boer, M. A., van Duinen, S. G., Febbraio, M., Mota, M. M. and Waters, A. P. (2005). "Murine malaria parasite sequestration: CD36 is the major receptor, but cerebral pathology is unlinked to sequestration." Proc Natl Acad Sci U S A **102**(32): 11468-73.

Franke-Fayard, B., Trueman, H., Ramesar, J., Mendoza, J., van der Keur, M., van der Linden, R., Sinden, R. E., Waters, A. P. and Janse, C. J. (2004). "A Plasmodium berghei reference line that constitutively expresses GFP at a high level throughout the complete life cycle." Mol Biochem Parasitol **137**(1): 23-33.

Franke-Fayard, B., Waters, A. P. and Janse, C. J. (2006). "Real-time *in vivo* imaging of transgenic bioluminescent blood stages of rodent malaria parasites in mice." Nat Protoc **1**(1): 476-85.

Frevert, U., Engelmann, S., Zougbede, S., Stange, J., Ng, B., Matuschewski, K., Liebes, L. and Yee, H. (2005). "Intravital observation of Plasmodium berghei sporozoite infection of the liver." PLoS Biol **3**(6): e192.

Frischknecht, F., Baldacci, P., Martin, B., Zimmer, C., Thiberge, S., Olivo-Marin, J. C., Shorte, S. L. and Menard, R. (2004). "Imaging movement of malaria parasites during transmission by Anopheles mosquitoes." Cell Microbiol **6**(7): 687-94.

Gardner, M. J., Hall, N., Fung, E., White, O., Berriman, M., Hyman, R. W., Carlton, J. M., Pain, A., Nelson, K. E., Bowman, S., Paulsen, I. T., James, K., Eisen, J. A., Rutherford, K., Salzberg, S. L., Craig, A., Kyes, S., Chan, M. S., Nene, V., Shallom, S. J., Suh, B., Peterson, J., Angiuoli, S., Pertea, M., Allen, J., Selengut, J., Haft, D., Mather, M. W., Vaidya, A. B., Martin, D. M., Fairlamb, A. H., Fraunholz, M. J., Roos, D. S., Ralph, S. A., McFadden, G. I., Cummings, L. M., Subramanian, G. M., Mungall, C., Venter, J. C., Carucci, D. J., Hoffman, S. L., Newbold, C., Davis, R. W., Fraser, C. M. and Barrell, B. (2002). "Genome sequence of the human malaria parasite Plasmodium falciparum." Nature **419**(6906): 498-511.

Garnham, P. C. (1966). "Malaria parasites and other haemosporidia." Blackwell Scientific Publications Ltd; Oxford.

Garnham, P. C. (1967). "Malaria in mammals excluding man." Adv Parasitol **5**: 139-204.

Gorantla, S., Dou, H., Boska, M., Destache, C. J., Nelson, J., Poluektova, L., Rabinow, B. E., Gendelman, H. E. and Mosley, R. L. (2006). "Quantitative magnetic

resonance and SPECT imaging for macrophage tissue migration and nanoformulated drug delivery." J Leukoc Biol **80**(5): 1165-74.

Graewe, S., Retzlaff, S., Struck, N., Janse, C. J. and Heussler, V. T. (2009). "Going live: a comparative analysis of the suitability of the RFP derivatives RedStar, mCherry and tdTomato for intravital and *in vitro* live imaging of Plasmodium parasites." Biotechnol J **4**(6): 895-902.

Grayson, M. H., Chaplin, D. D., Karl, I. E. and Hotchkiss, R. S. (2001). "Confocal fluorescent intravital microscopy of the murine spleen." J Immunol Methods **256**(1-2): 55-63.

Grayson, M. H., Hotchkiss, R. S., Karl, I. E., Holtzman, M. J. and Chaplin, D. D. (2003). "Intravital microscopy comparing T lymphocyte trafficking to the spleen and the mesenteric lymph node." Am J Physiol Heart Circ Physiol **284**(6): H2213-26.

Gretz, J. E., Norbury, C. C., Anderson, A. O., Proudfoot, A. E. and Shaw, S. (2000). "Lymph-borne chemokines and other low molecular weight molecules reach high endothelial venules via specialized conduits while a functional barrier limits access to the lymphocyte microenvironments in lymph node cortex." J Exp Med **192**(10): 1425-40.

Grun, J. L., Long, C. A. and Weidanz, W. P. (1985). "Effects of splenectomy on antibody-independent immunity to Plasmodium chabaudi adami malaria." Infect Immun **48**(3): 853-8.

Gruring, C., Heiber, A., Kruse, F., Ungefehr, J., Gilberger, T. W. and Spielmann, T. (2011). "Development and host cell modifications of Plasmodium falciparum blood stages in four dimensions." Nat Commun **2**: 165.

Gueirard, P., Tavares, J., Thiberge, S., Bernex, F., Ishino, T., Milon, G., Franke-Fayard, B., Janse, C. J., Menard, R. and Amino, R. (2010). "Development of the malaria parasite in the skin of the mammalian host." Proc Natl Acad Sci U S A **107**(43): 18640-5.

Guerra, C. A., Howes, R. E., Patil, A. P., Gething, P. W., Van Boeckel, T. P., Temperley, W. H., Kabaria, C. W., Tatem, A. J., Manh, B. H., Elyazar, I. R., Baird, J. K., Snow, R. W. and Hay, S. I. (2010). "The international limits and population at risk of Plasmodium vivax transmission in 2009." PLoS Negl Trop Dis **4**(8): e774.

Halin, C., Mora, J. R., Sumen, C. and von Andrian, U. H. (2005). "*In vivo* imaging of lymphocyte trafficking." Annu Rev Cell Dev Biol **21**: 581-603.

Hermsen, C. C., Mommers, E., van de Wiel, T., Sauerwein, R. W. and Eling, W. M. (1998). "Convulsions due to increased permeability of the blood-brain barrier in experimental cerebral malaria can be prevented by splenectomy or anti-T cell treatment." J Infect Dis **178**(4): 1225-7.

Heussler, V. and Doerig, C. (2006). "*In vivo* imaging enters parasitology." Trends Parasitol **22**(5): 192-5; discussion 195-6.

Ho, M. and White, N. J. (1999). "Molecular mechanisms of cytoadherence in malaria." Am J Physiol **276**(6 Pt 1): C1231-42.

Imbert, P., Rapp, C. and Buffet, P. A. (2009). "Pathological rupture of the spleen in malaria: analysis of 55 cases (1958-2008)." Travel Med Infect Dis **7**(3): 147-59.

Janse, C. J., Kroeze, H., van Wigcheren, A., Mededovic, S., Fonager, J., Franke-Fayard, B., Waters, A. P. and Khan, S. M. (2011). "A genotype and phenotype database of genetically modified malaria-parasites." Trends Parasitol **27**(1): 31-9.

Janse, C. J., Ramesar, J. and Waters, A. P. (2006). "High-efficiency transfection and drug selection of genetically transformed blood stages of the rodent malaria parasite Plasmodium berghei." Nat Protoc **1**(1): 346-56.

Karakas, H. M., Tuncbilek, N. and Okten, O. O. (2005). "Splenic abnormalities: an overview on sectional images." Diagn Interv Radiol **11**(3): 152-8.

Kaul, D. K., Liu, X. D., Nagel, R. L. and Shear, H. L. (1998). "Microvascular hemodynamics and *in vivo* evidence for the role of intercellular adhesion molecule-1 in the sequestration of infected red blood cells in a mouse model of lethal malaria." Am J Trop Med Hyg **58**(2): 240-7.

Khandoga, A. G., Khandoga, A., Reichel, C. A., Bihari, P., Rehberg, M. and Krombach, F. (2009). "*In vivo* imaging and quantitative analysis of leukocyte directional migration and polarization in inflamed tissue." PLoS One **4**(3): e4693.

Kherlopian, A. R., Song, T., Duan, Q., Neimark, M. A., Po, M. J., Gohagan, J. K. and Laine, A. F. (2008). "A review of imaging techniques for systems biology." BMC Syst Biol **2**: 74.

Kilejian, A. (1979). "Characterization of a protein correlated with the production of knob-like protrusions on membranes of erythrocytes infected with Plasmodium falciparum." Proc Natl Acad Sci U S A **76**(9): 4650-3.

Kim, A., Park, Y. K., Lee, J. S., Chung, M. H. and Kim, E. S. (2007). "A case of symptomatic splenic infarction in vivax malaria." Korean J Parasitol **45**(1): 55-8.

King, H. and Shumacker, H. B. (1952). "Splenic studies 1. Susceptibility to infection after splenectomy performed in infancy." Ann Surg **136**: 39-242.

Kitchen, S. K. (1938). "The infection of reticulocytes by Plasmodium vivax." Am J Trop Med Hyg **18**: 347.

Krotoski, W. A. (1985). "Discovery of the hypnozoite and a new theory of malarial relapse." Trans R Soc Trop Med Hyg **79**(1): 1-11.

Krucken, J., Mehnert, L. I., Dkhil, M. A., El-Khadragy, M., Benten, W. P., Mossmann, H. and Wunderlich, F. (2005). "Massive destruction of malaria-parasitized red blood cells despite spleen closure." Infect Immun **73**(10): 6390-8.

Kumar, S., Good, M. F., Dontfraid, F., Vinetz, J. M. and Miller, L. H. (1989). "Interdependence of CD4+ T cells and malarial spleen in immunity to Plasmodium vinckei vinckei. Relevance to vaccine development." J Immunol **143**(6): 2017-23.

Lamb, T. J., Brown, D. E., Potocnik, A. J. and Langhorne, J. (2006). "Insights into the immunopathogenesis of malaria using mouse models." Expert Rev Mol Med **8**(6): 1-22.

Landau, I. and Boulard, Y. (1978). "Life cycles and Morphology. In: Rodent Malaria (R. Killick-Kendrick and W. Peters, eds.)." Academic Press, London: 53-84.

Lee, S. H., Crocker, P. and Gordon, S. (1986). "Macrophage plasma membrane and secretory properties in murine malaria. Effects of Plasmodium yoelii blood-stage infection on macrophages in liver, spleen, and blood." J Exp Med **163**(1): 54-74.

Lewis, S. M. (1983). "The spleen--mysteries solved and unresolved." Clin Haematol **12**(2): 363-73.

Li, J. L. and Li, Y. J. (1987). "Inhibitory, opsonic and cytotoxic activities of monoclonal antibodies against asexual erythrocytic stages of Plasmodium falciparum." Parasitology **95 (Pt 2)**: 229-40.

Lindquist, R. L., Shakhar, G., Dudziak, D., Wardemann, H., Eisenreich, T., Dustin, M. L. and Nussenzweig, M. C. (2004). "Visualizing dendritic cell networks *in vivo*." Nat Immunol **5**(12): 1243-50.

Lokmic, Z., Lammermann, T., Sixt, M., Cardell, S., Hallmann, R. and Sorokin, L. (2008). "The extracellular matrix of the spleen as a potential organizer of immune cell compartments." Semin Immunol **20**(1): 4-13.

Looareesuwan, S., Suntharasamai, P., Webster, H. K. and Ho, M. (1993). "Malaria in splenectomized patients: report of four cases and review." Clin Infect Dis **16**(3): 361-6.

Martin-Jaular, L., Ferrer, M., Calvo, M., Rosanas-Urgell, A., Kalko, S., Graewe, S., Soria, G., Cortadellas, N., Ordi, J., Planas, A., Burns, J., Heussler, V. and del Portillo, H. A. (2011). "Strain-specific spleen remodelling in Plasmodium yoelii infections in Balb/c mice facilitates adherence and spleen macrophage-clearance escape." Cell Microbiol **13**(1): 109-22.

Matthews, K. R. (2011). "Controlling and coordinating development in vector-transmitted parasites." Science **331**(6021): 1149-53.

McAteer, M. A., Schneider, J. E., Ali, Z. A., Warrick, N., Bursill, C. A., von zur Muhlen, C., Greaves, D. R., Neubauer, S., Channon, K. M. and Choudhury, R. P. (2008). "Magnetic resonance imaging of endothelial adhesion molecules in mouse atherosclerosis using dual-targeted microparticles of iron oxide." Arterioscler Thromb Vasc Biol **28**(1): 77-83.

McGavern, D. and Dustin, M. (2009). Visualizing Immunity.

McGilvray, I. D., Serghides, L., Kapus, A., Rotstein, O. D. and Kain, K. C. (2000). "Nonopsonic monocyte/macrophage phagocytosis of Plasmodium falciparum-parasitized erythrocytes: a role for CD36 in malarial clearance." Blood **96**(9): 3231-40.

Mebius, R. E. and Kraal, G. (2005). "Structure and function of the spleen." Nat Rev Immunol **5**(8): 606-16.

Mendis, K., Sina, B. J., Marchesini, P. and Carter, R. (2001). "The neglected burden of Plasmodium vivax malaria." Am J Trop Med Hyg **64**(1-2 Suppl): 97-106.

Miller, L. H., Good, M. F. and Milon, G. (1994). "Malaria pathogenesis." Science **264**(5167): 1878-83.

Miller, L. H., Mason, S. J., Clyde, D. F. and McGinniss, M. H. (1976). "The resistance factor to Plasmodium vivax in blacks. The Duffy-blood-group genotype, FyFy." N Engl J Med **295**(6): 302-4.

Miller, M. J., Wei, S. H., Cahalan, M. D. and Parker, I. (2003). "Autonomous T cell trafficking examined *in vivo* with intravital two-photon microscopy." Proc Natl Acad Sci U S A **100**(5): 2604-9.

Mills, A., Lubell, Y. and Hanson, K. (2008). "Malaria eradication: the economic, financial and institutional challenge." Malar J **7 Suppl 1**: S11.

Mittelbrunn, M., Martinez del Hoyo, G., Lopez-Bravo, M., Martin-Cofreces, N. B., Scholer, A., Hugues, S., Fetler, L., Amigorena, S., Ardavin, C. and Sanchez-Madrid, F. (2009). "Imaging of plasmacytoid dendritic cell interactions with T cells." Blood **113**(1): 75-84.

Moghimi, S. M. (1995). "Mechanisms of splenic clearance of blood cells and particles: towards development of new splenotropic agents." Advanced Drug Delivery Reviews **17**(1): 103-115.

Molitoris, B. A. and Sandoval, R. M. (2005). "Intravital multiphoton microscopy of dynamic renal processes." Am J Physiol Renal Physiol **288**(6): F1084-9.

Morelli, A. E., Larregina, A. T., Shufesky, W. J., Zahorchak, A. F., Logar, A. J., Papworth, G. D., Wang, Z., Watkins, S. C., Falo, L. D., Jr. and Thomson, A. W. (2003). "Internalization of circulating apoptotic cells by splenic marginal zone dendritic cells: dependence on complement receptors and effect on cytokine production." Blood **101**(2): 611-20.

Mota, M. M., Brown, K. N., Holder, A. A. and Jarra, W. (1998). "Acute Plasmodium chabaudi chabaudi malaria infection induces antibodies which bind to the surfaces of parasitized erythrocytes and promote their phagocytosis by macrophages *in vitro*." Infect Immun **66**(9): 4080-6.

Mota, M. M., Pradel, G., Vanderberg, J. P., Hafalla, J. C., Frevert, U., Nussenzweig, R. S., Nussenzweig, V. and Rodriguez, A. (2001). "Migration of Plasmodium sporozoites through cells before infection." Science **291**(5501): 141-4.

Mota, M. M., Thathy, V., Nussenzweig, R. S. and Nussenzweig, V. (2001). "Gene targeting in the rodent malaria parasite Plasmodium yoelii." Mol Biochem Parasitol **113**(2): 271-8.

Mueller, I., Galinski, M. R., Baird, J. K., Carlton, J. M., Kochar, D. K., Alonso, P. L. and del Portillo, H. A. (2009). "Key gaps in the knowledge of Plasmodium vivax, a neglected human malaria parasite." Lancet Infect Dis **9**(9): 555-66.

Ngo, V. N., Korner, H., Gunn, M. D., Schmidt, K. N., Riminton, D. S., Cooper, M. D., Browning, J. L., Sedgwick, J. D. and Cyster, J. G. (1999). "Lymphotoxin alpha/beta and tumor necrosis factor are required for stromal cell expression of homing chemokines in B and T cell areas of the spleen." J Exp Med **189**(2): 403-12.

Nolte, M. A., Belien, J. A., Schadee-Eestermans, I., Jansen, W., Unger, W. W., van Rooijen, N., Kraal, G. and Mebius, R. E. (2003). "A conduit system distributes chemokines and small blood-borne molecules through the splenic white pulp." J Exp Med **198**(3): 505-12.

Orengo, J. M., Wong, K. A., Ocana-Morgner, C. and Rodriguez, A. (2008). "A Plasmodium yoelii soluble factor inhibits the phenotypic maturation of dendritic cells." Malar J **7**: 254.

Penet, M. F., Viola, A., Confort-Gouny, S., Le Fur, Y., Duhamel, G., Kober, F., Ibarrola, D., Izquierdo, M., Coltel, N., Gharib, B., Grau, G. E. and Cozzone, P. J. (2005). "Imaging experimental cerebral malaria *in vivo*: significant role of ischemic brain edema." J Neurosci **25**(32): 7352-8.

Peters, N. C., Egen, J. G., Secundino, N., Debrabant, A., Kimblin, N., Kamhawi, S., Lawyer, P., Fay, M. P., Germain, R. N. and Sacks, D. (2008). "*In vivo* imaging reveals an essential role for neutrophils in leishmaniasis transmitted by sand flies." Science **321**(5891): 970-4.

Piccio, L., Rossi, B., Scarpini, E., Laudanna, C., Giagulli, C., Issekutz, A. C., Vestweber, D., Butcher, E. C. and Constantin, G. (2002). "Molecular mechanisms involved in lymphocyte recruitment in inflamed brain microvessels: critical roles for P-selectin glycoprotein ligand-1 and heterotrimeric G(i)-linked receptors." J Immunol **168**(4): 1940-9.

Price, R. N., Tjitra, E., Guerra, C. A., Yeung, S., White, N. J. and Anstey, N. M. (2007). "Vivax malaria: neglected and not benign." Am J Trop Med Hyg **77**(6 Suppl): 79-87.

Quinn, T. C. and Wyler, D. J. (1980). "Resolution of acute malaria (Plasmodium berghei in the rat): reversibility and spleen dependence." Am J Trop Med Hyg **29**(1): 1-4.

Rogausch, H., Zwingmann, D., Trudewind, M., del Rey, A., Voigt, K. H. and Besedovsky, H. (2003). "Local and systemic autonomic nervous effects on cell migration to the spleen." J Appl Physiol **94**(2): 469-75.

Roozendaal, R., Mempel, T. R., Pitcher, L. A., Gonzalez, S. F., Verschoor, A., Mebius, R. E., von Andrian, U. H. and Carroll, M. C. (2009). "Conduits mediate transport of low-molecular-weight antigen to lymph node follicles." Immunity **30**(2): 264-76.

Ryan, J. R., Stoute, J. A., Amon, J., Dunton, R. F., Mtalib, R., Koros, J., Owour, B., Luckhart, S., Wirtz, R. A., Barnwell, J. W. and Rosenberg, R. (2006). "Evidence for transmission of Plasmodium vivax among a duffy antigen negative population in Western Kenya." Am J Trop Med Hyg **75**(4): 575-81.

Safeukui, I., Correas, J. M., Brousse, V., Hirt, D., Deplaine, G., Mule, S., Lesurtel, M., Goasguen, N., Sauvanet, A., Couvelard, A., Kerneis, S., Khun, H., Vigan-Womas, I., Ottone, C., Molina, T. J., Treluyer, J. M., Mercereau-Puijalon, O., Milon, G., David, P. H. and Buffet, P. A. (2008). "Retention of Plasmodium falciparum ring-infected erythrocytes in the slow, open microcirculation of the human spleen." Blood **112**(6): 2520-8.

Saito, H., Yokoi, Y., Watanabe, S., Tajima, J., Kuroda, H. and Namihisa, T. (1988). "Reticular meshwork of the spleen in rats studied by electron microscopy." Am J Anat **181**(3): 235-52.

Sanni, L. A., Fonseca, L. F. and Langhorne, J. (2002). "Mouse models for erythrocytic-stage malaria." Methods Mol Med **72**: 57-76.

Sayles, P. C., Cooley, A. J. and Wassom, D. L. (1991). "A spleen is not necessary to resolve infections with Plasmodium yoelii." Am J Trop Med Hyg **44**(1): 42-8.

Schaecher, K., Kumar, S., Yadava, A., Vahey, M. and Ockenhouse, C. F. (2005). "Genome-wide expression profiling in malaria infection reveals transcriptional changes associated with lethal and nonlethal outcomes." Infect Immun **73**(9): 6091-100.

Schmidt, E. E., MacDonald, I. C. and Groom, A. C. (1993). "Comparative aspects of splenic microcirculatory pathways in mammals: the region bordering the white pulp." Scanning Microsc **7**(2): 613-28.

Schnitzer, B., Sodeman, T., Mead, M. L. and Contacos, P. G. (1972). "Pitting function of the spleen in malaria: ultrastructural observations." Science **177**(44): 175-7.

Serghides, L., Smith, T. G., Patel, S. N. and Kain, K. C. (2003). "CD36 and malaria: friends or foes?" Trends Parasitol **19**(10): 461-9.

Singh, B., Kim Sung, L., Matusop, A., Radhakrishnan, A., Shamsul, S. S., Cox-Singh, J., Thomas, A. and Conway, D. J. (2004). "A large focus of naturally acquired Plasmodium knowlesi infections in human beings." Lancet **363**(9414): 1017-24.

Sipkins, D. A., Wei, X., Wu, J. W., Runnels, J. M., Cote, D., Means, T. K., Luster, A. D., Scadden, D. T. and Lin, C. P. (2005). "*In vivo* imaging of specialized bone marrow endothelial microdomains for tumour engraftment." Nature **435**(7044): 969-73.

Smith, J. D., Chitnis, C. E., Craig, A. G., Roberts, D. J., Hudson-Taylor, D. E., Peterson, D. S., Pinches, R., Newbold, C. I. and Miller, L. H. (1995). "Switches in expression of Plasmodium falciparum var genes correlate with changes in antigenic and cytoadherent phenotypes of infected erythrocytes." Cell **82**(1): 101-10.

Sponaas, A. M., Freitas do Rosario, A. P., Voisine, C., Mastelic, B., Thompson, J., Koernig, S., Jarra, W., Renia, L., Mauduit, M., Potocnik, A. J. and Langhorne, J. (2009). "Migrating monocytes recruited to the spleen play an important role in control of blood stage malaria." Blood **114**(27): 5522-31.

Steiniger, B., Barth, P. and Hellinger, A. (2001). "The perifollicular and marginal zones of the human splenic white pulp : do fibroblasts guide lymphocyte immigration?" Am J Pathol **159**(2): 501-12.

Stevenson, M. M., Tam, M. F., Wolf, S. F. and Sher, A. (1995). "IL-12-induced protection against blood-stage Plasmodium chabaudi AS requires IFN-gamma and TNF-alpha and occurs via a nitric oxide-dependent mechanism." J Immunol **155**(5): 2545-56.

Sturm, A., Amino, R., van de Sand, C., Regen, T., Retzlaff, S., Rennenberg, A., Krueger, A., Pollok, J. M., Menard, R. and Heussler, V. T. (2006). "Manipulation of host

hepatocytes by the malaria parasite for delivery into liver sinusoids." Science **313**(5791): 1287-90.

Su, X. Z., Heatwole, V. M., Wertheimer, S. P., Guinet, F., Herrfeldt, J. A., Peterson, D. S., Ravetch, J. A. and Wellems, T. E. (1995). "The large diverse gene family var encodes proteins involved in cytoadherence and antigenic variation of Plasmodium falciparum-infected erythrocytes." Cell **82**(1): 89-100.

Swirski, F. K., Nahrendorf, M., Etzrodt, M., Wildgruber, M., Cortez-Retamozo, V., Panizzi, P., Figueiredo, J. L., Kohler, R. H., Chudnovskiy, A., Waterman, P., Aikawa, E., Mempel, T. R., Libby, P., Weissleder, R. and Pittet, M. J. (2009). "Identification of splenic reservoir monocytes and their deployment to inflammatory sites." Science **325**(5940): 612-6.

Tarun, A. S., Baer, K., Dumpit, R. F., Gray, S., Lejarcegui, N., Frevert, U. and Kappe, S. H. (2006). "Quantitative isolation and *in vivo* imaging of malaria parasite liver stages." Int J Parasitol **36**(12): 1283-93.

Thiberge, S., Blazquez, S., Baldacci, P., Renaud, O., Shorte, S., Menard, R. and Amino, R. (2007). "*In vivo* imaging of malaria parasites in the murine liver." Nat Protoc **2**(7): 1811-8.

Togbe, D., de Sousa, P. L., Fauconnier, M., Boissay, V., Fick, L., Scheu, S., Pfeffer, K., Menard, R., Grau, G. E., Doan, B. T., Beloeil, J. C., Renia, L., Hansen, A. M., Ball, H. J., Hunt, N. H., Ryffel, B. and Quesniaux, V. F. (2008). "Both functional LTbeta receptor and TNF receptor 2 are required for the development of experimental cerebral malaria." PLoS One **3**(7): e2608.

Tong, K. A., Ashwal, S., Obenaus, A., Nickerson, J. P., Kido, D. and Haacke, E. M. (2008). "Susceptibility-weighted MR imaging: a review of clinical applications in children." AJNR Am J Neuroradiol **29**(1): 9-17.

Tsien, R. Y. (1998). "The green fluorescent protein." Annu Rev Biochem **67**: 509-44.

Udagama, P. V., David, P. H., Peiris, J. S., Ariyaratne, Y. G., Perera, K. L. and Mendis, K. N. (1987). "Demonstration of antigenic polymorphism in Plasmodium vivax malaria with a panel of 30 monoclonal antibodies." Infect Immun **55**(11): 2604-11.

Udomsanpetch, R., Thanikkul, K., Pukrittayakamee, S. and White, N. J. (1995). "Rosette formation by Plasmodium vivax." Trans R Soc Trop Med Hyg **89**(6): 635-7.

Urban, B. C., Ferguson, D. J., Pain, A., Willcox, N., Plebanski, M., Austyn, J. M. and Roberts, D. J. (1999). "Plasmodium falciparum-infected erythrocytes modulate the maturation of dendritic cells." Nature **400**(6739): 73-7.

Urban, B. C., Hien, T. T., Day, N. P., Phu, N. H., Roberts, R., Pongponratn, E., Jones, M., Mai, N. T., Bethell, D., Turner, G. D., Ferguson, D., White, N. J. and Roberts, D. J. (2005). "Fatal Plasmodium falciparum malaria causes specific patterns of splenic architectural disorganization." Infect Immun **73**(4): 1986-94.

van de Sand, C., Horstmann, S., Schmidt, A., Sturm, A., Bolte, S., Krueger, A., Lutgehetmann, M., Pollok, J. M., Libert, C. and Heussler, V. T. (2005). "The liver stage of Plasmodium berghei inhibits host cell apoptosis." Mol Microbiol **58**(3): 731-42.

van Krieken, J. H., Te Velde, J., Hermans, J. and Welvaart, K. (1985). "The splenic red pulp; a histomorphometrical study in splenectomy specimens embedded in methylmethacrylate." Histopathology **9**(4): 401-16.

Vanderberg, J. P. and Frevert, U. (2004). "Intravital microscopy demonstrating antibody-mediated immobilisation of Plasmodium berghei sporozoites injected into skin by mosquitoes." Int J Parasitol **34**(9): 991-6.

von Zur Muhlen, C., Sibson, N. R., Peter, K., Campbell, S. J., Wilainam, P., Grau, G. E., Bode, C., Choudhury, R. P. and Anthony, D. C. (2008). "A contrast agent recognizing activated platelets reveals murine cerebral malaria pathology undetectable by conventional MRI." J Clin Invest **118**(3): 1198-207.

Vyas, S., Gupta, V., Hondappanavar, A., Sakhuja, V., Bhardwaj, N., Singh, P. and Khandelwal, N. (2010). "Magnetic Resonance Imaging of Cerebral Malaria." J Emerg Med.

Weiss, L. (1989). "Mechanisms of splenic control of murine malaria: cellular reactions of the spleen in lethal (strain 17XL) Plasmodium yoelii malaria in BALB/c mice, and the consequences of pre-infective splenectomy." Am J Trop Med Hyg **41**(2): 144-60.

Weiss, L. (1990). "The spleen in malaria: the role of barrier cells." Immunol Lett **25**(1-3): 165-72.

Weiss, L. (1991). "Barrier cells in the spleen." Immunol Today **12**(1): 24-9.

Weiss, L., Geduldig, U. and Weidanz, W. (1986). "Mechanisms of splenic control of murine malaria: reticular cell activation and the development of a blood-spleen barrier." Am J Anat **176**(3): 251-85.

Weissleder, R. (2002). "Scaling down imaging: molecular mapping of cancer in mice." Nat Rev Cancer **2**(1): 11-8.

Winkel, K. D. and Good, M. F. (1991). "Inability of Plasmodium vinckei-immune spleen cells to transfer protection to recipient mice exposed to vaccine 'vectors' or heterologous species of plasmodium." Parasite Immunol **13**(5): 517-30.

Wong, K. A. and Rodriguez, A. (2008). "Plasmodium infection and endotoxic shock induce the expansion of regulatory dendritic cells." J Immunol **180**(2): 716-26.

Wyler, D. J., Quinn, T. C. and Chen, L. T. (1981). "Relationship of alterations in splenic clearance function and microcirculation to host defense in acute rodent malaria." J Clin Invest **67**(5): 1400-4.

Yadava, A., Kumar, S., Dvorak, J. A., Milon, G. and Miller, L. H. (1996). "Trafficking of Plasmodium chabaudi adami-infected erythrocytes within the mouse spleen." Proc Natl Acad Sci U S A **93**(10): 4595-9.

Yap, G. S. and Stevenson, M. M. (1994). "Differential requirements for an intact spleen in induction and expression of B-cell-dependent immunity to Plasmodium chabaudi AS." Infect Immun **62**(10): 4219-25.

9 Annex

9.1 *Generation of mCherry transgenic* P. yoelii *17X parasites*

Objectives

To generate *P. yoelii* 17X parasites transgenic for the red fluorescent protein mCherry, which has been used in *P. berghei* transfections giving brilliant and photostable fluorescence (Graewe *et al.*, 2009). With this aim, schizonts of *P. yoelii* 17X were obtained, transfected with pL0017-mCherry plasmid and injected into mice for *in vivo* selection of transfectants.

Methodology

P. yoelii 17X parasites were originally obtained from MR4 (www.mr4.org) and *Balb/c* mice were obtained from Charles River Laboratories. Three mice were infected intraperitoneally with *P. yoelii* 17X and, at 1-5% parasitemia, total blood was collected through intracardiac puncture in PBS/EDTA and washed in PBS. To obtain mature schizonts for transfection, the infected blood was cultured in RPMI 1640 (with L-Glutamin) media supplemented with 10mM Hepes, 50g/l Gentamicin, 50 uM 2-mercaptoethanol, 2,1 g/l sodium bicarbonate, 20% FCS and 1% PenStrep at 37°C, 5% CO_2. Under these conditions, 50% of pRBCs were mature schizonts after 22 hours in culture, as determined in Giemsa-stained blood smears. Schizonts were enriched by density centrifugation in 57% Nycodenz/PBS (Mota *et al.*, 2001), collected from the interphase, washed in PBS and used for transfection.

Cloning of the mCherry encoding sequence under the ubiquitous promoter of *P. berghei* elongation factor 1 (*Pbeef1α*) in vector pL0017 (MR4) was performed by S. Graewe and V. T. Heussler (Bernhard-Nocht Institute, Hamburg). This vector contains the *dhfr* gene for drug selection and it has been used in other researches to express GFP in *P. berghei* (Franke-Fayard *et al.*, 2004) and *P. yoelii* (Martin-Jaular *et al.*, 2011).

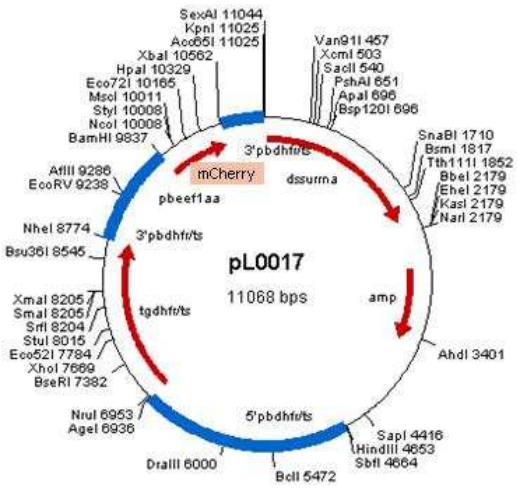

Transfection of *P. yoelii* parasites was performed using the Nucleofector technology of AMAXA, as described for *P. berghei* (Janse *et al.*, 2006) with slight modifications. Briefly, $4{\cdot}10^7$ *P. yoelii* 17X schizonts were mixed with five micrograms of pL0017-mCherry purified plasmid resuspended in 100 µl of Nucleofector solution and transfected using U033 program in AMAXA. Immediately after, 300 µl of PBS were added to the transfected parasites and the solution was injected intravenously into the tail vein of two *Balb/c* mice. Drug selection of transfected parasites was initiated 24 hours post-injection by administering pyrimethamine (0,07 g/l, pH 5.2) in drinking water. Parasitemia was followed thereafter in Giemsa-stained blood smears. At day 13 post-infection, when 4% parasitemia was reached, three Balb/c mice were infected intraperitoneally using a drop of tail blood from infected mice to generate stabilates and for phenotypic characterization.

Preliminary results

Time-course parasitemia of mCherry-*P. yoelii* 17X infected mice was comparable to that of wild-type *P. yoelii* 17X infected mice (figure 1A). All developmental stages were observed in Giemsa-stained peripheral blood smears. On average, 60% of pRBCs expressed mCherry, with variable intensities, as determined in DAPI-stained blood samples obtained from the tail of infected mice and visualized under a Leica TCS-SP5 microscope (Scientific-Technical Services, UB-IDIBAPS) (figure 1B). In order to enrich for parasites with brightest fluorescence for *in vivo* experiments, mCherry-pRBCs were sorted using a flow cytometry (FC) sorter equipped with a yellow-green laser (Scientific-Technical Services, UB-IDIBAPS) (figure 1C). In total, $3{\cdot}10^5$ mCherry-pRBCs were sorted into 400 µl of RPMI media with 10% FCS and injected intravenously into two Balb/c mice. The resulting infection gave 100% pRBCs fluorescent for mCherry.

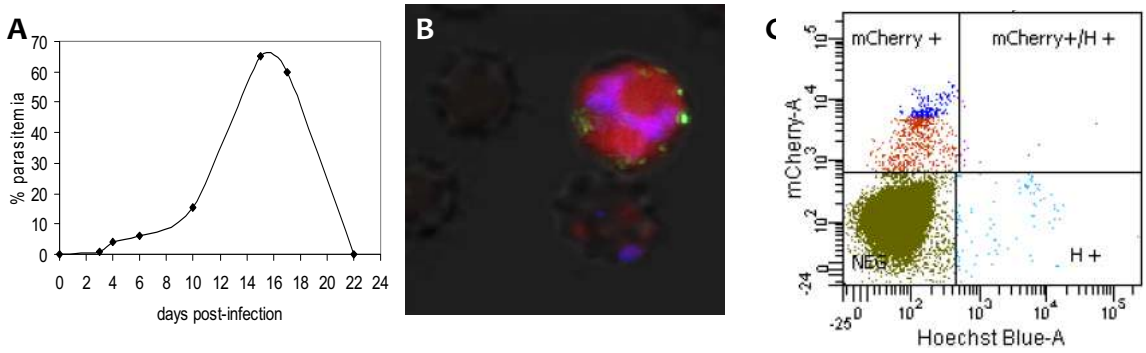

Figure 1- Generation of *P. yoelii* 17X-mCherry transgenic parasites. A: Time-course parasitemia in mCherry-*P. yoelii* 17X infected *Balb/c* mice. **B:** Confocal microscopy of pRBCs expressing mCherry (red). Nuclei are stained with DAPI (blue) and hemozoin is imaged using reflection contrast (green). **C:** FC sorting of the mCherry+ brightest population (blue). Gates were set using wild type *P. yoelii* 17X pRBCs for autofluorescence and Hoechst staining was used for identification of infected RBCs.

Future

The final objective is to obtain a stable clonal line of mCherry-*P. yoelii* 17X parasites in with the transgene integrated to the parasite genome. Therefore, PCR analysis will be performed to confirm integration and a clonal line will be obtained as described (Janse *et al.*, 2006).

Aknowledgements

To S. Graewe and V. Heussler for providing the plasmid and initial input in transfection experiments, to M. Bernabeu for helping in transfection experiments, to L. Martin-Jaular and C. González for helping in animal experiments and analysis, and to M. Calvo for image acquisition.

9.2 *Contributions*

9.2.1 Research article 1 :

Exosomes from* Plasmodium yoelii-*Infected Reticulocytes Protect Mice from Lethal Infections.

Lorena Martin-Jaular[1], Ernesto S. Nakayasu[2¤], Mireia Ferrer[1], Igor C. Almeida[2], Hernando A. del Portillo[1,3*]

1 Poverty-Related Diseases, Barcelona Centre for International Health Research, Barcelona, Spain, 2 The Border Biomedical Research Center, University of Texas at El Paso, El Paso, Texas, United States of America, 3Institució Catalana de Recerca i Estudis Avançats (ICREA), Barcelona, Spain

Abstract

Exosomes are 30–100-nm membrane vesicles of endocytic origin that are released after the fusion of multivesicular bodies (MVBs) with the plasma membrane. While initial studies suggested that the role of exosomes was limited to the removal of proteins during the maturation of reticulocytes to erythrocytes, recent studies indicate that they are produced by different types of cells and are involved in promoting inter-cellular communication and antigen presentation. Here, we describe the isolation and characterization of exosomes from peripheral blood of BALB/c mice infected with the reticulocyte-prone non-lethal *Plasmodium yoelii* 17X strain. Importantly, proteomic analysis revealed the presence of parasite proteins in these vesicles. Moreover, immunization of mice with purified exosomes elicited IgG antibodies capable of recognizing *P. yoelii*-infected red blood cells. Furthermore, lethal challenge of immunized mice with the normocyte-prone lethal *P. yoelii* 17XL strain caused a significant attenuation in the course of parasitaemia, increased survival time, and altered the cell tropism to reticulocytes. These results were obtained also when the exosomes were isolated from a *P. yoelii*-infected reticulocyte culture indicating that reticulocyte-derived exosomes carry antigens and are involved in immune modulation. Moreover, inclusion of CpG ODN 1826 in exosome immunizations elicited IgG2a and IgG2b antibodies and promoted survival, clearance of parasites and subsequent sterile protection of 83% of the animals challenged with *P. yoelli* 17XL. To our knowledge, this is the first report of immune responses elicited by exosomes derived from reticulocytes opening new avenues for the modulation of anti-malaria responses.

Published in: Plos One (accepted October 2011)

9.2.2 Research article 2:

Functional analysis of Plasmodium vivax *VIR proteins reveals different subcellular localizations and cytoadherence to the ICAM-1 endothelial receptor*

Bernabeu M[1], Lopez FJ[1], Ferrer M[1], Martin-Jaular L[1], Razaname A[2], Corradin G[2], Maier AG[3], del Portillo HA[1,4*] and Fernandez-Becerra C[1*]

1Barcelona Centre for International Health Research, Hospital Clinic-Universitat de Barcelona, Barcelona, Spain. 2Biochemistry Department, University of Lausanne, Epalinges, Switzerland 3LaTrobe Institute for Molecular Science, La Trobe University, Melbourne, Victoria 3086, Australia 4Institucio Catalana de Recerca i Estudis Avancats (ICREA), Barcelona, Spain.

Abstract

The subcellular localization and function of variant subtelomeric multigene families in Plasmodium vivax remain vastly unknown. Among them, the vir superfamily is putatively involved in antigenic variation and in mediating adherence to endothelial receptors. In the absence of a continuous *in vitro* culture system for P. vivax, we have generated P. falciparum transgenic lines expressing VIR proteins to infer location and function. We chose three proteins pertaining to subfamilies A (VIR17), C (VIR14) and D (VIR10), with domains and secondary structures that predictably traffic these proteins to different subcellular compartments. Here, we showed that VIR17 remained inside the parasite and around merozoites, whereas VIR14 and VIR10 were exported to the membrane of infected red blood cells (iRBCs) in an apparent independent pathway of Maurer's clefts. Remarkably, VIR14 was exposed at the surface of iRBCs and mediated adherence to different endothelial receptors expressed in CHO cells under static conditions. Under physiological flow conditions, however, cytoadherence was only observed to ICAM-1, which was the only receptor whose adherence was specifically and significantly inhibited by antibodies against conserved motifs of VIR proteins. Immunofluorescence studies using these antibodies also showed different sub-cellular localizations of VIR proteins in P. vivax-infected reticulocytes from natural infections. This data suggest that VIR proteins are trafficked to different cellular compartments and functionally demonstrates that VIR proteins can specifically mediate cytoadherence to the ICAM-1 endothelial receptor.

Submitted to: Cellular Microbiology (accepted November 2011)

9.2.3 Research article 3:

Expression of Non-TLR Pattern Recognition Receptors in the Spleen of Balb/c *Mice Infected with* Plasmodium yoelii *and* Plasmodium chabaudi chabaudi *AS*

Anna Rosanas-Urgell1*, Lorena Martin-Jaular2, Julio Ricarte-Filho3**, Mireia Ferrer2, Susana Kalko4, Edna Kimura3, Hernando A del Portillo1,2, 5***

1Departamento de Parasitologia, Instituto de Ciências Biomédicas, Universidade de São Paulo, Av. Prof. Lineu Prestes 1374, São Paulo, SP 05508-900, Brazil. 2Barcelona Centre for International Health Research, Barcelona, Spain. 3Departamento de Biologia Celular, Instituto de Ciências Biomédicas, Universidade de São Paulo, Av. Prof. Lineu Prestes 1524, São Paulo, SP 05508-900, Brazil. 4Bioinformatics Unit, IDIBAPS, Hospital Clinic, Barcelona, Spain. 5Institució Catalana de Recerca i Estudis Avançats (ICREA), Barcelona, Spain. * present address: Papua New Guinea Insitute of Medical Research, Madang 511, Papua New Guinea. ** present address: Memorial Sloan-Kettering Cancer Center, 1275 York Avenue New York, NY 10065, USA. *** present address: Barcelona Centre for International Health Research (CRESIB), Hospital Clinic/IDIBAPS, Universitat de Barcelona, Roselló 153, 1a planta, 08036, Barcelona, Spain

Abstract

Even though the spleen plays a crucial role in the development of immunity to malaria, the role of pattern recognition receptors (PRRs) expressed by splenic effector cells during malaria infection is poorly understood. The present study analyzed the expression profiles of splenic effector cells from selected PRRs in experimental infections of Balb/c mice with the *Plasmodium yoelii* 17XL lethal and 17X non-lethal strains as well as with the *P. chabaudi chabaudi* AS non-lethal strain. Results showed that expression profiles of all PRRs investigated were mostly not significant during AS infections whilst significant differences were observed in 17X and 17XL infections. Briefly, MRC1, MRC2 and F4/80 expression decreased at high parasitemias during 17X infections whereas MRC1 an MRC2 increased and F4/80 decreased in 17XL infections. Furthermore, MARCO and CD68 expression fluctuated during 17X infections whereas in 17XL infections both declined rapidly after initial parasitemias. SIGNR1 and SN expression demonstrated minor variations during infections with both strains. Noticeably, MSR1 and DECTIN2 expression increases at 50% parasitemia in infections with 17XL, with a similar trend observed at the protein level. Furthermore, a protective role of MSR1 was demostrated by increased lethality of MSR1 -/- KO mice infected with 17X. Our results suggest a dual role of these receptors which may contribute to the parasite clearance/protection in the 17X infections and to lethality in 17XL.

Submitted to: Memórias do Instituto Oswaldo Cruz (in revision)

9.2.4 Research article 4:

Postmortem characterization of patients with* P. vivax *malaria in the Brazilian Amazon

Marcus V G Lacerda[1,2,3], Silvio C P Fragoso[1,2], Maria G C Alecrim[1,2,3], Márcia A A Alexandre[1,2,3], Belisa M L Magalhães[1,2], André M Siqueira[1,2,3], Luiz C L Ferreira[1,2], José R Araújo[1], Maria Paula G Mourão[1,2,3], Jaume Ordi[4,5], Hernando del Portillo[4,6], Mireia Ferrer[4], Paola Castillo[5], Pedro Alonso[4] & Quique Bassat[4]

[1]Fundação de Medicina Tropical Dr. Heitor Vieira Dourado, Manaus, Brazil. [2]Universidade do Estado do Amazonas, Manaus, Brazil. [3]Universidade Nilton Lins, Manaus, Brazil. [4]Centre de Recerca en Salut Internacional de Barcelona (CRESIB), Hospital Clínic, Universitat de Barcelona, Barcelona, Spain. [5]Department of Pathology, Hospital Clínic, Universitat de Barcelona, Spain [6]Institució Catalana de Recerca i Estudis Avançats (ICREA), Barcelona, Spain.

Abstract

Despite of the number of *P. vivax* fatal cases worldwide, autopsic reports are scarce. In this case series of 17 autopsies, 12 cases could be attributed to *P. vivax* infection, with or without chronic co-morbidities. The major complication was acute respiratory distress syndrome (ARDS) and the finding of parasitized red blood cells inside pulmonary capillaries suggests that sequestration may be involved in pathogenesis of severe vivax malaria.

To be submitted to: Plos Medicine

9.2.5 Review 1:

On cytoadhesion of Plasmodium vivax*: raison d'être?*

Fabio TM Costa[I, +]; Stefanie CP Lopes[I]; Mireia Ferrer[II]; Juliana A Leite[I]; Lorena Martin-Jaular[II]; Maria Bernabeu[II]; Paulo A Nogueira[III]; Maria Paula G Mourão[IV]; Carmen Fernandez-Becerra[II]; Marcus VG Lacerda[IV]; Hernando del Portillo[II, V, +]

[I]Departamento de Genética, Evolução e Bioagentes, Instituto de Biologia, Universidade Estadual de Campinas, Campinas, SP, Brasil. [II]Barcelona Center for International Health Research, Barcelona, Spain. [III]Instituto Leônidas e Maria Deane-Fiocruz, Manaus, AM, Brasil. [IV]Fundação de Medicina Tropical Doutor Heitor Vieira Dourado, Manaus, AM, Brasil. [V]Institució Catalana de Recerca i Estudis Avançats, Barcelona, Spain

Abstract

It is generally accepted that *Plasmodium vivax*, the most widely distributed human malaria parasite, causes mild disease and that this species does not sequester in the deep capillaries of internal organs. Recent evidence, however, has demonstrated that there is severe disease, sometimes resulting in death, exclusively associated with *P. vivax* and that *P. vivax*-infected reticulocytes are able to cytoadhere *in vitro* to different endothelial cells and placental cryosections. Here, we review the scarce and preliminary data on cytoadherence in *P. vivax*, reinforcing the importance of this phenomenon in this species and highlighting the avenues that it opens for our understanding of the pathology of this neglected human malaria parasite.

Published in: Mem Inst Oswaldo Cruz. 2011 Aug;106 Suppl 1:79-84.

9.2.6 Review 2:

THE ROLE OF THE SPLEEN IN MALARIA

Hernando A. del Portillo1,2*, Mireia Ferrer1, Thibaut Brugat3, Lorena Martin-Jaular1, Jean Langhorne3, and Marcus VG Lacerda4

1Barcelona Centre for International Health Research (CRESIB), Barcelona, Spain. 2Institució Catalana de Recerca i Estudis Avançats (ICREA), Barcelona, Spain. 3Division of Parasitology, MRC National Institute for Medical Research, London, UK. 4Fundação de Medicina Tropical Dr. Heitor Vieira Dourado (FMT-HVD) and Universidade do Estado do Amazonas (UEA), Manaus, Brazil

Abstract

The spleen is a complex organ that is perfectly adapted to selectively filtering and destroying senescent red blood cells (RBCs), infectious microorganisms and *Plasmodium*-parasitized RBCs (pRBCs). Infection by malaria is the most common cause of spleen rupture and splenomegaly, albeit variably, a landmark of malaria infection. Here, the role of the spleen in malaria is reviewed with special emphasis in lessons learned from human infections and mouse models.

Submitted to: Cellular Microbiology (November 2011)

10 Aknowledgements

A tots vosaltres, que amb el vostre gra de sorra heu fet que fos possible. Gràcies.

I molt especialment...

... a l'Hernando, per la direcció d'aquesta tesi doctoral i la formació científica, biotecnològica i translacional que m'ha donat. Per descobrir-me el món fascinant de la malària vivax i la melsa. I si les barreres existeixen, que mai perdi aquesta força visionària per trencar-les.

… a la Lorena, amb qui he tingut la sort de fer aquest camí i aprendre'n moltíssim. I pel seu suport, el coneixement transmès, la humilitat científica i l'avaluació crítica d'aquesta tesi. Per tots els moments MILO i la sinèrgia que hem aconseguit, que no pari.

… a la Carmen i el Luis, per les discussions científiques i ensenyaments rebuts.

… a la Maria, el Pep, el Rui, Javi, Míriam i a tots els antonius, pels dies viscuts, l'equip que hem format i que ha fet que cada segon d'aquesta experiència fos únic. Perquè el més important és gaudir-ne, gràcies per viure'ls junts.

… a la Stefanie, la Juliana, la Bruna i la Wanessa, per l'ajuda rebuda i el treball en equip, i que ens retrobem aviat en l'"inferno" (per la calor) de Manaus.

... a tots els col·laboradors, per la feina realitzada i el seu involucrament en el projecte. I en concret, a la Maria C., per apropar-me al món màgic de les fluorescències i la imatge en viu, i perquè ens hi continuem endinsant.

… als falciparum i la resta del laboratori, ha sigut un plaer compartir-ho amb vosaltres.

... al tribunal d'aquesta tesi, per la seva avaluació crítica.

I també molt especialment als que ja formeu part de mi...

... papa, mama, Marc, Bernat, Isabel, iaia, dream i família, que sempre hi sereu.

... Pilaf, Kminal, Ester, Helen, Xarlo, Núria i Merxi, l'equip petit però invencible.

… Nora, Marina i Luis, per cuidar-me tant. I a l'artista (Nora) per les tapes d'aquesta tesi!

Us estimo.